Natural Resources Canada
Ressources naturelles Canada

Analytical details of single- and multicollection $^{40}Ar/^{39}Ar$ measurements for conventional step-heating and total-fusion age calculation using the Nu Noblesse at the Geological Survey of Canada

D. Kellett and N. Joyce

Geological Survey of Canada

Technical Note 8

2014

Canada

Geological Survey of Canada
Technical Note 8

Analytical details of single- and multicollection $^{40}Ar/^{39}Ar$ measurements for conventional step-heating and total-fusion age calculation using the Nu Noblesse at the Geological Survey of Canada

D. Kellett and N. Joyce

2014

ISSN 1914-525X
Catalogue No. M41-10/8-2014E-PDF
ISBN 978-1-100-23176-1
doi:10.4095/293465

A copy of this publication is also available for reference in depository libraries across Canada through access to the Depository Services Program's Web site at http://dsp-psd.pwgsc.gc.ca

This publication is available for free download through GEOSCAN
http://geoscan.ess.nrcan.gc.ca

Recommended citation

Kellett, D. and Joyce, N., 2014. Analytical details of single- and multicollection $^{40}Ar/^{39}Ar$ measurements for conventional step-heating and total-fusion age calculation using the Nu Noblesse at the Geological Survey of Canada; Geological Survey of Canada, Technical Note 8, 27 p. doi:10.4095/293465

Critical review
B. Davis

Authors
D. Kellett (Dawn.Kellett@NRcan-RNCan.gc.ca)
N. Joyce (Nancy.Joyce@NRcan-RNCan.gc.ca)
Geological Survey of Canada
601 Booth Street
Ottawa, Ontario
K1A 0E8

Correction date:

Analytical details of single- and multicollection $^{40}Ar/^{39}Ar$ measurements for conventional step-heating and total-fusion age calculation using the Nu Noblesse at the Geological Survey of Canada

D. Kellett and N. Joyce

Kellett, D. and Joyce, N., 2014. Analytical details of single- and multicollection $^{40}Ar/^{39}Ar$ measurements for conventional step-heating and total-fusion age calculation using the Nu Noblesse at the Geological Survey of Canada; Geological Survey of Canada, Technical Note 8, 27 p. doi:10.4095/293465

Abstract: This technical note outlines the sample preparation and data collection protocols for the Noble Gas Laboratory at the Geological Survey of Canada, including characteristics of the Nu Instruments Limited Noblesse multicollector mass spectrometer, for the purposes of $^{40}Ar/^{39}Ar$ geochronology.

Résumé : Cette note technique résume les protocoles de préparation d'échantillons et de collecte de données au laboratoire des gaz rares de la Commission géologique du Canada. Elle présente aussi les caractéristiques du spectromètre de masse à multicollecteur Noblesse de la société Nu Instruments Limited utilisé pour les analyses géochronologiques $^{40}Ar/^{39}Ar$.

INTRODUCTION

The Noble Gas Laboratory at the Geological Survey of Canada (GSC) in Ottawa, Ontario currently operates a Nu Instruments Limited Noblesse multicollector mass spectrometer that contains a fixed array of one Faraday and three discrete dynode ion counter detectors capable of simultaneous measurement of several noble gas isotopes. The instrument is used primarily for geochronology and thermochronology of K-bearing minerals and rocks by the $^{40}Ar/^{39}Ar$ method (*see* McDougall and Harrison, 1999, for a complete review). Multicollection mass spectrometry is relatively new to the field of noble gas measurement, and presents both great advantages and new challenges to the method (e.g. Cosca, 2007; Mark et al., 2009; Marrocchi et al., 2009; Coble et al., 2011). The primary advantages of this type of instrument are: higher precision of isotopic ratio measurements; suitability for a larger range of signal intensity compared to a single detector; significantly shorter collection times; and the ability to dedicate specific detectors to very small or contaminating signals. In addition, the Nu Instruments Limited Noblesse has a mass resolution sufficient to resolve common and problematic interfering isotopes (typically hydrocarbon and chlorine molecules) from Ar isotopes. The challenges lie in characterizing relative detector efficiency, linearity, and mass-dependent fractionation in the different collectors over a large dynamic range and under different tuning conditions (e.g. Turrin et al., 2010; Coble et al., 2011). In this case 'relative detector efficiency' is used to refer to the efficiency of detection of a collector relative to a reference detector. 'Mass-dependent fractionation' is used to refer to mass-dependent differences in ionization efficiency, mass effects on ion-current measurement, and any mass-dependent source effects, all of which cause the measured gas composition to deviate from its actual composition. Herein are detailed the methods used at the GSC for sample preparation and acquisition of laser step heating $^{40}Ar/^{39}Ar$ age data on the Noblesse.

SAMPLE PREPARATION DETAILS

Samples suitable for dating by the $^{40}Ar/^{39}Ar$ method are minerals or fine-grained volcanic rock samples that contain more than 0.5% K (*see* Table 1). Typically the most successfully dated materials are well preserved and unaltered biotite, muscovite, K-feldspar, hornblende, phlogopite, and whole-rock basalt. Undesirable contaminants and microchemical heterogeneities include alteration phases, mineral or fluid inclusions, mineral intergrowths, compositional zoning, exsolution lamellae, microveining, devitrification textures, vesicles, calcareous cements, hydrocarbon, and sulphide-mineral inclusions. Secondary Electron Microscope-Energy Dispersive Spectroscopy (SEM-EDS) microtextural and microchemical characterization is recommended prior to sample preparation to confirm sample quality and K content. Abundance of Ca and Cl should be verified as well, as undesired Ar isotopes produced in the reactor from these elements during irradiation can complicate analytical data interpretation and, more egregiously, contaminate the extraction line and mass-spectrometer system. Large amounts of Ca and Cl create noise that can elevate the overall background of a detector and can interfere with the proper trajectory of the critical Ar ion beams through the Noblesse flight tube. These effects can persist for days and even weeks after exposure to a 'dirty' sample.

Samples selected for $^{40}Ar/^{39}Ar$ analysis are gently crushed and sieved, and then rinsed several times with water to remove fine particles. A small amount of (typically) the 250–500 µm fraction of crushed material is placed in a Petri dish with ample amounts of ultra-pure ethyl alcohol. The best quality mineral grains are then picked under a binocular microscope and allowed to dry completely. Grains that are suspected to contain carbonate residue are subjected to a 15 minute bath in dilute (5%) acetic acid. Those from samples that have come into contact with organic heavy liquids from mineral separation processes are placed in an acetone ultrasonic bath for 15 minutes, and subsequently washed with de-ionized water and ultra-pure ethyl alcohol, and dried completely.

The can into which the mineral samples are loaded for irradiation is a custom-fabricated aluminum cylinder with six 35 mm deep tubular holes drilled into it, and a screw-on lid (Fig. 1). Individual mineral separates are loaded into 2–3 mm deep aluminum foil packets that are subsequently stacked vertically into 35 mm long foil tubes that once filled, are inserted into the tubular holes of the can. For samples with more than one target mineral (e.g. biotite and hornblende), both mineral phases are loaded into the same packet. Several flux monitor grains of Fish Canyon tuff sanidine (FCT-San) (28.02 ± 0.16 Ma (1σ); Renne et al. (1998)) are loaded into each sample packet for Phanerozoic and younger samples. In the case of Precambrian sample batches, individual packets containing PP-20 hornblende flux monitor grains are prepared (equivalent to monitor Hb3gr, 1074 ± 5 Ma (1σ); Jourdan et al. (2006)), and included in these packets are several FCT-San grains intended for use as secondary standards. A minimum of four PP-20 packets per tube are interspersed among the sample packets in the irradiation can.

The position of each sample packet in the can is defined by the distance of the top of the packet from the bottom of its tube. Positions are determined as packets are loaded two at a time into the tube. The height of the first packet (A) of each pair is measured using a ruler and recorded as the position of A, and after the two packets A and B are together pushed gently to the bottom of the tube, a glass rod marked with millimetre measurements is inserted into the tube until it reaches the packets, and the height read from the rod is recorded as the position of packet B. This process is repeated until the foil tube is filled. Each irradiation can is also loaded with a packet containing both Crystran (CaF_2) and K-glass (a potassium-rich zero-age natural volcanic glass), which are analyzed to determine reactor-induced correction factors

Table 1. Minerals potentially suitable for $^{40}Ar/^{39}Ar$ dating and their typical K contents.

Mineral	Formula	K (approximate %)	Source
Alkali feldspar: sanidine, microcline, orthoclase, adularia	$(K,Na)AlSi_3O_8$	3–16	Deer et al., 1992
Hornblende	$(Na,K)_{0-1}Ca_2(Mg,Fe,Al)_5Si_{6-7.5}Al_{2-0.5}O_{22}(OH)_2$	0.1–1.5	Deer et al., 1992
Biotite, (phlogopite(Mg)-annite(Fe) end members)	$K_2(MgFe)_{4-6}(Fe,Al,Ti)_{0-2}[Si_{5-6}Al_{2-3}O_{20}](OH,F)_4$	7–10	Deer et al., 1992
Fuchsite (Cr mica)	$K_2(Al,Cr)_6[Si_6O_{20}](OH)_4$	7–10	Deer et al., 1992
Illite (clay, fault gouge clay)	$K_{1.5-1}Al_4[Si_{6.5-7}Al_{1.5-1}O_{20}](OH)_4$	6–7	
Lepidolite (pegmatite, hydrothermal veins)	$K_2(Li,Al)_{5-6}[Si_{6-7}Al_{2-1}O_{20}](OH,F)_4$	7–10	Deer et al., 1992
Zinnwaldite (pegmatite, hydrothermal veins)	$K_2(Fe,Li,Al)_{5-6}[Si_{5-6}Al_{2-3}O_{20}](OH,F)_4$	7–10	Deer et al., 1992
Leucite (found in K-rich basic lavas)	$K[AlSi_2O_6]$	18	
Manganese oxides (cryptomelane (K)-hollandite (Ba), etc.)	$(K,Ba)_{1-2}Mn_8O_{16}.xH_2O$	1–5	McDougall and Harrison, 1999
Muscovite (also phengite, Si/Al>3, high-P equivalents)	$K_2Al_4[Si_6Al_2O_{20}](OH,F)_4$	7–10	Deer et al., 1992
Nepheline (found in alkaline igneous rocks)	$Na_3(Na,K)[Al_4Si_4O_{16}]$	7	Deer et al., 1992
Plagioclase	$Na[AlSi_3O_8]$-$Ca[Al_2Si_2O_8]$	0–1	Deer et al., 1992
Roscoelite (epithermal deposits)	$K_2(Fe,Li,Al)_{5-6}[Si_{5-6}Al_{2-3}O_{20}](OH,F)_4$	10	
Sericite (fine-grained muscovite and/or paragonite)	$K_2Al_4[Si_6Al_2O_{20}](OH,F)_4$	<7–10	
Glauconite (authigenic mineral in marine sediments)	$(K,Ca,Na)_{1.6}(Fe,Al,Mg)_4Si_{7.3}Al_{0.7}O_{20}(OH)_4$	<6.5	McDougall and Harrison, 1999
Stilpnomelane	$(K,Ca,Na)_{0.6}(Mg,Fe)_6Si_8Al(O,OH)_{27}.2\text{-}4H_2O$	1–2	Deer et al., 1992
Alunite (Al)-Jarosite (Fe) (alteration sulphate minerals)	$K(Al,Fe)_3(SO_4)_2(OH)_6$	1–12	McDougall and Harrison, 1999
Sylvite (evaporate) (also carnallite, polyhalite, langbeinite)	KCl	50	
Whole rock (volcanic rocks, slate, phyllite)			
Glass (tektite, pseudotachylite)			

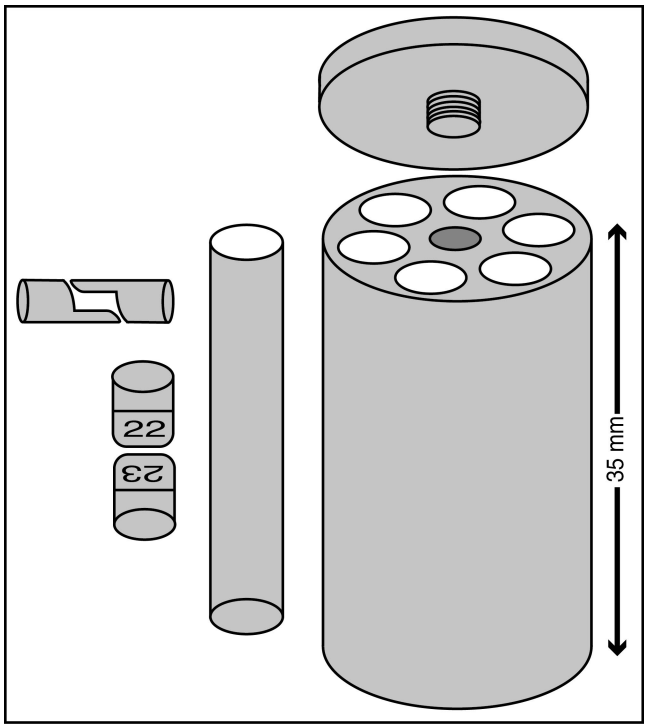

Figure 1. Illustration of an irradiation can used to contain samples for nuclear irradiation at the McMaster Nuclear Reactor. Numbered foil packets are stacked vertically into six cylindrical tubes radially distributed around the can.

(RCFs). Prepared irradiation cans are submitted for irradiation in one of three medium flux positions (position 8B, 8C, or 8E) at the research nuclear reactor of McMaster University (MNR) in Hamilton, Ontario. Neutron flux is either approximately 0.9×10^{13} neutrons/cm^2/s or 1.3×10^{13} neutrons/cm^2/s depending on whether the reactor is operating at a 2 MW or 3 MW power level, respectively. Duration of the irradiation depends on the estimated age range of the sample batch, and on the operating conditions of the reactor. Cadmium shielding (1 mm thick) is typically placed around the can during irradiation in order to reduce the effects of thermal neutrons on the samples, as well as to reduce the efficiency of the reactor-induced ^{40}K(n,p) ^{40}Ar reaction. Correction factors for typical interference species produced by thermal neutrons during irradiation are outlined in the 'Interfering isotopes and reaction-induced correction factors (RCFs)' section.

EXTRACTION LINE

The extraction line at the GSC is a dual system comprising two separate source chambers coupled to either a CO_2 or a UV laser. The tubulation from each chamber converges at a manifold upstream of the getters and ion pump, so that one line can be manually isolated and pumped with an auxiliary ion pump while the other line is in use. The ultrahigh vacuum in the main portion of the extraction line is maintained using a Gamma Titan 25S ion pump. There are two getters in the extraction line, including 1) a cylinder containing two SAES™ NP-10 getters of St 707 alloy (Zr-V-Fe) held at about 400°C to remove nitrogen, oxygen, hydrocarbon, water, and other active gases, and 2) a room-temperature getter containing HY-STOR® 201 calcium-nickel alloy pellets to getter hydrogen (Villeneuve and MacIntyre, 1997).

Routine atmospheric ^{40}Ar/^{36}Ar analyses are included during an analytical session using aliquots of air transferred to the extraction line from a secondary air reservoir, in order to monitor mass fractionation and detector efficiencies. Air from this reservoir is extracted via a Becker Systems automated pipette assembly comprising back-to-back Swagelok spring-to-close actuating valves separated by a 0.2 mL volume. Air shots are in a typical dynamic range for samples and standards on the Faraday and ion counters (^{40}Ar ~1–10 mV and ^{36}Ar ~4–34 μV). This secondary air tank is refreshed by means of a primary air reservoir that delivers large air aliquots through a manual pipette. Primary reservoir air shots are suitable for measurement of both ^{40}Ar (~10 V) and ^{36}Ar (~30 mV) on the Faraday collector. The secondary air reservoir is refreshed from the Faraday tank when necessary (typically every two to three months). The residual air in the secondary tank is then pumped away with a turbomolecular pump followed by the ion pump. Replenishment of the secondary air tank is accomplished by expanding a split of air from the primary tank, equilibrating and gettering within the line, and finally trapping the air in the secondary reservoir. Air shots dispensed from the reservoirs are fixed volumes; however, a broad range of ^{40}Ar and ^{36}Ar signal intensities can be obtained by dispensing and combining multiple air shots, or by splitting a single shot one or more times as needed by trapping a portion of it behind a valve and measuring the residual volume, or by pumping the residual away and re-expanding the trapped component.

Following irradiation, the irradiated can is returned from the research nuclear reactor of McMaster University and unpacked. Each sample is divided into two or more aliquots; samples and monitor aliquots are loaded into individual 1.5 mm or 3.0 mm diameter holes in a copper planchet (*see* map of planchet layout in Fig. 2). A KBr cover slip is seated on the planchet, separated from direct contact with the copper by 1 mm gold wire spacers, and the planchet assembly is then placed under vacuum in a chamber with a 2 inch (51 mm) diameter anti-reflective-coated Geo-Optics Cleartran™ differentially pumped ZnS viewport. The bellows connecting the source chamber to the extraction line is baked overnight at 200–250°C using a custom-fabricated oven, while open to a turbomolecular pump. Once the bellows has cooled, a heat lamp is placed over the viewport to gently degas (~100°C) the source chamber and planchet prior to switching from the turbo pump to the ion pump.

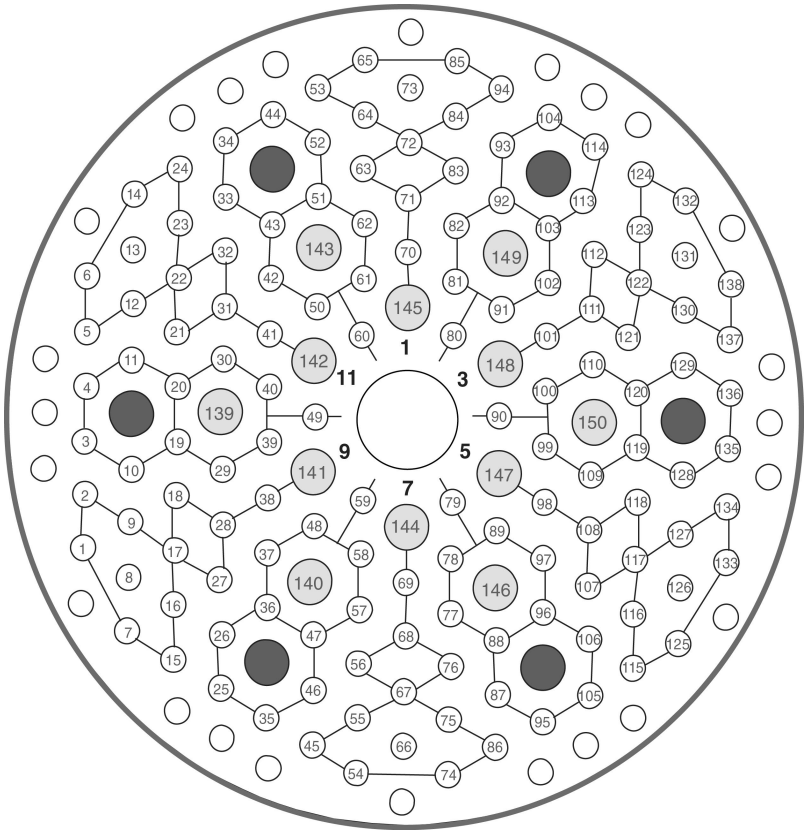

Figure 2. Illustration of the copper planchet used to hold samples during CO_2 laser heating for Ar isotopic analysis. The planchet consists of two copper pieces held together by screws (dark grey circles); the copper top plate seen here, featuring holes 3 mm deep and either 1.5 mm or 3 mm in diameter, and the solid base plate (not visible) that forms the floor of the holes. This base is separated from the top plate and polished to a mirror shine using 9 µm and 1 µm diamond suspension paste at every planchet cleaning. The network of lines and the large dark numbers are etched into the top plate to serve as visual landmarks for navigation under the laser camera. Numbers 1–150 are programmed laser-stage positions that allow Mass Spec to drive hole to hole during automated run sequences.

CO_2 LASER

Heating of individual sample aliquots either by total fusion or in steps of incrementally higher laser power (and hence higher temperature) is achieved using a Photon Machines, Inc. Fusions 10.6 55 W CO_2 laser. This laser is equipped with an optical beam-flattening homogenizer lens that distributes and homogenizes the laser beam over the full area of a planchet pit for uniform heating of the grain(s). Without the homogenizer lens, the laser beam would form a Gaussian power density distribution with a central 'hot spot' and result in uneven heating of the sample.

For total-fusion experiments (flux monitors and standards, for example), the sample is fused in a single heating step at high (~5–6 W) laser power for 60 s. For step-heating experiments, a general schedule of 5–20 heating increments is followed depending on the particular mineral being analyzed. These experimentally determined heating schedules are designed to progressively release argon gas from the sample in as many equal-volume steps as possible. A typical Mesozoic biotite analysis would consist of the following laser power steps (30 s heating time with 10 s power ramp-up, in watts): 0.20 W, 0.25 W, 0.30 W, 0.40 W, 0.45 W, 0.50 W, 0.55 W, 0.60 W, 0.65 W, 0.70 W, 0.75 W, 0.80 W, 0.90 W, 1.0 W, 1.1 W, 1.2 W, 1.5 W, 2.6 W, 3.5 W, and finally fusion at 6.0 W. The CO_2 laser Chromium software is operated remotely by Mass Spec software (Deino, 2001), allowing for integration of the laser step heating and total-fusion experiment schedules into a fully automated analytical routine. Mass Spec software incorporates a jog feature in which random short steps of the stage occur during heating experiments to better achieve coupling of the aliquot with the laser.

Argon gas released from the sample during each heating step is cleaned by passive equilibration with the getters on the extraction line for a period of 3–4 minutes, after which time the gas is admitted to the Nu Instruments Limited Noblesse multicollector mass spectrometer for isotopic analysis.

NOBLESSE INSTRUMENT DETAILS

The Nu Instruments Limited Noblesse (model 018) is a single-focusing, Nier-source, 75° magnetic sector multicollector noble gas mass spectrometer equipped with two quadrupole lens arrays. The Noblesse used at the GSC features one Faraday cup (FAR) with a $10^{11}\Omega$ resistor, and three ETP® discrete dynode ion-counting multipliers (IC0 ('axial'), IC1, and IC2; *see* Fig. 3) in a fixed array. The Faraday cup collects and transfers the signal current to an amplifier that measures the voltage drop across the resistor, yielding a signal intensity in volts, whereas the ion counters measure in units of counts per second (cps), with 62 500 cps = 1 mV. The overlapping working range between the Faraday and ion counters is approximately 2–20 mV, equivalent to approximately 125 000–1 250 000 cps. The collector configuration allows for the measurement, for example, of large ^{40}Ar

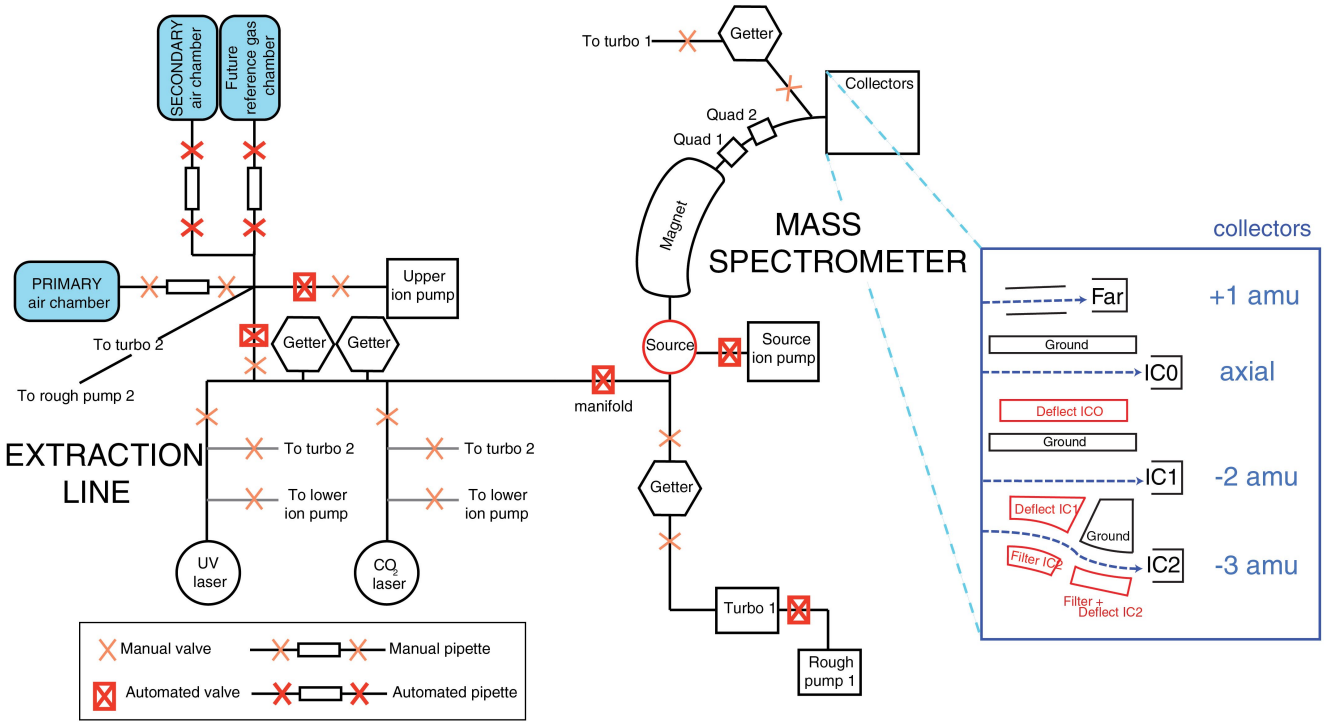

Figure 3. Schematic diagram of the extraction line and Noblesse mass spectrometer at the Geological Survey of Canada, illustrating Noblesse 018 collector cup configuration. Also shown are the deflector and filter blocks that can be used to either steer the beam into or away from the collector.

signals in the Faraday cup while simultaneously collecting ^{39}Ar in IC0, ^{37}Ar in IC1, and ^{36}Ar in IC2 in full multicollection mode. The ^{37}Ar has a fairly short half-life of about 35 days, and radioactive decay of implanted ^{37}Ar in ion counters causes noisy and high background levels; however, the accuracy of the ^{36}Ar measurement, critical for the atmospheric Ar correction, depends on the precise measurement of typically very small ^{36}Ar signals, and thus requires a stable and minimized background. The ability to maintain dedicated detectors for ^{37}Ar (for which implantation is an issue) and ^{36}Ar (which typically yields very small signals) is a principal advantage of this configuration.

The Noblesse is equipped with a wide collector slit, a feature that allows for the mass resolving power (MRP) of its collectors to exceed 1500 (MRP = m/Δm, where m is the mass of the peak, and Δm is the mass difference at 5% peak height between 5% and 95% of the peak height). This capacity for high resolution between peaks with very similar masses allows for measurement of critical masses in the absence of interfering species (discussed further in 'Collectors'). Nu Instruments Limited provides a simple software routine for determining MRP for the Noblesse collectors. For the GSC Noblesse, the MRP of the ion counters is in the range of 2300 (IC0), 2500 (IC1), and 2500 (IC2).

Typical background values measured in blank runs following a three minute isolation in the extraction line for the various isotopes are: ^{40}Ar: 8500 cps (2.5×10^{-16} mol), ^{39}Ar: 20 cps (5.9×10^{-19} mol), ^{38}Ar: 60 cps (1.8×10^{-18} mol), ^{37}Ar: 140 cps (4.1×10^{-18} mol), and ^{36}Ar: 80 cps (2.4×10^{-18} mol).

SENSETIVITY

Sensitivity of the mass spectrometer is determined by measuring the intensity of ^{40}Ar released from weighed grains of FCT-San and other well characterized K-bearing age reference materials by total fusion achieved using the CO_2 laser. The FCT-San grains are weighed on a microbalance prior to laser fusion, and moles of ^{40}Ar are calculated for each grain, based on 12.06% K_2O (Dazé et al., 2003), and the accepted age of 28.02 ± 0.16 Ma (1σ) (Renne et al., 1998). For analysis, ^{40}Ar is measured in the Faraday detector and ^{36}Ar is measured in IC2. The IC2 measurements of ^{36}Ar for the atmospheric correction are corrected to Faraday intensities in millivolts using an intercalibration factor based on air measurements (*see* details on intercalibration factors in 'Collectors'). Moles of ^{40}Ar in each weighed grain are calculated and compared to the measured intensity of ^{40}Ar on the mass spectrometer, following corrections for dead time, procedural blank, and atmospheric ^{40}Ar ($^{40}Ar^* = {}^{40}Ar_m - 298.56 \times {}^{36}Ar_m$, where '*' signifies radiogenic, 298.56 is the accepted ^{40}Ar/^{36}Ar of the atmosphere (Lee et al., 2006; Mark et al., 2011) and 'm' signifies measured).

Typical sensitivity measurements during 2010–2013 range 5.6–5.9 Amps/mol (Table 2). Normalizing to the full extraction line + mass spectrometer volume yields a range in sensitivity of 7.1–7.5 Amps/mol.

COLLECTORS

Tuning

Tuning of the source region is optimized by maximizing the ^{40}Ar signal (typically of ^{40}Ar from an air shot), as recommended by Nu Instruments Limited. Tuning of the quadrupole lenses is conducted after tuning of the source region, and after performing any necessary adjustment of plateau voltages for the ion counters. Quadrupole lens tuning manipulates both peak shape and peak alignment, and is sensitive to mass station. Thus the quadrupole values used during data collection are optimally tuned for each mass station used, and identical quadrupole values are used during blank, unknown, flux monitor, and air analyses. Two main quadrupole tuning configurations are used, for the following mass stations: quadrupole tuning 1 (^{39}Ar in IC0) and quadrupole tuning 2 (^{40}Ar in IC0). Exceptions are discussed below in the 'Data collection' section.

Interfering near-isobaric species such as hydrocarbons can produce small, but significant composite peaks at most of the masses of interest (Fig. 4). To avoid measurement of the interfering species, quadrupole tuning for peak alignment is performed such that measurement occurs on the low-mass Ar shoulder (Fig. 4b) of any significant composite peaks (typically ^{39}Ar, ^{38}Ar, ^{37}Ar, and ^{36}Ar). Since peak centring of the ^{40}Ar peak is typically performed to position the magnet, a small mass offset (~0.01–0.02 amu) may be applied to ensure that measurement occurs in the peak flat

Table 2. Sensitivity measurements.

	Weight	^{40}K	^{40}Ar	^{40}Ar$_m$	Intensity*		
	(µg)	(nmol)	(nmol)	(mV)	(mol/V)	(V/g)	(Amps/mol†)
June 2013 PP20							
Hole 119	51.4	0.0018709	1.596E-04	102.585	1.559E-12	1991.2	6.4
Hole 120	33.9	0.0012339	1.052E-04	60.121	1.761E-12	1762.9	5.7
Hole 121	37.5	0.0013650	1.164E-04	68.500	1.706E-12	1819.7	5.9
Hole 122	26.6	0.0009682	8.257E-05	40.520	2.040E-12	1522.0	4.9
Hole 123	41.2	0.0014997	1.279E-04	63.497	2.017E-12	1539.2	8.0
Hole 124	34.6	0.0012594	1.074E-04	56.336	1.923E-12	1614.4	5.2
Hole 125	41.9	0.0015251	1.301E-04	59.301	2.198E-12	1412.3	4.5
Hole 126	35.8	0.0013031	1.111E-04	58.133	1.915E-12	1620.7	5.2
Hole 127	28.9	0.0010519	8.971E-05	47.918	1.877E-12	1653.8	5.3
Hole 128	25.3	0.0009209	7.853E-05	44.582	1.768E-12	1756.2	5.7
Hole 129	26.3	0.0009573	8.164E-05	47.450	1.730E-12	1794.5	5.8
Hole 130	26.4	0.0009609	8.195E-05	49.861	1.655E-12	1875.4	6.0
						Mean	**5.7**
						Standard deviation	**0.88**
January 2013 PP20							
Hole 140	52.9	0.0019255	1.642E-04	101.800	1.646E-12	1885.8	6.1
Hole 141	37.1	0.0013504	1.152E-04	81.923	1.594E-12	1947.3	6.3
Hole 142	33.0	0.0012012	1.024E-04	49.521	2.076E-12	1495.1	4.8
Hole 143	22.0	0.0008008	6.829E-05	37.380	1.880E-12	1651.3	5.3
Hole 144	31.1	0.0011320	9.654E-05	51.005	1.896E-12	1637.0	5.3
Hole 145	35.9	0.0013067	1.114E-04	68.700	1.625E-12	1910.4	6.2
						Mean	**5.7**
						Standard deviation	**0.61**
Feb/12 FCT-SAN						**Mean**	**5.9**
						Standard deviation	**0.97**
Jan/10 FCT-SAN						**Mean**	**5.6**
						Standard deviation	**0.73**

^{40}Ar$_m$ is corrected for the procedural blank and atmospheric Ar (*see* text for details).
† Faraday amplifier contains a 10^{11} Ω resistor.
*Intensity has not been normalized to the full extraction line + mass spectrometer volume. The measured extraction line volume is about 0.79 of the total volume.

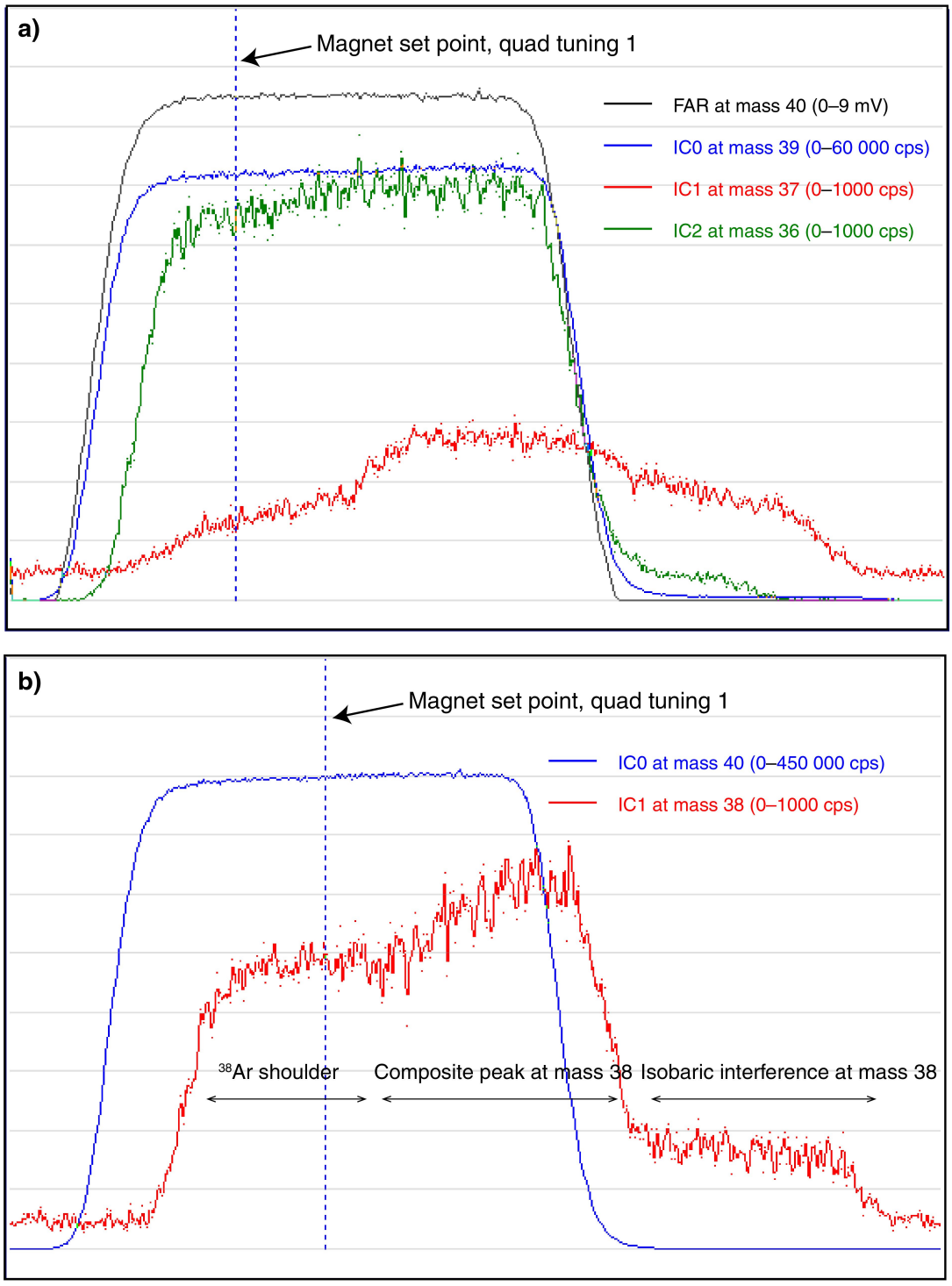

Figure 4. Peak alignment using **a)** quadrupole tuning 1 and **b)** quadrupole tuning 2 (see Table 4 for details), and illustrating typical mass resolution of composite 36, 37, 38, and 39 peaks (Ar component forms the low-mass component for all composite peaks, as labelled for the 38 peak). Vertical line shows the magnet set point. Peaks are tuned such that measurement occurs on the low-mass Ar shoulder of composite peaks. Scales used for each mass are indicated in parentheses.

of the Ar shoulders of composite peaks. The mass resolution of the Noblesse sufficiently separates Ar from interfering species for measurement of the peak flat on these shoulders.

Dead-time correction

The detector response of an ion counter involves a short time delay known as dead time. For a linear system, incident ions which strike the electron multiplier system during the period of dead time do not produce a corresponding pulse, and thus are not counted. At higher count rates, more counts are missed. A dead-time correction is applied to ion counting data after extrapolation to time zero (t = 0) and before baseline corrections as follows:

$$cps_{DTc} = cps_m/(1 - cps_m \times d_t) \quad (1)$$

in which cps_{DTc} is the dead-time–corrected signal in counts per second, cps_m is the measured signal in counts per second, and d_t is the dead-time correction in nanoseconds (Turrin et al., 2010). For a detailed discussion of dead time in ion counting systems, *see* Fahey (1998).

Dead time and any collector nonlinearity are measured on IC0 using multiples of secondary reservoir air shots (1 to 4 pipetted volumes) such that the ^{40}Ar intensity is 2×10^5 to 1×10^6 cps. This intensity range brackets typical ^{40}Ar measurement intensities of unknowns and is within the dynamic range of the Faraday cup and ion counters. The ^{40}Ar is measured in both the Faraday and IC0 collectors, and ^{36}Ar is measured in IC0, in order to implement two different methods for dead-time determination. Direct measurement of dead time is not made on IC1 and IC2 because the tuning conditions necessary to make the measurements would not be representative of the measurement of unknowns; however, IC1/IC0 and IC2/IC0 gains have been found to be constant over a range of intensities, and thus the characteristic dead time determined for IC0 is thought to be representative of the other collectors as well. Importantly, IC2 and IC1 collectors are used to measure ^{36}Ar and ^{37}Ar, respectively, which are typically small signals, much less than 100 000 cps, and thus measurements made in those collectors should be negligibly affected by dead time.

For method 1, the relative deviation of the measured $^{40}Ar/^{36}Ar$ ratio from the accepted $^{40}Ar/^{36}Ar$ ratio was plotted against the measured intensity of the smaller isotope (^{36}Ar). The slope is proportional to the dead time, and yielded DT = 27 ± 3 ns (Fig. 5a; Table 3). (e.g. Fahey, 1998; Nelms et al., 2001). Note that in plot Figure 5a, the y-intercept also gives a measure of the mass fractionation for the IC0 detector.

In method 2, the $^{40}Ar_{ICO}/^{40}Ar_{FAR}$ ratio was plotted against $^{40}Ar_{ICO}$ intensity. The slope of a best-fit line through this data is related to dead time through the following equation:

$$d_t = \text{-slope/y-intercept} \quad (2)$$

Using the same analytical runs as in method 1, this yields a dead time of 27 ± 8 ns (Fig. 5c). Note that in this method, the y-intercept also yields the gain of the IC0 detector relative to the Faraday detector. Both approaches assume linearity of the collector, which is likely an oversimplification (Richter et al., 2001).

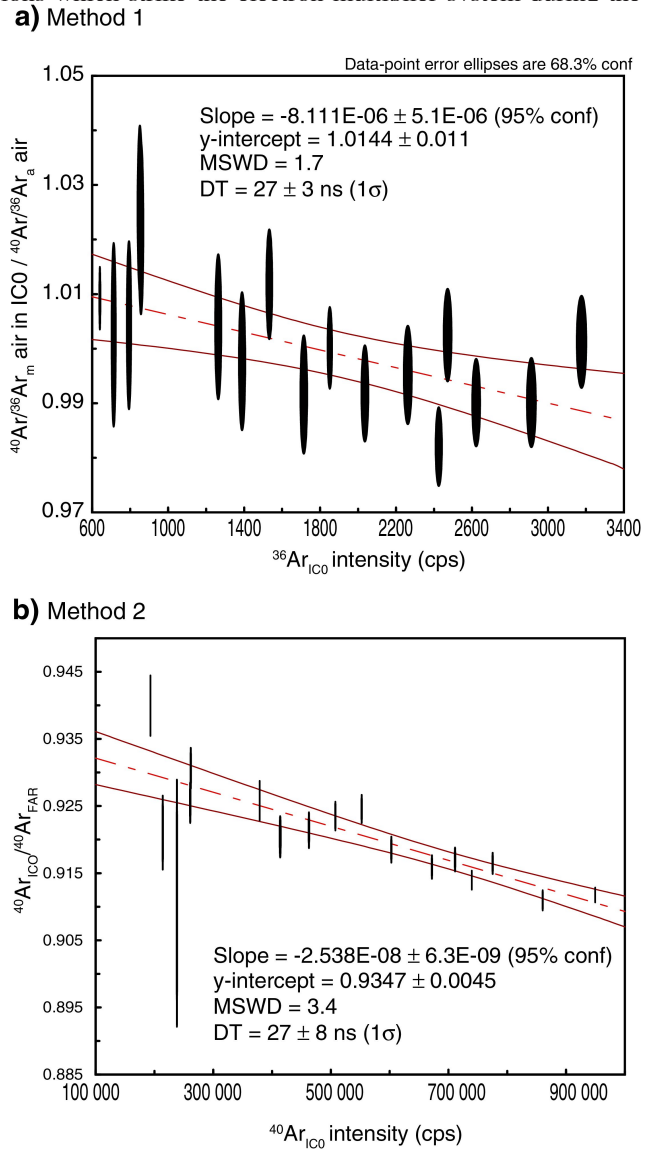

Figure 5. Dead-time correction calculations. **a)** Method 1: measured (uncorrected for dead time) atmospheric $^{40}Ar/^{36}Ar$ relative to the accepted value of 298.56 in the y-axis, plotted against $^{36}Ar_{ICO}$ signal intensity in the x-axis. The slope is proportional to dead time by d_t = -slope*298.56/y-intercept. **b)** Method 2: The measured ^{40}Ar in IC0 relative to that in the Faraday collector in the y-axis is plotted against the $^{40}Ar_{IC0}$ intensity. The slope is proportional to dead time by d_t = -slope/y-intercept. Subscripts 'm' and 'a' in Figure 5a denote measured and accepted.

Table 3. Experiments used to calculate IC0 dead time.

SEM air shots	$^{40}Ar_{FAR}$ (cps*), corr	1σ (cps)	$^{40}Ar_{IC0}$ (cps), corr	1σ (cps)	$^{36}Ar_{IC0}$ (cps), corr	1σ (cps)	$^{40}Ar_{IC0}/^{40}Ar_{FAR}$ method 2	1σ	$^{40}Ar_{IC0}/^{36}Ar_{IC0}$ method 1	1σ
1X	280827	593	261343	125	856	9	0.9306	0.0020	305.2	3.1
1X	281437	596	260468	138	851	8	0.9255	0.0020	306.2	3.0
2X	550240	809	508138	208	1717	12	0.9235	0.0014	296.0	2.1
3X	810826	798	741013	250	2476	14	0.9139	0.0010	299.3	1.6
4X	1044115	769	951939	288	3185	17	0.9117	0.0007	298.9	1.6
1X	261402	3500	237999	112	794	8	0.9105	0.0122	299.8	3.0
2X	502850	954	463311	181	1534	10	0.9214	0.0018	302.1	2.0
3X	735002	907	673186	190	2266	13	0.9159	0.0012	297.1	1.8
4X	947217	994	862811	256	2919	16	0.9109	0.0010	295.6	1.6
1X	231790	660	213476	586	713	8	0.9210	0.0036	299.3	3.3
2X	450144	740	414304	603	1391	11	0.9204	0.0020	297.9	2.5
3X	657241	899	603638	189	2039	12	0.9184	0.0013	296.1	1.7
4X	847136	939	776332	246	2626	14	0.9164	0.0011	295.6	1.5
1X	204804	641	192510	110	639	2	0.9400	0.0030	301.3	1.1
2X	409171	848	378790	164	1264	11	0.9258	0.0020	299.7	2.6
3X	598808	865	553624	203	1854	9	0.9245	0.0014	298.6	1.4
4X	777067	960	712553	256	2430	12	0.9170	0.0012	293.2	1.4

*Measured in mV and converted to equivalent cps by 1 mV = 62 500 cps; corr = baseline and procedural blank corrected.
1σ errors include errors in the procedural blank, all data are uncorrected for dead time.

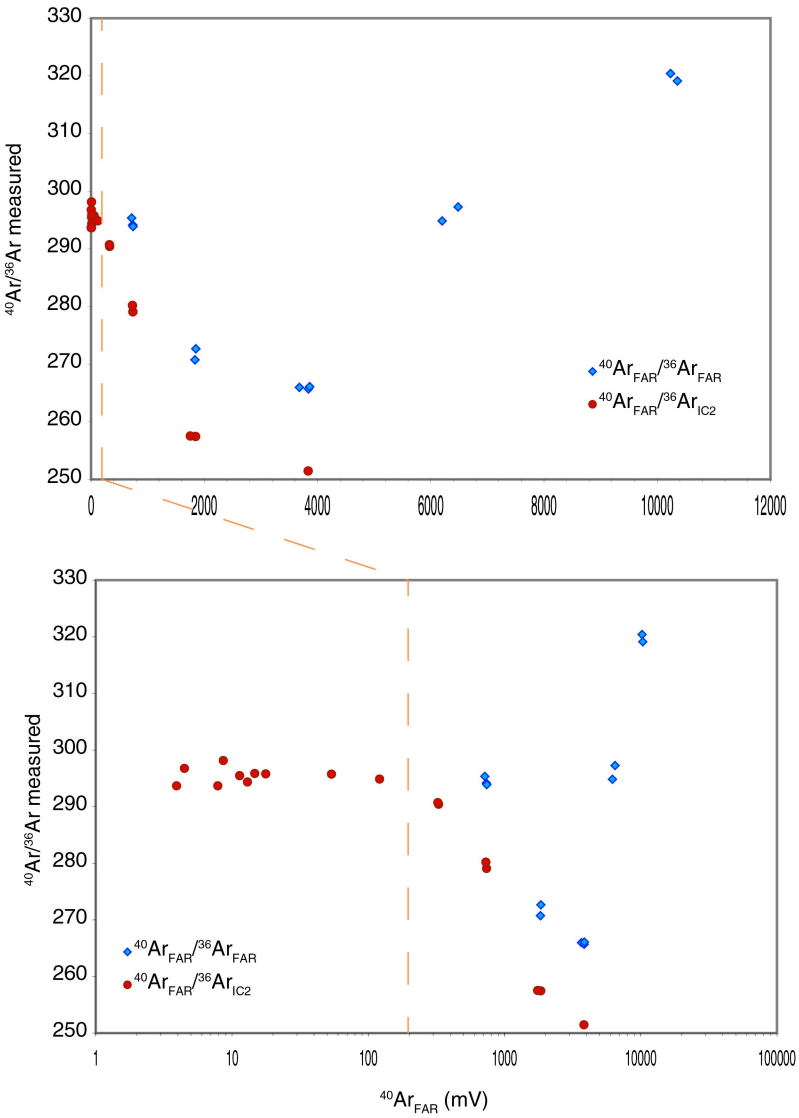

Figure 6. Observed behaviour of mass spectrometer for large Ar gas aliquots, interpreted to reflect pressure effects in the source region. Two sets of experiments are plotted together in **a)** a standard x-y plot and **b)** a log plot. Data have not been corrected for mass fractionation or relative gain. In the first set of experiments, $^{40}Ar/^{36}Ar$ from air shots of varying pressure were collected by measuring ^{40}Ar in the Faraday cup and ^{36}Ar in IC2, and ^{40}Ar intensity ranged 3–4000 mV. In the second set, $^{40}Ar/^{36}Ar$ was measured with both ^{40}Ar and ^{36}Ar in the Faraday cup, and ^{40}Ar intensity ranged 700–11000 mV. Note that there is a difference in $^{40}Ar/^{36}Ar$ where experiments overlap (~800–4000 mV), because data are uncorrected for relative gain of the IC2 detector relative to the Faraday cup. The orange line denotes the cut off above which the instrument displays an apparent pressure-dependent effect.

Pressure-dependent fractionation

Pressure-dependent fractionation was examined using air shots with a large range of pressures over the course of two sets of experiments (Fig. 6). Small volumes were measured with ^{40}Ar in the Faraday collector and ^{36}Ar in IC2 in the first set of experiments, and large volumes were measured solely using the Faraday detector in the second set of experiments. For Faraday-only measurements, the ^{40}Ar gas load ranged from 2.0×10^{-12} mol to 2.8×10^{-11} mol, resulting in Faraday signals between 0.7 V and 10.5 V, and measurements were repeated in two different analytical sessions with near-identical results. Note that the two sets of analyses are not directly compatible because ^{36}Ar was measured in different collectors, but the results show the same overall trend (Fig. 6). For ^{40}Ar signals under 150 mV (9.4×10^6 cps equivalent), the measured $^{40}Ar/^{36}Ar$ is independent of Ar pressure; however, over 200 mV, the measured $^{40}Ar/^{36}Ar$ begins to deviate. As signal size increases, $^{40}Ar/^{36}Ar$ systematically decreases to about 90% of the value measured at lower gas pressure. Beyond about 4 V, the $^{40}Ar/^{36}Ar$ value increased, until it reaches about 110% of the value measured at low intensities. Since the same effect is observed in both the ion counter and the Faraday collector, this may be a reflection of pressure interferences in the source region rather than at the detectors. Regardless of their cause, such large signals are effectively outside the calibration window of the air shots used for relative efficiency and mass-fractionation intercalibrations and would require a significant and difficult to characterize pressure-dependent correction. To avoid these pressure-dependent fractionation effects, an overpressure routine (*see* section 'Multicollector scheme for all samples MC-O') is triggered to split large gas loads such that the measured intensity of the most abundant measured isotope (typically ^{40}Ar, measured in the Faraday cup) never exceeds 160 mV.

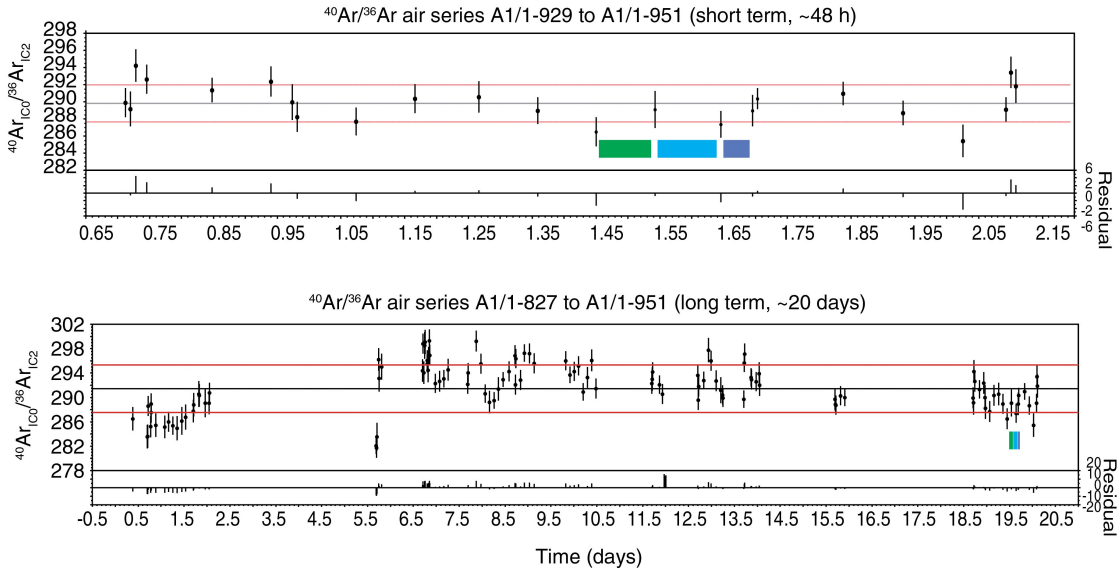

Figure 7. The $^{40}Ar_{IC0}/^{36}Ar_{IC2}$ collected from a series of air shots **a)** A1/1-929 to A1/1-951, a time period of about 48 h, and **b)** A1/1-827 to A1/1-951, a time period of about 20 days. A single-grain step-heating experiment of reference material GA-1550 (biotite) described also in Figures 9 and 10 was collected during the time span of the three coloured bands.

DATA COLLECTION

Data collection and detector intercalibration corrections

Multicollector Ar data must be carefully corrected for detector intercalibration relative to a reference detector because of both efficiency differences between collectors, and mass fractionation of Ar isotopes at the source and within the detectors (e.g. Turrin et al., 2010; Coble et al., 2011). Furthermore, detector intercalibration requires continuous monitoring of efficiency and mass-fractionation behaviour over time (Coble et al., 2011). At the GSC Noble Gas Laboratory, the IC0 detector is used as the reference detector, and intercalibration factors (ICFs) are applied to the other detectors relative to IC0.

In Figure 7 are examples of both short-term (48 hour) and longer term (~20 days) drift in the $^{40}Ar_{IC0}/^{36}Ar_{IC2}$ ratio of air shots. Individual measurements encompass both the efficiency of IC2 relative to IC0, as well as mass fractionation as measured at the detectors. In the short-term, there is a drift on the order of hours, resulting in a somewhat high standard deviation of 0.75% for the average value over the 2 days of data collection; however, for the longer time span of about 20 days, the range of drift is considerably higher, and results in a standard deviation of 1.34% for the average value over the period of data collection. Furthermore, there are periods of days during the longer time span for which all data are consistently above or below the average long-term value. Thus both in the short and the long time span, a time dependent drift in ICF (encompassing both detector efficiency and mass fractionation for this example) is apparent between the two detectors. Whereas these data were collected under constant tuning conditions, any tuning of source or quadrupole lenses, or adjustment of ion counter plateau voltages will impact ICFs (e.g. Coble et al., 2011).

In the previous example, relative detector efficiency and mass fractionation were considered together, making it difficult to isolate which effect makes a greater contribution to the observed time-dependent drift. In Figure 8 the authors isolate these effects to compare drift in relative detector efficiency over time with drift in mass fractionation over the same period. To do this 100 air shots were measured over approximately three days, monitoring $^{40}Ar_{FAR}$, $^{40}Ar_{IC0}$ and $^{36}Ar_{IC0}$. The $^{40}Ar_{FAR}/^{40}Ar_{IC0}$ is a measure of the efficiency of the Faraday cup relative to IC0, whereas $^{40}Ar_{IC0}/^{36}Ar_{IC0}$ is a measure of mass fractionation in IC0. Although the relative standard deviation for ratios is similar (0.5% for $^{40}Ar_{FAR}/^{40}Ar_{IC0}$ versus 0.4% for $^{40}Ar_{IC0}/^{36}Ar_{IC0}$), the latter measurement is considerably less precise due to counting statistics of the small ^{36}Ar signal compared to ^{40}Ar in air. It is immediately clear from a visual inspection that there is far less time-dependent drift for IC0 mass fractionation than for FAR/IC0 relative efficiency. This observation follows the common observation for many single-collector noble gas machines that mass fractionation is found to exhibit little to no variation over a time scale of weeks to months and therefore need only be measured occasionally and adjusted rarely; however, it is expected that relative efficiency between detectors will show much more variability over the short and long term as observed here. This may be due to the more rapid deterioration in efficiency of ion counters relative

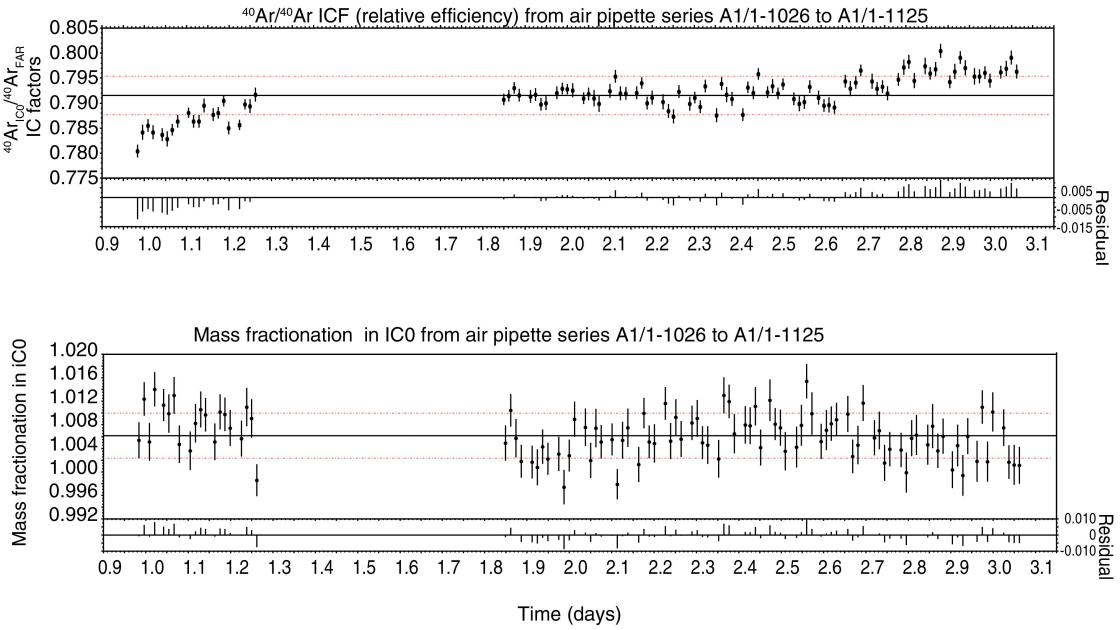

Figure 8. One hundred air shots analyzed over three days (A1/1-1026 to A1/1-1125); **a)** plot of relative efficiency between the Faraday collector and IC0 is plotted. The average value over the three days is shown with the solid black line, whereas the dashed red lines are the standard deviation at 0.5%. Note that Mass Spec software applies a multiplicative factor to the Faraday measurement for plotting purposes, thus the ratios are offset from the true efficiency by a constant. **b)** The mass fractionation determined from comparing measured $^{40}Ar/^{36}Ar$ in the IC0 detector relative to the accepted value of 298.56. Over the three days the standard deviation of the average value is at 0.4%.

to Faraday cups, differences in aging of the ion counters due to regularly responding to total accumulated counts (e.g. a dedicated detector for the typically very small ^{36}Ar signal), as well as effects of temperature, humidity, internal heating, etc. influencing efficiency in different collectors differently. Thus it is clear from this example that relative efficiency between detectors, particularly between the Faraday and IC0 detectors (across which the critical $^{40}Ar/^{39}Ar$ ratio may be measured), must be monitored on a relatively short time scale of hours, whereas mass fractionation varies little in time and though monitored regularly is not observed to change significantly in time, with the exception of minor shifts in response to tuning conditions and plateau voltages.

It is not practicable to independently determine efficiency and mass fractionation for each detector, as the tuning conditions and gas loads required for the exercise (measuring ^{40}Ar and ^{36}Ar in each detector) would deviate considerably from the conditions of data collection for unknowns (Coble et al., 2011), and the errors introduced in the multiple corrections would be highly undesirable (Turrin et al., 2010). Rather than independently measuring efficiency between each detector and mass fractionation at each detector, intercalibration factors (ICFs) are determined that capture either efficiency and/or mass fractionation in the detectors of interest, depending on the collector configuration. The ICFs are interpolated from periodic air shots, relative to the IC0 detector. Thus there are a maximum of three required ICF corrections to make, for FAR, IC1, and IC2, depending on the collector configuration used. These ICF corrections are detailed below as they are applied in the specific collection schemes described below.

With the particular cup configuration and tuning capabilities of the Noblesse at the Geological Survey of Canada (Fig. 3) there are three sampling routines best suited for $^{40}Ar/^{39}Ar$ age analysis: single collection (SC), multicollection for small ^{40}Ar signals (i.e. Phanerozoic samples, MC-Y), and multicollection for large ^{40}Ar signals (Precambrian samples, MC-O) (Table 4). A single routine for measurement of atmospheric Ar is used to determine ICFs for all three types of analyses. Baselines are considered to be implicit in the procedural blank correction, with the exception of the FAR baseline, which is prone to short-term drift and measured before and after each analysis. Procedural blank measurements mimic exactly the measurement scheme of gas analyses and typically bracket every four to six unknowns during an analytical session. Blanks are typically used to forward correct unknowns unless there is an obvious reason (e.g. a particularly large gas load in the analytical step proceeding the blank measurement) to interpolate or average bracketing blanks.

Table 4. Nu Instruments Limited Noblesse collector configurations used at the Geological Survey of Canada. Each row represents a change in axial mass (peak hop) during a single measurement cycle. For example, in single collection, five peak hops are conducted in each measurement cycle. Quad tuning 1: tuned for peak shape and alignment with ^{39}Ar in IC0. Quad tuning 2: tuned for peak shape and alignment with ^{40}Ar in IC0. SC = single collection, MC-Y = multicollection, young, MC-O = multicollection, old. All analyses terminate their current after 400 s.

	FAR (+1 amu)	IC0 (axial)	Count time (s)	IC1 (-2 amu)	IC2 (-3 amu)	Use	Quad tuning
SC		**^{40}Ar**	10			Typically Phanerozoic samples	1
		^{39}Ar	10				1
		^{38}Ar	10				1
		^{37}Ar	10				1
		^{36}Ar	10				1
MC-Y	**^{40}Ar**	**^{40}Ar**	10	**^{38}Ar**	^{37}Ar**	Phanerozoic samples	2
		^{39}Ar	12	**^{37}Ar**	**^{36}Ar**		1
MC-O	**^{40}Ar**	**^{39}Ar**	40	**^{37}Ar**	**^{36}Ar**	Typically PreCambrian samples	1
	^{39}Ar	**^{38}Ar**	3	*^{36}Ar*	^{35}Cl		1
Air		^{40}Ar	8	^{38}Ar	^{37}Ar	Inter-calibration of detectors	2
	^{40}Ar	^{39}Ar	12	^{37}Ar	^{36}Ar		1
	^{39}Ar	*^{38}Ar*	8	^{36}Ar	*^{35}Cl*		1
	^{37}Ar	^{36}Ar	8				2

Bold = used for data reduction and age calculation.
Normal = measured, but not used.
Italicized = not measured.
Underlined = data used to calculate intercalibration factors.
**Deflected away from collector using filter.

Single-collector scheme (SC)

This collection scheme is for young samples that yield sufficiently small ^{40}Ar signals for measurement on an ion counter (ideally $<1 \times 10^6$ cps per analysis, whether step heating or total fusion). All isotopes are measured in IC0 by peak hopping, using 'standard' quadrupole tuning 1, in which quadrapole lenses 1 and 2 are tuned to achieve optimal peak shape and alignment of Ar isotopes while ^{39}Ar occupies IC0. This data collection scheme requires no correction for collector efficiency, and mass fractionation is determined from $^{40}Ar_{IC0}/^{36}Ar_{IC0}$ measured with air shots (e.g. Fig. 8). By using a single collector, correction factors are simplified, but IC0 is subject to the undesirable analytical side effects of exposure to ^{37}Ar, and the data collection time is longer, thus the main advantages of multicollection are lost (Table 4).

Multicollector scheme for young samples (MC-Y)

The MC-Y scheme is used for young samples (typically Phanerozoic) or small gas loads for which ^{40}Ar is best measured in an ion counter, i.e. the Faraday cup is not used (Table 4). It comprises the same first two peak hops as the air analysis. To protect IC2 from implantation of ^{37}Ar atoms at the first mass position, the ^{37}Ar beam is deflected away from the collector by applying a voltage to the IC2 filter. The ICFs are determined for ^{37}Ar and ^{38}Ar in IC1 and ^{36}Ar in IC2 by using the $^{40}Ar_{IC0}/^{36}Ar_{IC1}$ and $^{40}Ar_{IC0}/^{36}Ar_{IC2}$ ratios measured in air. Quadrupole settings for ICFs are identical to quadrupole settings used for unknown measurements (*see* Table 4). These ICFs incorporate both relative efficiency and mass fractionation as described in 'Data collection and detector intercalibration corrections'. Since these effects are not isolated, it is not possible to isolate and calculate the true, per atomic mass unit mass fractionation value. Thus the mass fractionation component of the correction is slightly overestimated. For IC2 this method effectively applies a 4 amu mass fractionation factor determined from $^{40}Ar_{IC0}/^{36}Ar_{IC2}$ to the $^{36}Ar_{IC2}$ value when it is corrected against $^{39}Ar_{IC0}$, a 3 amu difference. Similarly, the $^{40}Ar_{IC0}/^{36}Ar_{IC1}$ ratio results in applying a 4 amu mass fractionation to the 2 amu difference between $^{37}Ar_{IC1}$ and $^{39}Ar_{IC0}$; however, since the mass fractionation factor is less than 1% (0.6% in the IC0 example of Fig. 8) this should have a negligible effect on the age of a sample, except perhaps in the case of very large Ca/K ratios (>100), for which the Ca correction on ^{39}Ar from ^{37}Ar is significant. The $^{40}Ar_{IC0}/^{39}Ar_{IC0}$ measurement is intentionally not corrected for mass fractionation. The mass fractionation correction would be applied to the ^{40}Ar/^{39}Ar ratio used to calculate both the sample and the J ratio, and if this correction is relatively constant, therefore cancels out in the age calculation. Since flux monitors are measured in an identical manner to unknowns, and since, as demonstrated above, the mass fractionation of the IC0 detector shows little to no variation with time, this correction and its uncertainty can be avoided (e.g. Brumm et al., 2010).

Multicollector scheme for old samples (MC-O)

This scheme uses a highly desirable configuration for ^{40}Ar/^{39}Ar analyses as ^{37}Ar and ^{36}Ar are measured on dedicated collectors, and all the main isotopes of interest are measured in a single analytical cycle. It is primarily used for Precambrian samples for which the ^{40}Ar signal is large compared to other signals. The main cycle measures ^{40}Ar in the Faraday cup, ^{39}Ar in IC0, ^{37}Ar in IC1, and ^{36}Ar in IC2 (Table 4). A second, brief cycle monitors Cl by measurement of ^{38}Ar in IC0 and ^{35}Cl in IC2. This measurement scheme takes full advantage of

Table 5. Typical measurements of reactor-induced correction factors.

Irradiation batch	Flux position	Cd-shielded	K-glass $(^{40}Ar/^{39}Ar)_K$	Crystran $(^{39}Ar/^{37}Ar)_{Ca}$	Crystran $(^{36}Ar/^{37}Ar)_{Ca}$	Reference
GSC RAD#66[a]	8A	No	0.058	0.000743	0.000258	
GSC RAD#63	5C	Yes	~0	0.000743	0.000277	
GSC RAD#57[b]	5C	No	0.026	0.000764	0.000228	
GSC RAD#55[b]	5C	Yes	0.0031	0.000945	0.000273	
	5C	No	No data	0.000739	0.000277	Ross and Sharp, 1988

a: GSC RAD#66 sample batch was irradiated in medium-flux site 8A. All other data in this table is for samples irradiated in high-flux site 5C of McMaster Nuclear Reactor.
b: Data from VG3600 prior to acquisition of Nu Noblesse, for comparison.

the multicollection capabilities of Noblesse. Intercalibration factors are determined for the Faraday, IC1, and IC2 detectors using the following measured air ratios: $^{40}Ar_{FAR}/^{40}Ar_{IC0}$, $^{40}Ar_{IC0}/^{36}Ar_{IC1}$, and $^{40}Ar_{IC0}/^{36}Ar_{IC2}$. The FAR/IC0 ICF is basically a relative efficiency correction determined by correcting the measured $^{40}Ar_{FAR}$ to equivalent counts per second of $^{40}Ar_{IC0}$ (or $^{40}Ar_{EqICO}$). As mentioned in 'Multicollector scheme for young samples (MC-Y)', traditionally the $^{40}Ar_{IC0}/^{39}Ar_{IC0}$ is corrected for mass fractionation; however, unknowns and J monitors are measured in an identical fashion for all irradiations such that any IC0 mass fractionation cancels out between the J monitors and unknowns. The IC0/IC1 ICF is determined using $^{40}Ar_{IC0}/^{36}Ar_{IC1}$, and the IC0/IC2 ICF is determined using $^{40}Ar_{IC0}/^{36}Ar_{IC2}$ as for MC-Y. This scheme requires that air-shot data are collected at four different mass stations (*see* Table 4). Drift of ICFs, particularly the FAR/IC0 ICF, occurs on the time scale of hours to days (Fig. 7) and is thus monitored by analyzing air shots periodically throughout each analytical session, approximately every tenth analysis.

Avoiding overpressure during analyses

Large gas loads resulting in large signal sizes can trip the ion counters during an analytical session, and over time can significantly decrease their lifespan. Large signals can also raise background to undesirable levels. Finally, very large gas loads appear to cause major deviations in measured gas composition from the actual gas composition, resulting in pressure-dependent mass fractionation (*see* 'Pressure-dependent fractionation'). For these reasons, it is desirable to limit measurement of signals to less than 160 mV in the Faraday collector and prevent inlet of signals more than 1×10^6 cps into the ion counters.

To ensure this, the signal intensity of a selected isotope is measured in the first seconds of inlet of gas into the mass spectrometer from the extraction line during each analysis. During an MC-O analysis, the largest signal, $^{40}Ar_{FAR,}$ is monitored and if its intensity exceeds 160 mV, an autoroutine is triggered to split the gas. Based on the authors' experiments of pressure-dependent fractionation, this should ensure that measurements are well below the threshold for pressure-dependent interferences at the source. The gas-splitting procedure is as follows: the manifold valve is closed, the mass spectrometer fraction of the gas is pumped away, and the extraction line portion of the gas (~20%) is then re-expanded into the mass spectrometer. This subroutine is repeated as many times as necessary to achieve an acceptable gas load as determined by measurement on the Faraday detector upon inlet to the mass spectrometer. The procedure followed for an MC-Y analysis is similar except that ^{40}Ar is placed briefly into the Faraday collector and the subroutine triggers if the inlet intensity for $^{40}Ar_{FAR}$ exceeds about 13 mV (~8×10^5 cps equivalent in IC0).

INTERFERING ISOTOPES AND REACTOR-INDUCED CORRECTION FACTORS (RCFS)

Irradiation of samples in the McMaster Nuclear Reactor causes several additional Ar-producing nuclear reactions, many of which are insignificant (*see* McDougall and Harrison (1999) for a complete list). Significant corrections include ^{40}Ar produced from irradiation of K and ^{36}Ar and ^{39}Ar produced from irradiation of Ca. To correct for these products, the following RCFs are determined for each irradiation: $(^{40}Ar/^{39}Ar)_K$, $(^{39}Ar/^{37}Ar)_{Ca}$, and $(^{36}Ar/^{37}Ar)_{Ca}$.

Reactor-induced K reactions

Each can sent to the McMaster reactor is loaded with a few crystals of zero-age, Ca-free K-glass. Using the unknown analysis routine and total fusion or step heating (depending on the length of the irradiation and the size of the crystals) with the CO_2 laser, ^{40}Ar, ^{39}Ar, and ^{36}Ar are measured and corrected for baseline, dead time, procedural blanks, and mass fractionation. The ^{40}Ar produced from K irradiation is calculated by:

$$(^{40}Ar/^{39}Ar)_K = (^{40}Ar_m - (^{36}Ar_m * 298.56))/^{39}Ar_m \quad (3)$$

where the subscript 'm' denotes the measured (corrected) intensities, and '$^{36}Ar_m$ * 298.56' yields the atmospheric ^{40}Ar component (McDougall and Harrison, 1999). Typically two or three measurements are made per irradiation. Typical corrections determined for irradiations with and without Cd shielding (which significantly reduces the amount of ^{40}Ar produced from K) are shown in Table 5.

Reactor-induced Ca reactions

Irradiation cans are also loaded with a few crystals of Crystran, a K-free CaF_2. Total fusion analyses, again with the CO_2 laser, are conducted and ^{40}Ar, ^{39}Ar, ^{37}Ar, and ^{36}Ar are measured and corrected for baseline, dead time, procedural blanks, and mass fractionation. The resulting $^{39}Ar_m/^{37}Ar_m$ yields the $(^{39}Ar/^{37}Ar)_{Ca}$ RCF. The ^{36}Ar produced from Ca irradiation is calculated by:

$$(^{36}Ar/^{37}Ar)_{Ca} = (^{36}Ar_m - (^{40}Ar_m/298.56))/^{37}Ar_m \quad (4)$$

where $^{40}Ar_m/298.56$ yields the atmospheric component of ^{36}Ar (McDougall and Harrison, 1999). As for the K-glass, two to three measurements are typically made per can and averaged. Table 5 shows typical RCFs for Ca. Uncertainties in reactor-induced correction factors are propagated into age calculations, but typically have a negligible influence on error in age.

$^{40}Ar/^{39}Ar$ GEOCHRONOLOGY

Measurement of flux monitors

Neutron flux gradients are determined by measurement of several age-appropriate standards (usually FCT-San for Phanerozoic samples and PP-20 for Precambrian samples) as flux monitors, which are interspersed among the sample packets throughout each tube in the six-tube sample canister, and interpolating an appropriate fit against calculated J-factor and sample position for each tube. For example, in Figure 9, a J flux gradient is determined for GSC irradiation Rad#66, tube E. In this example, FCT-San was used as the flux monitor. The J calculations were made for grains measured at positions 3 mm, 6 mm, 9 mm, 13 mm, 16 mm, 20 mm, 23 mm, 27 mm, and 33 mm. These data were used to apply a linear or parabolic best-fit regression (linear in this case) to the monitors, and the resulting J values and error in J are applied to unknowns. In addition to the flux monitors, secondary standards including

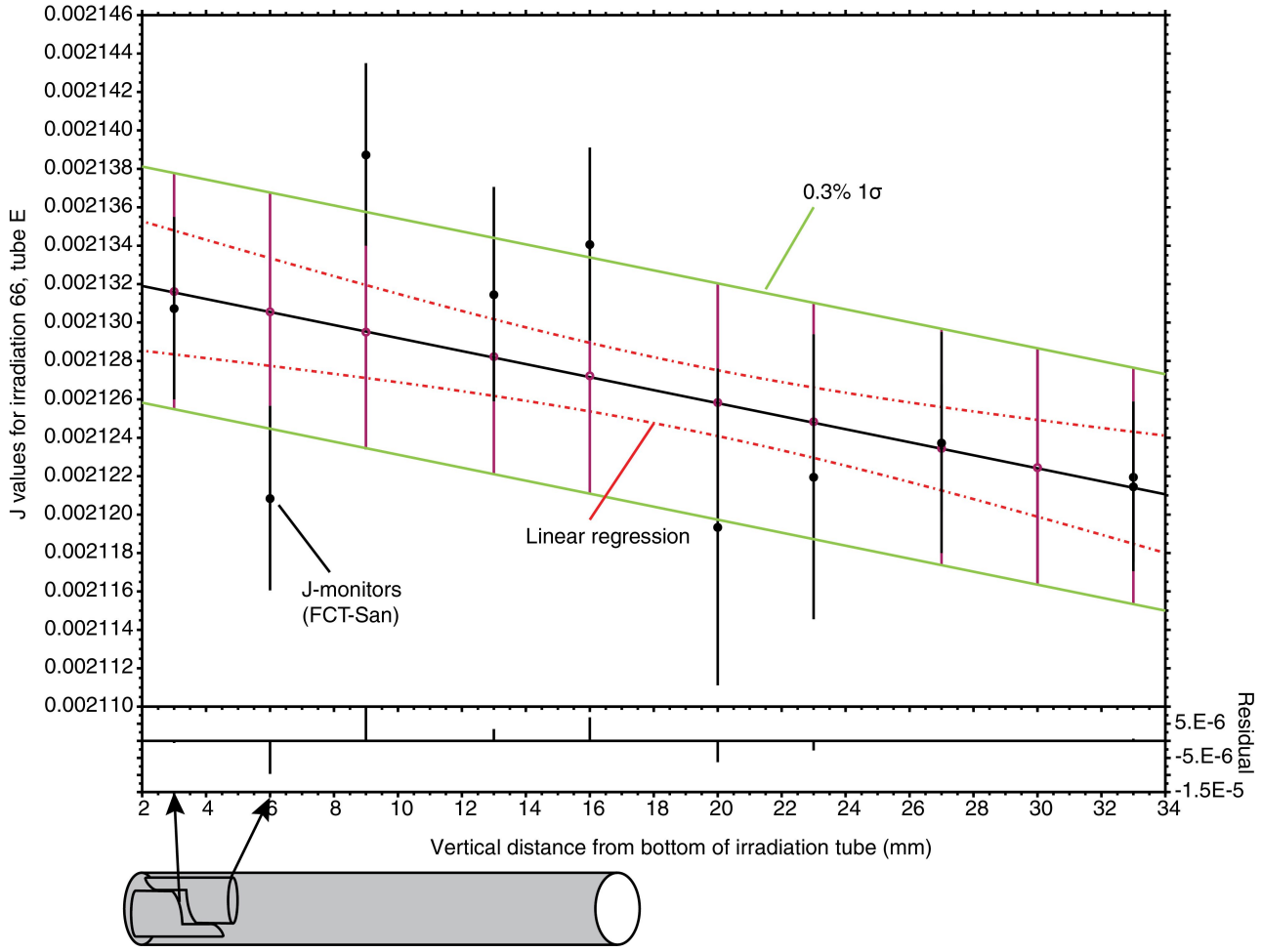

Figure 9. One-dimensional fit of J values in GSC irradiation Rad#66, tube E. The illustration shows how sample position is measured as a vertical distance from the bottom of the irradiation tube for each packet within the tube. Monitors, in this case FCT-San, are measured at several positions in the tube. Black dots and error bars are J values calculated from monitors. The red dashed lines show the 1σ error envelope for a linear regression through the monitor data. The green lines show the 1σ error envelope for a more conservative 0.6% 2σ error in J.

one or more of FCT-San (in Precambrian batches), PP-20 (in Phanerozoic batches), or GA-1550 biotite (98.5 ± 0.8 Ma (1σ); Spell and McDougall (2003); in either Precambrian or Phanerozoic batches) are also distributed through the sample packets and used to verify the resulting J values by treating them as unknowns and evaluating whether the resulting age is within error of the accepted age (e.g. Fig. 10). Although for some tubes, the best-fit regression through the monitors may be less than 0.2% 2σ, this is likely an underestimation of the error in J. A regression of ±0.6% (2σ) is more common, and results in a better match for secondary standard data. Thus the authors apply 0.6% 2σ as a conservative estimate of the error in J for all tubes where the best-fit results in an error less than 0.6% 2σ (as demonstrated in Fig. 9).

Measurement and calculation of age data

Data reduction and age calculations are performed using Mass Spec software version 7.93 and constants outlined in Table 6. Details regarding data reduction, error propagation, and age calculation are in Deino (2001). The software applies and propagates errors for all corrections, including ICFs, described above.

To apply ICFs to unknowns as described in 'Data collection', air shots are measured approximately each 10 analyses, and ICFs are interpolated between air shots. Interpolation can be done in a number of ways. In Figure 11, the IC0/IC2 ICFs from a number of air shots are used to interpolate the ICF for a step-heating analysis of a grain of GA-1550 reference material. Three different interpolations are applied: average, linear versus parabolic best-fit (linear provides the best fit in this case) and linear interpolation with smoothing. Whereas it can be argued that the linear regression underestimates the variability in ICF and hence error over the course of the experiment, all three options result in an identical result for both plateau and integrated age, demonstrating the relatively small impact on age of the error propagated from the ICF interpolation. Typically, the last option, linear interpolation with smoothing, is used to interpolate ICFs over the course of a step-heating experiment in order to capture the error in the individual ICF measurements as well as time-dependent drift in ICF that occurs on a time scale of hours (Fig. 7, 11).

Secondary standard age results

In Figure 10, secondary standard data from three irradiations analyzed during 2013 are presented. Analytical data are presented in Appendix tables A1, A2, and A3. The secondary standard which has been analyzed most frequently is FCT-San from irradiation batches Rad#64 and Rad#65 (Fig. 10a), irradiation times for which were optimized for Precambrian samples (960 MWH). Despite the fact that FCT-San was over-irradiated ($^{40}Ar/^{39}Ar$ was commonly <1), the weighted mean of integrated ages from 33 separate analyses (20 step-heating and 13 single-fusion runs) was 27.99 ± 0.18 Ma (2σ). These analyses were run using the MC-O scheme (*see* 'Multicollector scheme for old samples (MC-O)'), and the accurate age the authors are consistently able to obtain for FCT-San in static multicollection mode validates that instrument settings and detector intercalibrations, particularly between Far (^{40}Ar) and IC0 (^{39}Ar), are appropriate for the analysis of unknowns.

Secondary standards that are included in younger sample batches, such as GA-1550 biotite and PP-20 hornblende from Rad#66 (160 MWH), were analyzed using the MC-Y scheme (*see* 'Multicollector scheme for young samples (MC-Y)'). Figure 10b shows the weighted mean of integrated ages for six step-heated grains of GA-1550 biotite (98.4 ± 1.1 Ma, 2σ). Note that two additional analyses were statistically rejected from the weighted mean (>1.5 nMADs from median age (MAD = mean absolute deviation)). One is slightly young, but overlaps at the 2σ level with the accepted age for GA-1550. The other is clearly too old, possibly indicating a spurious grain, or contamination of that sample pit. No analytical issues could be identified for that data. The PP-20 hornblende, although significantly under-irradiated ($^{40}Ar/^{39}Ar$ was ~400), yielded a weighted mean of integrated step-heating ages of 1062 ± 10 Ma (n = 4, 2σ, Fig. 10c). This age is slightly younger than but overlaps within the 2σ error of the accepted age for PP20 of 1074 ± 10 Ma. Whereas both secondary standard data sets are small, the age reproducibility illustrates that the present MC-Y analytical approach is suitable for the analysis of young unknowns. With future irradiations of sample batches this secondary standard data set will be further expanded to larger n, and also will include analyses of other available age reference material.

ACKNOWLEDGMENTS

This work would not have been possible without the years of dedication and the vision of M. Villeneuve in the GSC Noble Gas Laboratory. Full automation of the lab and refinement of the analytical methods were achieved with the assistance of many. T. Pestaj from the GSC SHRIMP II Lab is thanked for his wizardry with wiring and pneumatic systems. The authors are grateful to M. Carisse and R. Martin from CANMET Engineering and Technical Services for always coming through on seemingly endless electrical and machine shop requests; the authors appreciate their creativity, cheerfulness, and high standard for quality workmanship. T. Becker from Berkeley Geochronology Center is acknowledged for providing automated air pipettes and useful advice. A. Deino from Berkeley Geochronology Center is thanked for installing Mass Spec and assisting and advising in the integration of hardware and software components. J. Saxton from Nu Instruments and J. Roy and S. Pinkham from Photon Machines, Inc. provided excellent advice and assistance throughout the automation process. Laboratory methods and protocols were determined after countless hours of isotopic analyses, experimentation, and data manipulation and analysis, with the assistance of E. Knight and numerous student assistants with infinite patience. B. Davis is thanked for many fruitful discussions and for a thoughtful review that helped to improve this manuscript.

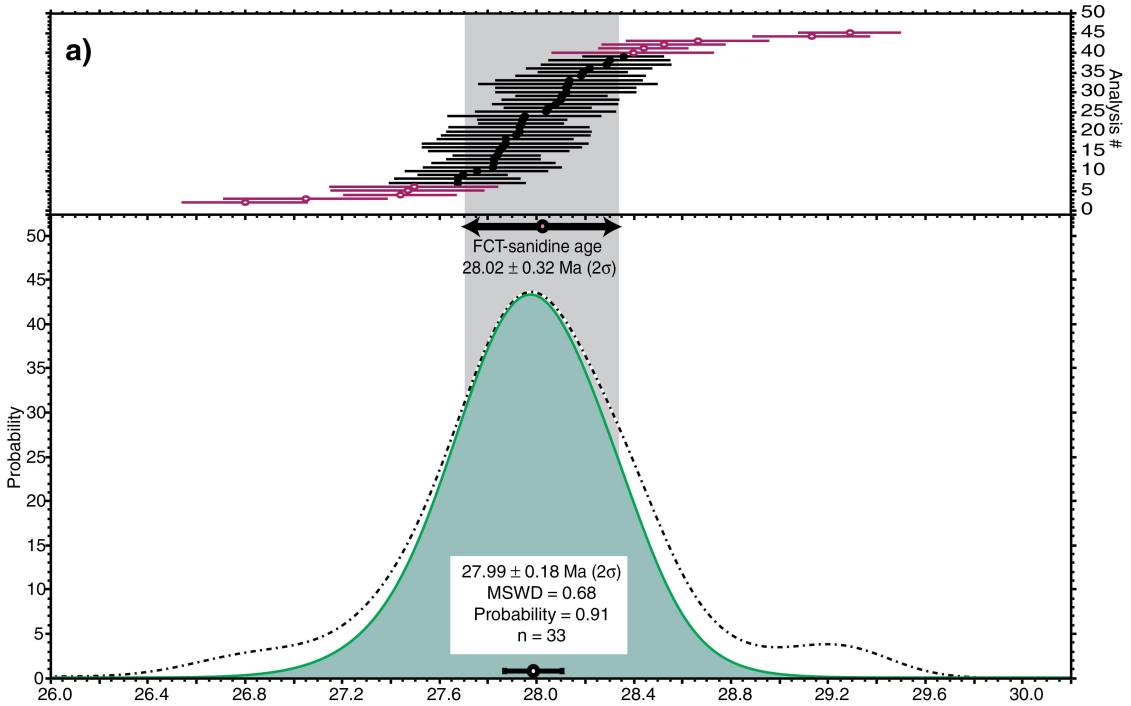

Figure 10. Secondary standard data; error bars and values reported are all 2σ. **a)** The probability distribution of integrated ages for FCT-San analyses from Precambrian irradiation batches Rad#64 and Rad#65 is shown. The weighted mean age of 27.99 ± 0.18 Ma falls within the accepted age of 28.02 ± 0.3 Ma for FCT-San from Renne et al. (1998). The dotted line shows the trend of the probability curve should the outlier data points in purple be included.

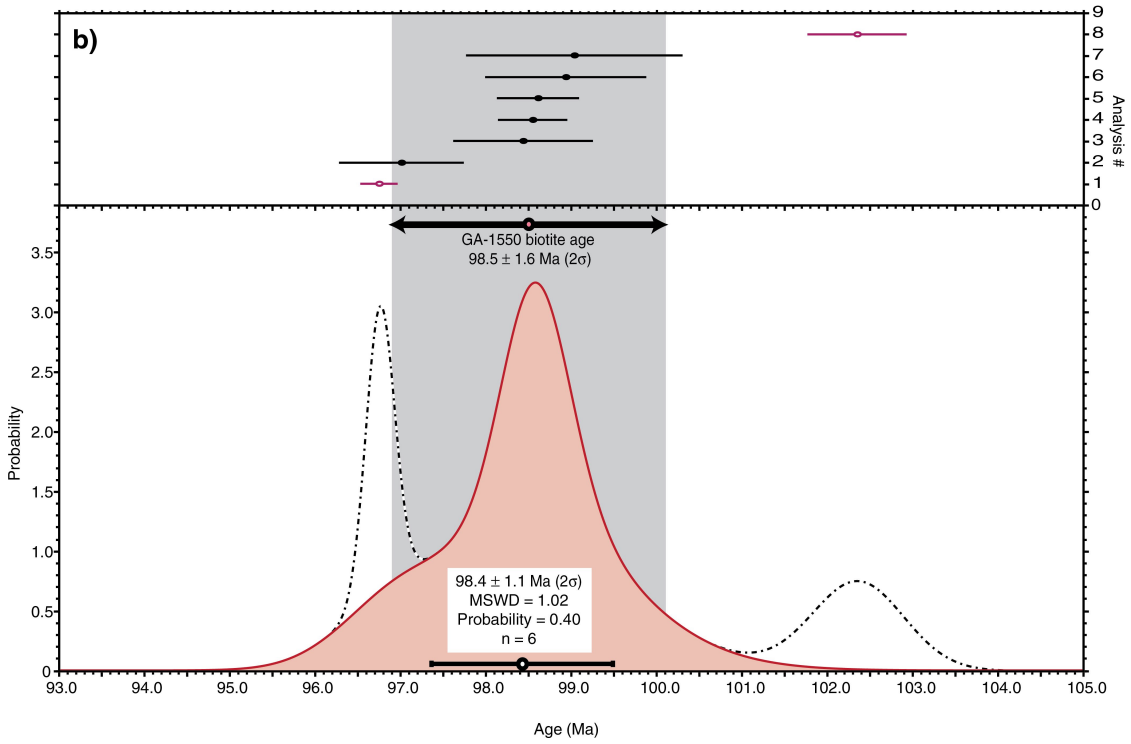

Figure 10. (Continued) Secondary standard data; error bars and values reported are all 2σ. The probability curves for analyses of **b)** GA-1550 biotite and **c)** PP-20 hornblende are shown, respectively. Both the GA-1550 and PP-20 were from Phanerozoic irradiation batch Rad#66. *See* text for discussion of data.

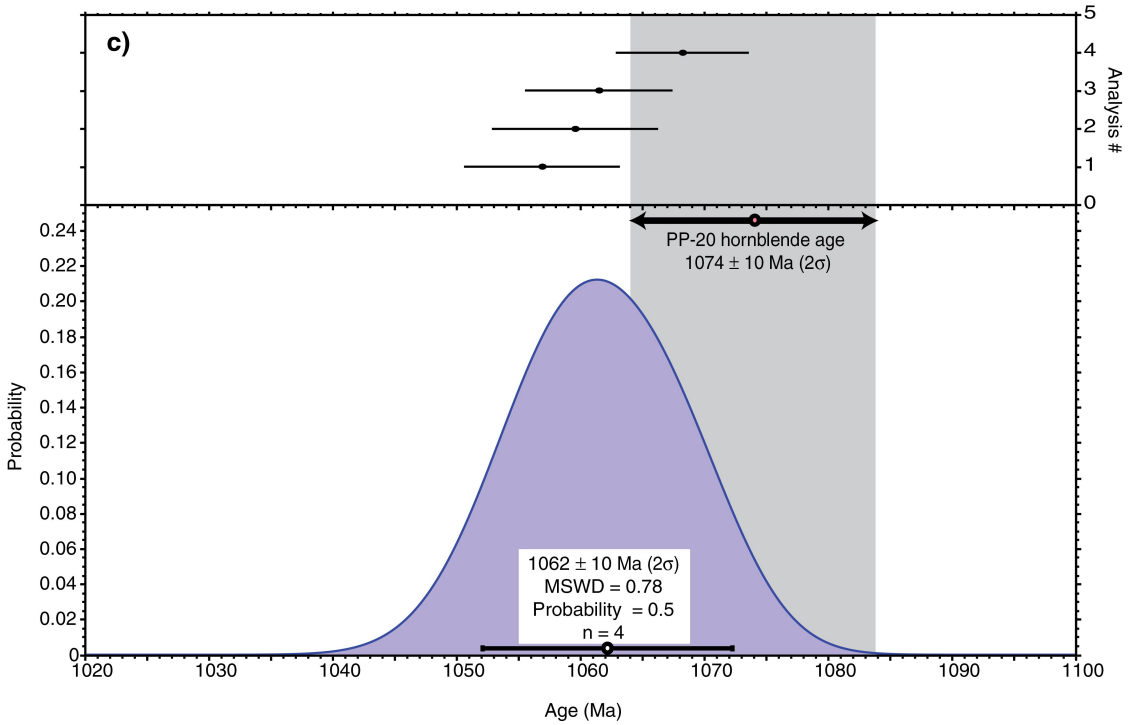

Figure 10. (Continued) Secondary standard data; error bars and values reported are all 2σ. The probability curves for analyses of **b)** GA-1550 biotite and **c)** PP-20 hornblende are shown, respectively. Both the GA-1550 and PP-20 were from Phanerozoic irradiation batch Rad#66. *See* text for discussion of data.

Table 6. Constants used for data reduction at the Geological Survey of Canada.

Constants used	Source
Atmospheric argon ratios	
$(^{40}Ar/^{36}Ar)_A = 298.56 \pm 0.31$	Lee et al., 2006
$(^{40}Ar/^{38}Ar)_A = 0.1885 \pm 0.0003$	Lee et al., 2006
Decay constants	
$^{40}K\ \lambda_\varepsilon$ $5.81e^{-11} \pm 1.70e^{-12}\ a^{-1}$	Steiger and Jäger, 1977
$^{40}K\ \lambda_\beta$ $4.962e^{-10} \pm 8.60e^{-12}\ a^{-1}$	Steiger and Jäger, 1977
^{39}Ar $2.58e^{-3} \pm 0.00003\ a^{-1}$	Stoenner et al., 1965
^{37}Ar $7.2088 \pm 0.02\ a^{-1}$	Stoenner et al., 1965
$^{36}Cl\ \lambda_\beta$ $2.30e^{-6}\ a^{-1}$	McDougall and Harrison, 1999

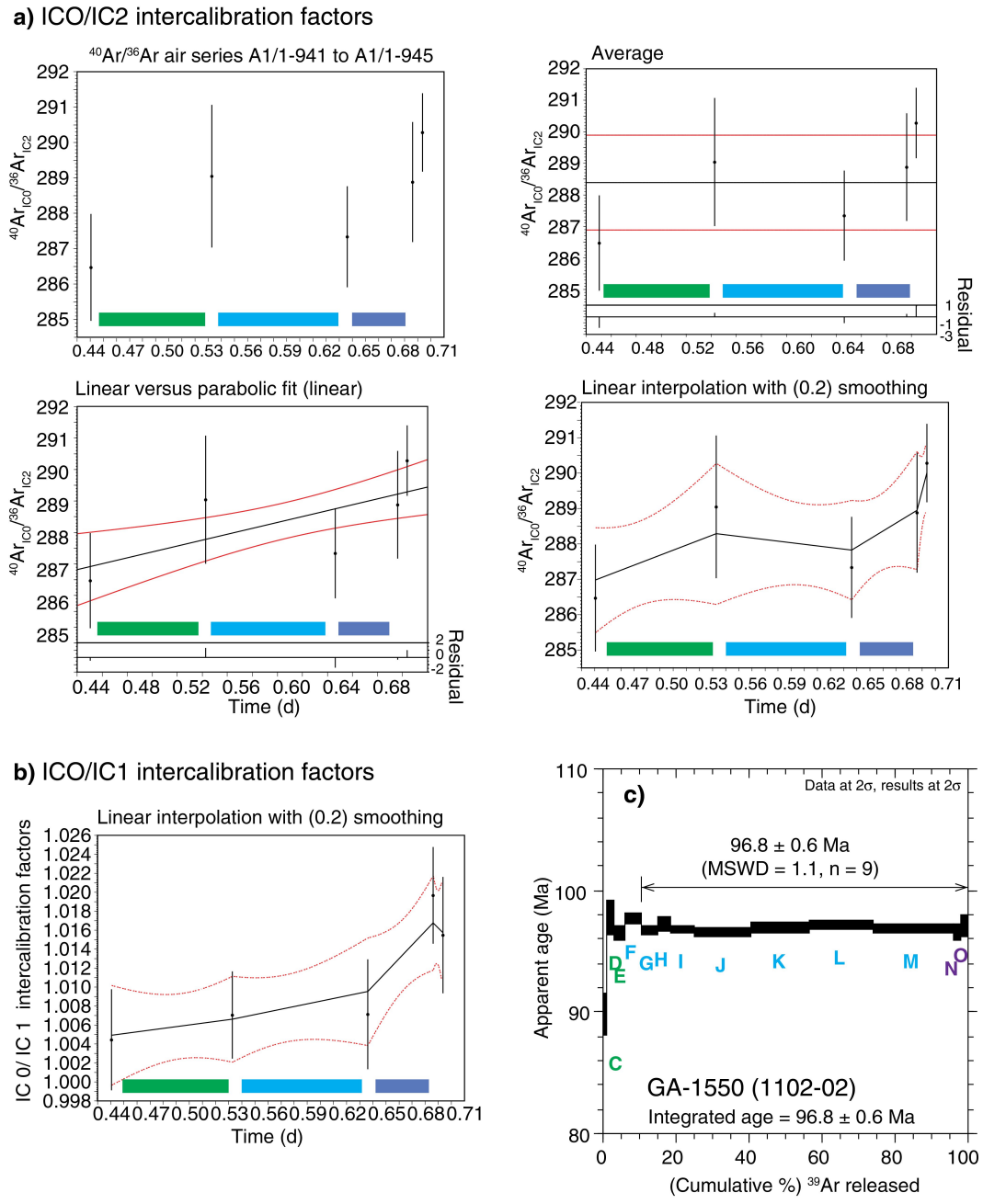

Figure 11. Interpolation of intercalibration factors (ICFs). **a)** The ICFs are determined for IC0/IC2 based on air measurements of $^{40}Ar_{IC0}/^{36}Ar_{IC2}$. Step heating of GA-1550 occurred in the intervals shown with the coloured bars: steps A–E during the green interval, steps F–M during the blue interval and steps N-Q during the purple interval. Error bars for data and regressions are 1σ in Figures 11a and 11b, and 2σ in 11c. Three different approaches to interpolation are shown: average; linear versus parabolic; and; linear interpolation with smoothing. The error envelopes for each fit are propagated into the error for the corrected isotopes and ultimately into the age equation. **b)** The ICFs for IC0/IC1 based on air measurements of $^{40}Ar_{IC0}/^{36}Ar_{IC1}$ with a linear interpolation with smoothing. **c)** The resulting step-heat Ar release spectrum for the grain of GA-1550 biotite. Regardless of the type of fit used for ICF interpolation, there is no change to the resulting age or error in age in this example. Only heating steps comprising more than 1% of total ^{39}Ar released were included in the integrated and plateau age calculations.

REFERENCES

Brumm, A., Jensen, G.M., van den Bergh, G.D., Morwood, M.J., Kurniawan, I., Aziz, F., and Storey, M., 2010. Hominins on Flores, Indonesia, by one million years ago; Nature, v. 464, p. 748–752. doi:10.1038/nature08844

Coble, M.A., Grove, M., and Calvert, A.T., 2011. Calibration of Nu-Instruments Noblesse multicollector mass spectrometers for argon isotopic measurements using a newly developed reference gas; Chemical Geology, v. 290, p. 75–87. doi:10.1016/j.chemgeo.2011.09.003

Cosca, M., 2007. $^{40}Ar/^{39}Ar$ geochronology by multicollector mass spectrometry; EOS Transactions of the American Geophysical Union, v. 88, Fall Meet Supplement, Abstract V32B-05.

Dazé, A., Lee, J.K.W., and Villeneuve, M., 2003. An intercalibration study of the Fish Canyon sanidine and biotite $^{40}Ar/^{39}Ar$ standards and some comments on the age of the Fish Canyon Tuff; Chemical Geology, v. 199, p. 111–127. doi:10.1016/S0009-2541(03)00079-2

Deer, W.A., Howie, R.A., and Zussman, J., 1992. An Introduction to the Rock-Forming Minerals; Pearson Education Limited, Harlow, London, United Kingdom, 696 p.

Deino, A.L., 2001. Users manual for Mass Spec v. 5.02; Berkeley Geochronology Center, Special Publication 1a, Berkeley Geochronology Center, Berkley, California, 119 p.

Fahey, A.J., 1998. Measurements of dead time and characterization of ion counting systems for mass spectrometry; The Review of Scientific Instruments, v. 69, p. 1282–1288. doi:10.1063/1.1148796

Jourdan, F., Verati, C., and Féraud, G., 2006. Intercalibration of the Hb3gr $^{40}Ar/^{39}Ar$ dating standard; Chemical Geology, v. 231, p. 177–189. doi:10.1016/j.chemgeo.2006.01.027

Lee, J.-Y., Marti, K., Severinghaus, J.P., Kawamura, K., Yoo, H.-S., Lee, J.B., and Kim, J.S., 2006. A redetermination of the isotopic abundances of atmospheric Ar; Geochimica et Cosmochimica Acta, v. 70, p. 4507–4512. doi:10.1016/j.gca.2006.06.1563

Mark, D.F., Barfod, D., Stuart, F.M., and Imlach, J., 2009. The ARGUS multicollector noble gas mass spectrometer: performance for $^{40}Ar/^{39}Ar$ geochronology; Geochemistry, Geophysics, Geosystems, v. 10, 9 p. doi:10.1029/2009GC002643

Mark, D.F., Stuart, F.M., and de Podesta, M., 2011. New high-precision measurements of the isotopic composition of atmospheric argon; Geochimica et Cosmochimica Acta, v. 75, p. 7494–7501. doi:10.1016/j.gca.2011.09.042

Marrocchi, Y., Burnard, P.G., Hamilton, D., Colin, A., Pujol, M., Zimmermann, L., and Marty, B., 2009. Neon isotopic measurements using high-resolution, multicollector noble gas mass spectrometer: HELIX-MC; Geochemistry, Geophysics, Geosystems, v. 10, 8 p. doi:10.1029/2008GC002339

McDougall, I. and Harrison, T.M., 1999. Geochronology and Thermochronology by the $^{40}Ar/^{39}Ar$ Method; Oxford University Press, New York, New York, 269 p. (second edition).

Nelms, S.M., Quetel, C.R., Prohaska, T., Vogl, J., and Taylor, P.D.P., 2001. Evaluation of detector dead time calculation models for ICP-MS; Journal of Analytical Atomic Spectrometry, v. 16, p. 333–338. doi:10.1039/b007913h

Renne, P.R., Swisher, C.C., Deino, A.L., Karner, D.B., Owens, T.L., and DePaolo, D.J., 1998. Intercalibration of standards, absolute ages and uncertainties in $^{40}Ar/^{39}Ar$ dating; Chemical Geology, v. 145, p. 117–152. doi:10.1016/S0009-2541(97)00159-9

Richter, S., Goldberg, S.A., Mason, P.B., Traina, A.J., and Schwieters, J.B., 2001. Linearity tests for secondary electron multipliers used in isotope ratio mass spectrometry; International Journal of Mass Spectrometry, v. 206, p. 105–127. doi:10.1016/S1387-3806(00)00395-X

Ross, J.A. and Sharp, W.D., 1988. The effects of sub-blocking temperature metamorphism on the K/Ar systematics of hornblendes: $^{40}Ar/^{39}Ar$ dating of polymetamorphic garnet amphibolite from the Franciscan Complex, California; Contributions to Mineralogy and Petrology, v. 100, p. 213–221. doi:10.1007/BF00373587

Spell, T.L. and McDougall, I., 2003. Characterization and calibration of $^{40}Ar/^{39}Ar$ dating standards; Chemical Geology, v. 198, p. 189–211. doi:10.1016/S0009-2541(03)00005-6

Steiger, R.H. and Jäger, E., 1977. Subcommission on geochronology: convention on the use of decay constants in geo- and cosmochronology; Earth and Planetary Science Letters, v. 36, p. 359–362. doi:10.1016/0012-821X(77)90060-7

Stoenner, R.W., Schaeffer, O.A., and Katcoff, S., 1965. Half-lives of argon-37, argon-39, and argon-42; Science, v. 148, p. 1325–1328. doi:10.1126/science.148.3675.1325

Turrin, B.D., Swisher III, C.C., and Deino, A.L., 2010. Mass discrimination monitoring and intercalibration of dual collectors in noble gas mass spectrometer systems; Geochemistry, Geophysics, Geosystems, v. 11, 20 p. doi:10.1029/2009GC003013

Villeneuve, M.E. and MacIntyre, D.G., 1997. Laser $^{40}Ar/^{39}Ar$ ages of the Babine porphyries and Newman Volcanics, Fulton Lake map area, west-central British Columbia; *in* Radiogenic Age and Isotopic Studies: Report 10; Geological Survey of Canada, Current Research 1997-F, p. 131–139.

Geological Survey of Canada Project 33040INU62

Appendix A

Table A1. Analytical data for Fish Canyon Tuff sanidine secondary standards from irradiation batches #64 and #65.

Lab ID#[b]	Sample	Material	Watts	Irrad.[c]	J (x 10^{-3}) ± 1σ		Relative isotopic abundances[a]										Background relative isotopic abundances										Derived results								w/±J ±1σ
							^{40}Ar ±1σ		^{39}Ar ±1σ		^{38}Ar ±1σ		^{37}Ar ±1σ		^{36}Ar ±1σ		^{40}Ar Bkgd ±1σ		^{39}Ar Bkgd ±1σ		^{38}Ar Bkgd ±1σ		^{37}Ar Bkgd ±1σ		^{36}Ar Bkgd ±1σ		^{39}Ar Mol x 10^{-14}	^{39}Ar % of total	%(^{36}Ar)$_{Ca}$	Ca/K ±1σ		%^{40}Ar*	Age (Ma) ±1σ		
1009-01A	FCT-San	SAN	1.0	64b	21.454	0.034	1742290.0	6222.8	2373105.0	673.4	28001.5	202.1	2617.2	17.0	33.72	14.61	949.0	360.0	52.7	1.3	99.2	6.9	421.6	1.9	137.40	1.80	8.37	75.8	12.7	0.013	0.000	99.5	27.92	0.16	0.16
1009-01B	FCT-San	SAN	1.5	64b	21.454	0.034	553614.7	1951.9	756784.9	176.2	8974.4	63.3	839.3	4.1	17.67	3.55	949.0	360.0	52.7	1.3	99.2	6.9	421.6	1.9	137.44	1.80	2.67	24.2	7.8	0.013	0.000	99.1	27.72	0.15	0.15
1007-01A	*FCT-San*	*SAN*	*0.6*	*64b*	*21.410*	*0.054*	*1138877.0*	*4368.7*	*1561350.0*	*471.4*	*18492.6*	*293.9*	*1678.5*	*17.9*	*98.69*	*15.51*	*949.0*	*360.0*	*52.7*	*1.3*	*99.2*	*6.9*	*421.6*	*1.9*	*137.40*	*1.80*	*5.51*	*40.4*	*2.8*	*0.012*	*0.000*	*97.5*	*27.13*	*0.18*	*0.19*
1007-01B	*FCT-San*	*SAN*	*1.5*	*64b*	*21.410*	*0.054*	*1681084.0*	*6055.8*	*2305173.0*	*734.7*	*26507.7*	*281.7*	*2470.3*	*20.4*	*27.56*	*16.42*	*949.0*	*360.0*	*52.7*	*1.3*	*99.2*	*6.9*	*421.6*	*1.9*	*137.40*	*1.80*	*8.13*	*59.6*	*14.7*	*0.012*	*0.000*	*99.6*	*27.70*	*0.16*	*0.17*
1011-01A	FCT-San	SAN	0.4	64b	21.494	0.054	42634.1	576.7	52811.7	46.6	686.0	25.0	88.7	3.7	13.00	3.37	5098.0	340.0	43.0	1.0	109.6	7.3	428.9	1.8	129.46	1.70	0.19	0.9	1.2	0.020	0.001	91.0	28.14	0.84	0.85
1011-01B	FCT-San	SAN	0.5	64b	21.494	0.054	67925.0	562.0	95217.9	57.9	1093.0	32.3	93.6	3.3	0.00	2.78	5098.0	340.0	43.0	1.0	109.6	7.3	428.9	1.8	129.46	1.70	0.34	1.6	0.0	0.012	0.000	101.2	27.64	0.41	0.42
1011-01C	FCT-San	SAN	1.0	64b	21.494	0.054	1361050.0	5931.7	1886186.0	544.9	22527.7	171.6	1947.8	17.6	28.66	13.60	5098.0	340.0	43.0	1.0	109.6	7.3	428.9	1.8	129.50	1.70	6.65	32.3	11.6	0.012	0.000	99.5	27.48	0.17	0.19
1011-01D	FCT-San	SAN	4.0	64b	21.494	0.054	2778254.0	11556.8	3800405.0	734.7	44378.3	263.4	4003.8	21.9	83.26	13.78	5098.0	340.0	43.0	1.0	109.6	7.3	428.9	1.8	129.50	1.70	13.41	65.1	8.2	0.013	0.000	99.2	27.77	0.16	0.17
1031-01A	FCT-San	SAN	0.5	64e	23.287	0.046	1962671.0	8082.4	2885612.0	795.9	36340.5	569.4	3053.1	20.6	73.36	13.01	3109.0	380.0	41.3	1.1	101.9	2.8	424.7	2.0	123.10	1.50	10.18	53.9	7.1	0.013	0.000	99.0	27.92	0.17	0.17
1031-01B	FCT-San	SAN	0.8	64e	23.287	0.046	368405.2	1576.2	542983.0	138.5	6536.1	70.6	560.4	4.3	12.01	2.95	3109.0	380.0	41.3	1.1	101.9	2.8	424.7	2.0	123.09	1.50	1.92	10.1	8.0	0.012	0.000	99.1	27.89	0.17	0.18
1031-01C	FCT-San	SAN	1.0	64e	23.287	0.046	346218.5	1499.2	510794.3	138.5	5920.3	81.9	530.8	4.3	6.66	3.03	3109.0	380.0	41.3	1.1	101.9	2.8	424.7	2.0	123.09	1.50	1.80	9.5	13.6	0.012	0.000	99.5	27.97	0.18	0.18
1031-01D	FCT-San	SAN	1.3	64e	23.287	0.046	394405.4	1663.9	582945.0	176.2	6881.9	49.2	586.3	4.3	13.97	3.05	3109.0	380.0	41.3	1.1	101.9	2.8	424.7	2.0	123.09	1.50	2.06	10.9	7.2	0.012	0.000	99.0	27.79	0.17	0.18
1031-01E	FCT-San	SAN	4.0	64e	23.287	0.046	563403.4	2324.8	830177.8	226.6	9726.7	54.8	839.0	4.9	13.00	3.24	4631.0	350.0	52.1	2.0	124.4	8.6	421.6	2.1	123.22	1.70	2.93	15.5	11.0	0.012	0.000	99.4	27.98	0.16	0.17
1001-01A	FCT-San	SAN	0.4	64a	21.994	0.072	1944779.0	8049.9	2686257.0	734.7	31588.5	165.5	2701.0	18.7	83.73	11.48	4631.0	350.0	52.1	2.0	124.4	8.6	421.6	2.1	123.20	1.70	9.48	56.0	5.5	0.012	0.000	98.8	28.02	0.16	0.18
1001-01B	FCT-San	SAN	0.8	64a	21.994	0.072	671853.8	2743.1	930524.2	239.2	10942.1	37.5	885.7	4.8	2.09	3.02	4631.0	350.0	52.1	2.0	124.4	8.6	421.6	2.1	123.22	1.70	3.28	19.4	72.3	0.011	0.000	100.0	28.28	0.16	0.18
1001-01C	FCT-San	SAN	1.0	64a	21.994	0.072	550972.4	2274.9	763014.5	188.8	8889.1	31.4	712.1	4.8	15.39	3.06	4631.0	350.0	52.1	2.0	124.4	8.6	421.6	2.1	123.22	1.70	2.69	15.9	7.9	0.011	0.000	99.2	28.08	0.16	0.18
1001-01D	FCT-San	SAN	1.3	64a	21.994	0.072	188049.6	925.0	259656.3	102.0	2807.6	68.5	244.1	3.8	2.84	3.12	4631.0	350.0	52.1	2.0	124.4	8.6	421.6	2.1	123.22	1.70	0.92	5.4	14.7	0.011	0.000	99.6	28.27	0.22	0.24
1001-01E	FCT-San	SAN	4.0	64a	21.994	0.072	126581.4	677.8	161254.7	69.3	1943.6	29.3	149.0	3.4	21.62	3.05	2754.0	330.0	47.9	1.7	118.8	9.7	421.6	1.9	123.85	1.80	0.57	3.4	1.2	0.011	0.000	95.0	29.20	0.29	0.31
1003-01A	FCT-San	SAN	0.4	64a	21.793	0.045	1496435.0	6254.6	2060942.0	673.4	24325.2	165.4	2199.9	18.1	39.77	12.25	2446.0	350.0	47.6	1.3	89.6	4.4	423.2	1.8	118.10	1.70	7.27	57.7	9.5	0.013	0.000	99.3	27.99	0.17	0.18
1003-01B	FCT-San	SAN	0.8	64a	21.793	0.045	417657.3	1740.4	579017.0	163.7	6810.1	46.8	570.6	4.0	6.09	2.92	2446.0	350.0	47.7	1.3	89.6	4.4	423.2	1.8	118.11	1.70	2.04	16.2	16.0	0.012	0.000	99.6	27.91	0.16	0.17
1003-01C	FCT-San	SAN	1.0	64a	21.793	0.045	336929.1	1430.2	464648.3	138.5	5412.2	53.1	466.2	4.0	0.93	2.82	2446.0	350.0	47.7	1.3	89.6	4.4	423.2	1.8	118.11	1.70	1.64	13.0	85.6	0.012	0.000	100.0	28.15	0.17	0.18
1003-01D	FCT-San	SAN	1.3	64a	21.793	0.045	262729.5	1155.5	362394.8	112.0	4238.4	24.3	368.6	3.9	10.06	2.93	2446.0	350.0	47.7	1.3	89.6	4.4	423.2	1.8	118.11	1.70	1.28	10.1	6.3	0.012	0.000	98.9	27.85	0.18	0.19
1003-01E	FCT-San	SAN	4.0	64a	21.793	0.045	73461.6	559.6	103446.5	51.6	1221.6	33.7	99.1	3.2	6.14	2.67	6075.0	310.0	48.8	1.6	74.8	12.0	420.0	2.0	118.83	1.70	0.36	2.9	2.8	0.012	0.000	97.6	26.91	0.38	0.38
1005-01A	*FCT-San*	*SAN*	*0.4*	*64a*	*21.693*	*0.060*	*666016.3*	*2701.8*	*897556.5*	*188.8*	*11036.8*	*80.2*	*833.1*	*4.7*	*21.56*	*2.97*	*6075.0*	*310.0*	*48.8*	*1.6*	*74.8*	*12.0*	*420.0*	*2.0*	*118.83*	*1.70*	*3.17*	*64.4*	*6.6*	*0.011*	*0.000*	*99.1*	*28.42*	*0.16*	*0.17*
1005-01B	*FCT-San*	*SAN*	*0.8*	*64a*	*21.693*	*0.060*	*118358.4*	*696.2*	*161086.2*	*71.8*	*1946.6*	*25.6*	*139.2*	*3.4*	*4.21*	*3.01*	*6075.0*	*310.0*	*48.8*	*1.6*	*74.8*	*12.0*	*420.0*	*2.0*	*118.83*	*1.70*	*0.57*	*11.6*	*5.7*	*0.010*	*0.000*	*99.0*	*28.11*	*0.29*	*0.30*
1005-01C	*FCT-San*	*SAN*	*1.0*	*64a*	*21.693*	*0.060*	*66071.4*	*549.9*	*94439.4*	*52.9*	*1142.5*	*32.5*	*80.3*	*3.3*	*1.38*	*2.91*	*6075.0*	*310.0*	*48.8*	*1.6*	*74.8*	*12.0*	*420.0*	*2.0*	*118.83*	*1.70*	*0.33*	*6.8*	*10.0*	*0.010*	*0.000*	*99.4*	*26.89*	*0.43*	*0.44*
1005-01D	*FCT-San*	*SAN*	*1.3*	*64a*	*21.693*	*0.060*	*166446.5*	*821.2*	*221420.5*	*80.6*	*2614.9*	*30.7*	*192.3*	*3.7*	*1.81*	*2.97*	*2476.0*	*360.0*	*48.8*	*1.7*	*96.5*	*5.6*	*421.2*	*1.9*	*118.36*	*1.80*	*0.78*	*15.9*	*18.2*	*0.010*	*0.000*	*99.7*	*28.97*	*0.23*	*0.24*
1005-01E	*FCT-San*	*SAN*	*4.0*	*64a*	*21.693*	*0.060*	*15075.2*	*489.4*	*18743.7*	*22.7*	*230.5*	*28.3*	*9.4*	*3.2*	*0.60*	*2.79*	*2476.0*	*360.0*	*48.8*	*1.7*	*96.5*	*5.6*	*421.2*	*1.9*	*118.36*	*1.80*	*0.07*	*1.3*	*2.7*	*0.006*	*0.002*	*98.9*	*30.72*	*1.99*	*1.99*
1013-01A	FCT-San	SAN	0.4	64c	22.178	0.050	432885.5	1794.0	614367.7	151.1	7287.9	90.8	732.4	4.7	10.96	3.08	2476.0	360.0	48.8	1.7	96.5	5.6	421.2	1.9	118.36	1.80	2.17	23.6	11.4	0.014	0.000	99.3	27.65	0.16	0.17
1013-01B	FCT-San	SAN	0.8	64c	22.178	0.050	163182.9	814.7	234238.1	95.7	2707.9	29.5	271.3	3.6	2.90	3.06	2476.0	360.0	48.8	1.7	96.5	5.6	421.2	1.9	118.36	1.80	0.83	9.0	16.0	0.014	0.000	99.6	27.40	0.23	0.24
1013-01C	FCT-San	SAN	1.0	64c	22.178	0.050	38799.4	543.6	52438.5	37.8	650.3	25.6	59.8	3.2	0.00	2.54	2409.0	370.0	53.6	1.8	76.3	4.5	419.6	1.8	119.49	1.40	0.19	2.0	0.0	0.014	0.001	103.5	30.25	0.71	0.71
1013-01D	FCT-San	SAN	1.3	64c	22.178	0.050	37816.3	504.9	52943.6	36.6	640.8	18.2	60.2	3.1	1.68	2.94	2409.0	370.0	53.6	1.8	76.3	4.5	419.6	1.8	119.49	1.40	0.19	2.0	6.2	0.014	0.001	98.8	27.87	0.76	0.76
1013-01E	FCT-San	SAN	4.0	64c	22.178	0.050	1166556.0	4984.4	1650466.0	538.8	19260.9	214.3	1901.1	19.3	0.00	10.46	2409.0	370.0	53.6	1.8	76.3	4.5	419.6	1.8	119.50	1.40	5.82	63.4	0.0	0.014	0.000	100.4	28.03	0.17	0.18
1015-01A	FCT-San	SAN	0.4	64c	22.210	0.050	466692.2	1925.0	664849.0	176.2	7823.4	41.8	709.1	4.5	16.24	2.98	2409.0	370.0	53.6	1.8	76.3	4.5	419.6	1.8	119.49	1.40	2.35	26.2	7.5	0.013	0.000	99.0	27.51	0.16	0.17
1015-01B	FCT-San	SAN	0.8	64c	22.210	0.050	406993.5	1705.8	581262.2	163.7	6937.9	55.5	584.4	4.5	0.43	2.86	3661.0	350.0	53.1	1.9	90.3	3.6	413.8	1.8	121.05	1.60	2.05	22.9	231.0	0.012	0.000	100.1	27.72	0.16	0.17
1015-01C	FCT-San	SAN	1.0	64c	22.210	0.050	655503.8	2665.9	941377.9	214.0	11071.2	53.0	918.6	4.8	0.00	2.76	3661.0	350.0	53.1	1.9	90.3	3.6	413.8	1.8	121.05	1.60	3.32	37.0	0.0	0.012	0.000	100.2	27.61	0.15	0.17
1015-01D	FCT-San	SAN	1.3	64c	22.210	0.050	153295.1	792.5	219796.8	89.4	2634.1	41.7	225.2	3.5	0.00	2.75	3661.0	350.0	53.1	1.9	90.3	3.6	413.8	1.8	121.05	1.60	0.78	8.6	0.0	0.012	0.000	101.1	27.89	0.23	0.24
1015-01E	FCT-San	SAN	4.0	64c	22.210	0.050	95502.7	639.7	134221.3	61.7	1556.6	30.4	131.7	3.3	0.00	2.85	3661.0	350.0	53.1	1.9	90.3	3.6	413.8	1.8	121.05	1.60	0.47	5.3	0.0	0.012	0.000	101.1	28.46	0.33	0.33
1017-01A	FCT-San	SAN	0.4	64c	22.245	0.050	1362088.0	5759.7	1926375.0	612.2	22238.1	263.4	2158.9	17.4	0.00	12.09	2980.0	370.0	49.9	1.8	106.1	10.0	415.9	2.0	119.30	1.60	6.80	72.6	0.0	0.014	0.000	100.3	28.10	0.17	0.18
1017-01B	FCT-San	SAN	0.8	64c	22.245	0.050	253858.3	1130.7	359023.1	103.2	4127.4	31.8	386.5	3.9	0.19	2.76	2980.0	370.0	49.9	1.8	106.1	10.0	415.9	2.0	119.34	1.60	1.27	13.5	357.1	0.013	0.000	100.1	28.04	0.18	0.19
1017-01C	FCT-San	SAN	1.0	64c	22.245	0.050	59440.4	568.7	83578.9	45.4	907.6	23.6	87.8	3.2	0.00	2.84	2980.0	370.0	49.9	1.8	106.1	10.0	415.9	2.0	119.34	1.60	0.29	3.1	0.0	0.013	0.000	102.6	28.91	0.49	0.50
1017-01D	FCT-San	SAN	1.3	64c	22.245	0.050	99612.1	644.3	139616.9	66.7	1599.1	25.9	153.3	3.6	0.79	2.95	2980.0	370.0	49.9	1.8	106.1	10.0	415.9	2.0	119.34	1.60	0.49	5.3	33.2	0.013	0.000	99.8	28.23	0.32	0.33
1017-01E	FCT-San	SAN	4.0	64c	22.245	0.050	106761.8	646.0	146251.8	66.7	1752.2	35.5	150.4	3.2	8.23	2.74	2668.0	340.0	45.8	1.5	71.4	4.3	413.6	1.7	113.00	1.70	0.52	5.5	3.1	0.012	0.000	97.8	28.28	0.30	0.30
1019-01A	FCT-San	SAN	0.4	64d	23.211	0.079	1268827.0	5392.7	1870273.0	569.4	22201.4	244.9	2060.5	16.8	29.29	11.57	2668.0	340.0	45.8	1.5	71.4	4.3	413.6	1.7	113.00	1.70	6.60	57.2	12.1	0.013	0.000	99.4	27.88	0.18	0.20
1019-01B	FCT-San	SAN	0.8	64d	23.211	0.079	395140.6	1674.5	584859.1	151.1	6807.3	39.3	620.2	4.3	5.19	2.90	2668.0	340.0	45.8	1.5	71.4	4.3	413.6	1.7	113.00	1.70	2.06	17.9	20.5	0.013	0.000	99.7	27.85	0.17	0.19
1019-01C	FCT-San	SAN	1.0	64d	23.211	0.079	301303.7	1305.6	446324.3	125.9	5142.6	34.3	481.8	4.0	5.76	2.99	2668.0	340.0	45.8	1.5	71.4	4.3	413.6	1.7	113.00	1.70	1.57	13.7	14.4	0.013	0.000	99.5	27.77	0.18	0.20
1019-01D	FCT-San	SAN	1.3	64d	23.211	0.079	194203.6	919.3	289896.5	104.5	3577.7	80.7	310.5	3.9	0.00	2.73	4169.0	330.0	47.9	1.7	77.2	5.1	410.4	1.9	118.66	1.70	1.02	8.9	0.0	0.013	0.000	100.5	27.82	0.20	0.22
1019-01E	FCT-San	SAN	4.0	64d	23.211	0.079	53550.1	517.0	77375.3	45.4	853.9	13.6	78.2	3.5	2.55	2.74	4169.0	330.0	47.9	1.7	77.2	5.1	410.4	1.9	118.66	1.70	0.27	2.4	5.3	0.012	0.001	98.6	28.22	0.53	0.53
1021-01A	FCT-San	SAN	0.4	64d	23.199	0.049	5918.5	478.0	3354.8	10.3	74.0	7.9	16.2	3.2	10.55	2.94	4169.0	330.0	47.9	1.7	77.2	5.1	410.4	1.9	118.66	1.70	0.01	0.1	0.3	0.058	0.011	46.9	34.19	12.22	12.22
1021-01B	FCT-San	SAN	0.8	64d	23.199	0.049	1945055.0	8133.7	2891681.0	795.9	33675.6	257.2	3188.6	18.5	6.93	11.09	4169.0	330.0	47.9	1.7	77.2	5.1	410.4	1.9	118.70	1.70	10.20	56.6	79.3	0.013	0.000	100.0	27.79	0.16	0.17
1021-01C	FCT-San	SAN	1.0	64d	23.199	0.049	1077061.0	4744.5	1596655.0	538.8	18537.3	98.0	1734.7	16.0	3.91	12.08	3362.0	390.0	53.0	1.7	59.4	3.9	414.9	1.9	116.30	1.50	5.63	31.2	76.3	0.013	0.000	100.0	27.87	0.19	0.19
1021-01D	FCT-San	SAN	1.3	64d	23.199	0.049	315277.0	1396.9	465346.5	138.5	5510.7	35.5	499.9	4.3	4.46	2.90	3362.0	390.0	53.0	1.7	59.4	3.9	414.9	1.9	116.29	1.50	1.64	9.1	19.3	0.013	0.000	99.7	27.90	0.18	0.19
1021-01E	FCT-San	SAN	4.0	64d	23.199	0.049	104189.8	698.0	153476.3	73.0	1777.2	24.2	159.6	3.4	5.27	2.71	3362.0	390.0	53.0	1.7	59.4	3.9	414.9	1.9	116.29	1.50	0.54	3.0	5.2	0.013	0.000	98.6	27.65	0.31	0.31
1023-01A	FCT-San	SAN	0.4	64d	23.189	0.076	184099.9	912.0	264295.3	85.6	3139.7	36.7	261.4	3.5	15.34	2.83	3362.0	390.0	53.0	1.7	59.4	3.9	414.9	1.9	116.29	1.50	0.93	7.5	2.9	0.012	0.000	97.6	28.08	0.22	0.24
1023-01B	FCT-San	SAN	0.8	64d	23.189	0.076	1241392.0	5341.4	1843317.0	612.2	21832.9	196.0	1734.0	16.5	11.74	11.04	2780.0	370.0	46.7	1.7	72.0	5.5	407.8	1.8	115.20	1.60	6.50	52.3	25.5	0.011	0.000	99.8	27.76	0.17	0.20

Notes:
a: Relative isotopic abundances corrected for blank, radioactive decay, and mass discrimination
b: 4-digit number indicates the RunID number in Mass Spec, -01 denotes the aliquot number, letter suffix indicates the heating step
c: Number indicates the irradiation batch number, letter refers to the tube in which the sample was loaded in the irradiation can. Rads #64 and #65 were both 960 MWH, done in medium-flux positions at McMaster Nuclear Reactor (positions 8D and 8C, respectively), with Cd shielding.
Data in italics were analyses excluded from integrated age calculations.
All negative values in the table were replaced with "0".
Decay constants and isotopic abundances after Steiger and Jäger (1977).
Ages calculated relative to PP20 Hornblende flux monitor at 1074 Ma (Jourdan et al., 2006)
Nucleogenic interference correction factors (±2σ)
(^{39}Ar/^{37}Ar)Ca = 0.0007 ± 0.000054
(^{36}Ar/^{37}Ar)Ca = 0.00028 ± 0.00017
(^{40}Ar/^{39}Ar)K = 0.003 ± 0.005
Bkgd = background

Table A1. (Continued)

Lab ID#[b]	Sample	Material	Watts	Irrad.[c]	*J* (x 10^{-3}) ± 1σ		Relative isotopic abundances[a]										Background relative isotopic abundances										Derived results								w/±*J* ±1σ
							^{40}Ar ±1σ		^{39}Ar ±1σ		^{38}Ar ±1σ		^{37}Ar ±1σ		^{36}Ar ±1σ		^{40}Ar Bkgd ±1σ		^{39}Ar Bkgd ±1σ		^{38}Ar Bkgd ±1σ		^{37}Ar Bkgd ±1σ		^{36}Ar Bkgd ±1σ		^{39}Ar Mol x 10^{-14}	^{39}Ar % of total	%(^{36}Ar)$_{Ca}$	Ca/K ±1σ		%^{40}Ar*	Age (Ma) ±1σ		
1023-01C	FCT-San	SAN	1.0	64d	23.189	0.076	359360.7	1562.3	531135.4	138.5	6254.6	61.9	501.8	4.2	3.56	2.94	2780.0	370.0	46.7	1.7	72.0	5.5	407.8	1.8	115.20	1.60	1.87	15.1	24.3	0.011	0.000	99.8	27.88	0.17	0.20
1023-01D	FCT-San	SAN	1.3	64d	23.189	0.076	246926.5	1146.9	363255.4	117.1	4232.2	49.4	346.6	3.8	0.05	2.75	2780.0	370.0	46.7	1.7	72.0	5.5	407.8	1.8	115.20	1.60	1.28	10.3	1208.0	0.012	0.000	100.1	28.10	0.19	0.21
1023-01E	FCT-San	SAN	4.0	64d	23.189	0.076	358654.2	1561.4	525016.2	138.5	6217.8	68.2	493.7	4.2	8.87	2.69	2780.0	370.0	46.7	1.7	72.0	5.5	407.8	1.8	115.20	1.60	1.85	14.9	9.6	0.011	0.000	99.3	28.03	0.17	0.19
1025-01A	FCT-San	SAN	0.4	64e	23.301	0.043	90655.3	636.1	121374.7	61.7	1787.2	26.7	167.5	3.2	25.25	2.82	1992.0	360.0	53.4	1.9	61.8	3.9	408.5	1.7	112.72	1.60	0.43	3.0	1.1	0.017	0.000	91.8	28.46	0.37	0.38
1025-01B	FCT-San	SAN	0.8	64e	23.301	0.043	584502.7	2463.1	870395.0	214.0	10284.2	68.1	978.0	5.3	3.23	2.84	1992.0	360.0	53.4	1.9	61.8	3.9	408.5	1.7	112.72	1.60	3.07	21.6	52.3	0.014	0.000	99.9	27.85	0.16	0.17
1025-01C	FCT-San	SAN	1.0	64e	23.301	0.043	1738504.0	7404.4	2564387.0	673.4	29860.2	287.8	2821.7	19.6	39.94	11.11	1992.0	360.0	53.4	1.9	61.8	3.9	408.4	1.7	112.70	1.60	9.05	63.6	12.2	0.013	0.000	99.4	27.97	0.17	0.17
1025-01D	FCT-San	SAN	1.3	64e	23.301	0.043	292953.4	1312.6	434922.8	122.1	5029.2	69.3	488.7	4.3	6.15	2.85	1992.0	360.0	53.4	1.9	61.8	3.9	408.5	1.7	112.72	1.60	1.53	10.8	13.7	0.014	0.000	99.5	27.80	0.18	0.19
1025-01E	FCT-San	SAN	4.0	64e	23.301	0.043	30315.5	494.7	43017.4	30.3	525.2	18.1	40.7	3.0	7.31	2.81	2269.0	340.0	54.0	1.9	67.2	4.2	411.4	1.7	114.22	1.50	0.15	1.1	1.0	0.011	0.001	92.9	27.17	0.94	0.94
1027-01A	FCT-San	SAN	0.4	64e	23.295	0.029	21349.7	506.6	20850.4	24.0	302.5	15.7	51.2	2.9	17.41	2.75	2269.0	340.0	54.0	1.9	67.2	4.2	411.4	1.7	114.22	1.50	0.07	0.5	0.5	0.030	0.002	75.7	32.18	1.91	1.91
1027-01B	FCT-San	SAN	0.8	64e	23.295	0.029	1342145.0	5894.6	1998430.0	593.9	23064.0	189.8	2008.6	16.8	9.92	10.52	2269.0	340.0	54.0	1.9	67.2	4.2	411.4	1.7	114.20	1.50	7.05	45.2	35.0	0.012	0.000	99.9	27.83	0.17	0.18
1027-01C	FCT-San	SAN	1.0	64e	23.295	0.029	141458.7	776.0	210151.4	78.1	2472.7	30.5	204.9	3.4	0.82	2.79	2269.0	340.0	54.0	1.9	67.2	4.2	411.4	1.7	114.22	1.50	0.74	4.8	43.4	0.012	0.000	99.9	27.90	0.25	0.25
1027-01D	FCT-San	SAN	1.3	64e	23.295	0.029	177315.8	914.0	257255.6	93.2	3026.9	41.9	254.4	3.6	2.64	2.66	2391.0	350.0	49.6	1.7	70.0	5.4	414.7	1.8	117.22	1.40	0.91	5.8	16.6	0.012	0.000	99.6	28.49	0.22	0.22
1027-01E	FCT-San	SAN	4.0	64e	23.295	0.029	1310792.0	5799.9	1937018.0	600.0	22285.3	159.3	1887.6	17.3	0.00	11.02	2391.0	350.0	49.6	1.7	70.0	5.4	414.7	1.8	117.20	1.40	6.83	43.8	0.0	0.012	0.000	100.4	28.17	0.18	0.18
1001-02A	FCT-San	SAN	0.4	64a	21.994	0.072	20942.2	469.2	17196.2	21.4	246.3	12.6	10.5	2.7	2.20	2.68	3541.0	350.0	40.7	1.2	81.9	5.6	361.7	1.8	115.47	1.60	0.06	1.0	1.2	0.011	0.003	96.9	46.09	2.09	2.09
1001-02B	FCT-San	SAN	0.8	64a	21.994	0.072	549757.4	1993.9	766969.0	151.1	8853.3	79.5	516.7	3.8	6.22	2.59	3541.0	350.0	40.7	1.2	81.9	5.6	361.7	1.8	115.47	1.60	2.71	43.2	21.2	0.012	0.000	99.7	28.01	0.15	0.17
1001-02C	FCT-San	SAN	1.0	64a	21.994	0.072	251636.4	1016.4	350380.6	99.5	4116.5	28.3	232.4	3.3	0.27	2.59	3541.0	350.0	40.7	1.2	81.9	5.6	361.7	1.8	115.47	1.60	1.24	19.7	219.3	0.012	0.000	100.0	28.15	0.17	0.20
1001-02D	FCT-San	SAN	1.3	64a	21.994	0.072	98671.7	564.4	138290.1	64.2	1622.8	29.3	84.5	3.0	0.00	2.68	5377.0	280.0	46.6	1.5	92.9	4.6	366.2	1.5	117.09	1.60	0.49	7.8	0.0	0.011	0.000	100.6	28.12	0.29	0.31
1001-02E	FCT-San	SAN	4.0	64a	21.994	0.072	358919.1	1345.6	503807.3	125.9	5723.0	58.1	331.9	3.2	0.00	2.68	5377.0	280.0	46.6	1.5	92.9	4.6	366.2	1.5	117.09	1.60	1.78	28.4	0.0	0.012	0.000	100.4	28.01	0.16	0.18
1003-02A	FCT-San	SAN	0.4	64a	21.793	0.045	12617.1	451.9	3212.9	9.8	119.3	11.2	2.1	2.7	25.42	2.70	5377.0	280.0	46.6	1.5	92.9	4.6	366.2	1.5	117.09	1.60	0.01	0.2	0.0	0.012	0.015	39.9	60.44	10.94	10.94
1003-02B	FCT-San	SAN	0.8	64a	21.793	0.045	145806.5	692.7	196052.9	84.4	2478.3	63.1	137.9	2.9	14.31	2.60	5377.0	280.0	46.6	1.5	92.9	4.6	366.2	1.5	117.09	1.60	0.69	12.6	2.5	0.013	0.000	97.1	28.05	0.23	0.23
1003-02C	FCT-San	SAN	1.0	64a	21.793	0.045	527565.3	1935.7	737243.4	151.1	8536.2	80.8	511.8	3.7	12.48	2.73	5899.0	360.0	42.1	1.4	93.8	6.7	359.2	1.8	110.89	1.50	2.60	47.3	10.5	0.012	0.000	99.4	27.61	0.15	0.16
1003-02D	FCT-San	SAN	1.3	64a	21.793	0.045	122265.0	668.7	170093.1	71.8	1965.1	42.1	124.2	3.3	13.17	2.44	5899.0	360.0	42.1	1.4	93.8	6.7	359.2	1.8	110.89	1.50	0.60	10.9	2.4	0.013	0.000	96.9	27.03	0.25	0.25
1003-02E	FCT-San	SAN	4.0	64a	21.793	0.045	382856.4	1456.4	453659.3	125.9	5456.7	37.1	314.8	3.3	118.93	3.23	5899.0	360.0	42.1	1.4	93.8	6.7	359.2	1.8	110.89	1.50	1.60	29.1	0.7	0.012	0.000	90.8	29.74	0.18	0.19
1005-02A	FCT-San	SAN	0.4	64a	21.693	0.060	19182.3	502.5	22435.5	25.2	293.2	14.3	26.9	2.9	11.12	2.53	5899.0	360.0	42.1	1.4	93.8	6.7	359.2	1.8	110.89	1.50	0.08	1.0	0.6	0.021	0.002	82.8	27.37	1.56	1.56
1005-02B	FCT-San	SAN	0.8	64a	21.693	0.060	757118.0	2739.3	1039929.0	188.8	12173.2	75.1	759.1	4.2	8.09	2.63	4930.0	350.0	38.0	1.3	73.8	11.0	363.8	1.7	107.34	1.80	3.67	48.5	24.0	0.013	0.000	99.8	28.07	0.14	0.16
1005-02C	FCT-San	SAN	1.0	64a	21.693	0.060	104624.2	650.4	140344.7	64.2	1691.8	28.6	104.2	2.9	10.42	2.71	4930.0	350.0	38.0	1.3	73.8	11.0	363.8	1.7	107.34	1.80	0.50	6.5	2.6	0.013	0.000	97.1	27.98	0.30	0.31
1005-02D	FCT-San	SAN	1.3	64a	21.693	0.060	63370.9	538.2	84624.6	54.1	953.8	44.2	56.8	2.9	7.16	2.80	4930.0	350.0	38.0	1.3	73.8	11.0	363.8	1.7	107.34	1.80	0.30	3.9	2.0	0.012	0.001	96.7	27.98	0.46	0.47
1005-02E	FCT-San	SAN	4.0	64a	21.693	0.060	627330.2	2297.8	858513.2	188.8	10085.5	51.5	618.8	4.1	8.94	2.63	4930.0	350.0	38.0	1.3	73.8	11.0	363.8	1.7	107.34	1.80	3.03	40.0	17.7	0.013	0.000	99.7	28.14	0.15	0.16
1007-02A	FCT-San	SAN	0.4	64b	21.410	0.054	5860.1	481.5	1823.6	8.1	101.6	10.1	0.0	2.6	0.00	2.49	3266.0	330.0	48.1	2.0	136.7	4.5	365.5	1.7	116.68	1.60	0.01	0.1	1.5	0.000	0.026	105.9	126.66	17.51	17.51
1007-02B	FCT-San	SAN	0.8	64b	21.410	0.054	78359.0	567.8	103727.0	60.5	1136.0	19.4	82.8	3.1	0.00	2.58	3266.0	330.0	48.1	2.0	136.7	4.5	365.5	1.7	116.68	1.60	0.37	6.9	0.0	0.014	0.001	101.9	29.35	0.36	0.37
1007-02C	FCT-San	SAN	1.0	64b	21.410	0.054	199838.1	883.0	273815.2	85.6	3083.4	39.3	195.8	3.2	1.34	2.41	3266.0	330.0	48.1	2.0	136.7	4.5	365.5	1.7	116.68	1.60	0.97	18.2	37.5	0.013	0.000	99.9	27.80	0.18	0.20
1007-02D	FCT-San	SAN	1.3	64b	21.410	0.054	605268.4	2241.7	830471.1	163.7	9573.5	85.7	603.0	4.1	0.00	2.59	3266.0	330.0	48.1	2.0	136.7	4.5	365.5	1.7	116.68	1.60	2.93	55.1	0.0	0.013	0.000	100.1	27.82	0.14	0.16
1007-02E	FCT-San	SAN	4.0	64b	21.410	0.054	222697.3	939.5	297382.4	104.5	3365.1	51.9	221.6	3.3	1.42	2.62	4808.0	290.0	46.9	1.9	107.9	5.4	362.4	1.6	115.93	1.50	1.05	19.7	39.9	0.013	0.000	99.9	28.53	0.18	0.20
1011-02A	FCT-San	SAN	0.4	64b	21.494	0.054	20831.1	477.8	27310.0	27.8	350.0	8.9	22.5	2.6	0.00	2.53	4808.0	290.0	46.9	1.9	107.9	5.4	362.4	1.6	115.93	1.50	0.10	1.7	0.0	0.015	0.002	100.2	29.27	1.25	1.25
1011-02B	FCT-San	SAN	0.8	64b	21.494	0.054	412556.5	1581.7	571651.1	163.7	6704.9	45.6	387.0	3.6	0.00	2.62	4808.0	290.0	46.9	1.9	107.9	5.4	362.4	1.6	115.93	1.50	2.02	36.4	0.0	0.012	0.000	100.3	27.71	0.15	0.17
1011-02C	FCT-San	SAN	1.0	64b	21.494	0.054	185768.7	825.7	257459.6	88.1	2977.8	20.9	176.3	3.1	0.00	2.52	4808.0	290.0	46.9	1.9	107.9	5.4	362.4	1.6	115.93	1.50	0.91	16.4	0.0	0.012	0.000	100.7	27.83	0.19	0.20
1011-02D	FCT-San	SAN	1.3	64b	21.494	0.054	267615.9	1106.4	366409.4	123.4	4238.3	51.8	248.9	3.3	2.92	2.80	4213.0	380.0	43.3	1.8	89.5	4.4	362.4	1.6	110.57	1.80	1.29	23.4	21.9	0.012	0.000	99.8	27.90	0.17	0.19
1011-02E	FCT-San	SAN	4.0	64b	21.494	0.054	252192.1	1077.5	346214.5	91.9	4053.1	34.3	228.2	3.4	2.83	2.63	4213.0	380.0	43.3	1.8	89.5	4.4	362.4	1.6	110.57	1.80	1.22	22.1	20.7	0.012	0.000	99.7	27.82	0.18	0.19
1013-02A	*FCT-San*	*SAN*	*0.4*	*64c*	*22.178*	*0.050*	*26529.5*	*534.4*	*35013.5*	*30.3*	*441.0*	*15.7*	*32.9*	*3.0*	*2.25*	*2.71*	*4213.0*	*380.0*	*43.3*	*1.8*	*89.5*	*4.4*	*362.4*	*1.6*	*110.57*	*1.80*	*0.12*	*4.5*	*3.7*	*0.017*	*0.002*	*97.6*	*29.20*	*1.09*	*1.10*
1013-02B	*FCT-San*	*SAN*	*0.8*	*64c*	*22.178*	*0.050*	*66868.1*	*583.6*	*92518.6*	*51.6*	*1125.4*	*20.6*	*76.7*	*2.9*	*2.72*	*2.63*	*4213.0*	*380.0*	*43.3*	*1.8*	*89.5*	*4.4*	*362.4*	*1.6*	*110.57*	*1.80*	*0.33*	*12.0*	*7.2*	*0.015*	*0.001*	*98.9*	*28.23*	*0.43*	*0.43*
1013-02C	*FCT-San*	*SAN*	*1.0*	*64c*	*22.178*	*0.050*	*20347.9*	*538.8*	*26831.0*	*30.2*	*329.5*	*10.6*	*25.9*	*3.0*	*5.06*	*2.59*	*4924.0*	*400.0*	*38.6*	*1.5*	*94.1*	*4.0*	*360.8*	*1.7*	*109.61*	*1.60*	*0.09*	*3.5*	*1.3*	*0.017*	*0.002*	*92.7*	*27.77*	*1.39*	*1.39*
1013-02D	*FCT-San*	*SAN*	*1.3*	*64c*	*22.178*	*0.050*	*231986.2*	*1012.9*	*334646.1*	*117.1*	*3885.3*	*34.2*	*254.4*	*3.3*	*3.54*	*2.58*	*4924.0*	*400.0*	*38.6*	*1.5*	*94.1*	*4.0*	*360.8*	*1.7*	*109.61*	*1.60*	*1.18*	*43.3*	*18.4*	*0.014*	*0.000*	*99.6*	*27.29*	*0.18*	*0.19*
1013-02E	*FCT-San*	*SAN*	*4.0*	*64c*	*22.178*	*0.050*	*196239.1*	*906.5*	*283078.9*	*96.9*	*3275.7*	*34.2*	*207.7*	*3.2*	*3.24*	*2.58*	*4924.0*	*400.0*	*38.6*	*1.5*	*94.1*	*4.0*	*360.8*	*1.7*	*109.61*	*1.60*	*1.00*	*36.7*	*16.4*	*0.013*	*0.000*	*99.6*	*27.28*	*0.19*	*0.20*
1034-01A	FCT-San	SAN	0.4	65a	16.784	0.050	549200.4	1196.4	585162.4	151.1	6913.3	37.0	1713.6	5.2	12.85	2.70	2586.0	340.0	52.9	1.3	89.3	5.8	393.3	1.8	128.11	1.60	2.06	64.5	8.6	0.013	0.000	99.4	27.92	0.11	0.13
1034-01B	FCT-San	SAN	0.8	65a	16.784	0.050	114204.3	533.5	119612.2	60.4	1409.3	22.2	298.5	3.3	0.00	2.60	2586.0	340.0	52.9	1.3	89.3	5.8	393.3	1.8	128.11	1.60	0.42	13.2	0.0	0.011	0.000	100.7	28.78	0.25	0.26
1034-01C	FCT-San	SAN	1.0	65a	16.784	0.050	68879.1	507.8	71078.7	46.6	871.2	18.6	179.5	3.2	0.00	2.69	2586.0	340.0	52.9	1.3	89.3	5.8	393.3	1.8	128.11	1.60	0.25	7.8	0.0	0.011	0.000	100.4	29.11	0.41	0.41
1034-01D	FCT-San	SAN	1.3	65a	16.784	0.050	90320.2	483.9	93662.5	55.4	1092.7	24.6	233.4	3.0	0.00	2.69	2586.0	340.0	52.9	1.3	89.3	5.8	393.3	1.8	128.11	1.60	0.33	10.3	0.0	0.011	0.000	101.8	29.38	0.31	0.32
1034-01E	FCT-San	SAN	4.0	65a	16.784	0.050	37709.0	488.3	38367.7	31.5	463.1	15.5	109.1	2.9	4.10	2.85	5713.0	340.0	47.8	1.3	76.7	3.3	387.8	1.8	124.47	1.70	0.14	4.2	1.7	0.013	0.000	96.8	28.49	0.77	0.77
1036-01A	*FCT-San*	*SAN*	*0.4*	*65a*	*16.784*	*0.050*	*391263.7*	*933.4*	*420725.6*	*123.4*	*5034.8*	*34.1*	*1379.9*	*4.6*	*14.15*	*2.85*	*5713.0*	*340.0*	*47.8*	*1.3*	*76.7*	*3.3*	*387.8*	*1.8*	*124.47*	*1.70*	*1.48*	*24.9*	*6.3*	*0.015*	*0.000*	*99.0*	*27.56*	*0.12*	*0.14*
1036-01B	*FCT-San*	*SAN*	*0.8*	*65a*	*16.784*	*0.050*	*266937.3*	*720.7*	*289893.7*	*94.4*	*3458.8*	*20.4*	*803.8*	*4.0*	*10.15*	*2.66*	*5713.0*	*340.0*	*47.8*	*1.3*	*76.7*	*3.3*	*387.8*	*1.8*	*124.47*	*1.70*	*1.02*	*17.1*	*5.1*	*0.013*	*0.000*	*98.9*	*27.28*	*0.13*	*0.16*
1036-01C	*FCT-San*	*SAN*	*1.1*	*65a*	*16.784*	*0.050*	*142222.9*	*567.9*	*156279.5*	*71.8*	*1878.7*	*24.1*	*434.2*	*3.4*	*0.01*	*2.66*	*5713.0*	*340.0*	*47.8*	*1.3*	*76.7*	*3.3*	*387.8*	*1.8*	*124.47*	*1.70*	*0.55*	*9.2*	*2273.3*	*0.013*	*0.000*	*100.1*	*27.27*	*0.20*	*0.22*
1036-01D	*FCT-San*	*SAN*	*4.0*	*65a*	*16.784*	*0.050*	*85374.1*	*513.0*	*84112.1*	*46.6*	*991.1*	*30.8*	*234.4*	*3.4*	*25.16*	*3.00*	*5299.0*	*350.0*	*46.8*	*1.4*	*91.2*	*5.8*	*387.0*	*1.9*	*116.02*	*1.60*	*0.30*	*5.0*	*0.6*	*0.013*	*0.000*	*91.2*	*27.73*	*0.37*	*0.38*
1056-01A	*FCT-San*	*SAN*	*0.4*	*65d*	*16.555*	*0.091*	*718722.8*	*2522.1*	*740264.5*	*365.1*	*8828.6*	*35.7*	*1432.3*	*9.5*	*18.23*	*2.78*	*2968.0*	*300.0*	*39.2*	*1.2*	*78.6*	*5.6*	*591.5*	*2.2*	*93.56*	*1.50*	*2.61*	*56.3*	*7.1*	*0.012*	*0.000*	*99.3*	*28.47*	*0.13*	*0.20*
1056-01B	*FCT-San*	*SAN*	*0.8*	*65d*	*16.555*	*0.091*	*307919.7*	*1159.9*	*318667.3*	*119.6*	*3815.3*	*38.2*	*584.9*	*6.2*	*4.45*	*2.64*	*2968.0*	*300.0*	*39.2*	*1.2*	*78.6*	*5.6*	*591.5*	*2.2*	*93.56*	*1.50*	*1.12*	*24.2*	*11.9*	*0.012*	*0.000*	*99.6*	*28.42*	*0.15*	*0.22*
1056-01C	*FCT-San*	*SAN*	*1.1*	*65d*	*16.555*	*0.091*	*106999.1*	*579.7*	*108769.5*	*56.7*	*1252.9*	*27.0*	*188.7*	*5.2*	*0.00*	*2.63*	*2968.0*	*300.0*	*39.2*	*1.2*	*78.6*	*5.6*	*591.5*	*2.2*	*93.56*	*1.50*	*0.38*	*8.3*	*0.0*	*0.011*	*0.000*	*100.2*	*29.10*	*0.27*	*0.32*
1056-01D	*FCT-San*	*SAN*	*4.5*	*65d*	*16.555*	*0.091*	*133432.8*	*666.3*	*136632.8*	*61.7*	*1603.0*	*23.3*	*246.6*	*5.4*	*3.51*	*2.55*	*2968.0*	*300.0*	*39.2*	*1.2*	*78.6*	*5.6*	*591.5*	*2.2*	*93.56*	*1.50*	*0.48*	*10.4*	*6.3*	*0.011*	*0.000*	*99.3*	*28.62*	*0.23*	*0.28*

Table A1. (Continued)

Lab ID#[b]	Sample	Material	Watts	Irrad.[c]	*J* (x 10^{-3}) ± 1σ		Relative isotopic abundances[a]										Background relative isotopic abundances										Derived results								w/±*J* ±1σ
							^{40}Ar ±1σ		^{39}Ar ±1σ		^{38}Ar ±1σ		^{37}Ar ±1σ		^{36}Ar ±1σ		^{40}Ar Bkgd ±1σ		^{39}Ar Bkgd ±1σ		^{38}Ar Bkgd ±1σ		^{37}Ar Bkgd ±1σ		^{36}Ar Bkgd ±1σ		^{39}Ar Mol x 10^{-14}	^{39}Ar % of total	$\%(^{36}Ar)_{Ca}$	Ca/K ±1σ		$\%^{40}Ar^{*}$	Age (Ma) ±1σ		
1058-01A	*FCT-San*	*SAN*	*0.5*	*65d*	*16.667*	*0.061*	*10266.4*	*475.3*	*10579.8*	*15.2*	*144.9*	*16.6*	*22.2*	*3.4*	*0.00*	*2.27*	*2891.0*	*330.0*	*38.6*	*1.2*	*74.9*	*2.8*	*570.9*	*2.0*	*94.19*	*1.50*	*0.04*	*1.4*	*0.0*	*0.014*	*0.002*	*108.1*	*31.17*	*2.31*	*2.32*
1058-01B	*FCT-San*	*SAN*	*0.7*	*65d*	*16.667*	*0.061*	*305051.6*	*739.6*	*309520.6*	*138.5*	*3604.6*	*37.9*	*596.4*	*5.0*	*7.27*	*2.84*	*2891.0*	*330.0*	*38.6*	*1.2*	*74.9*	*2.8*	*570.9*	*2.0*	*94.19*	*1.50*	*1.09*	*40.9*	*7.8*	*0.013*	*0.000*	*99.3*	*29.10*	*0.13*	*0.17*
1058-01C	*FCT-San*	*SAN*	*1.2*	*65d*	*16.667*	*0.061*	*73772.6*	*517.9*	*74996.6*	*54.1*	*866.1*	*21.6*	*148.4*	*3.6*	*0.22*	*2.36*	*2891.0*	*330.0*	*38.6*	*1.2*	*74.9*	*2.8*	*570.9*	*2.0*	*94.19*	*1.50*	*0.26*	*9.9*	*65.3*	*0.013*	*0.000*	*100.0*	*29.23*	*0.35*	*0.37*
1058-01D	*FCT-San*	*SAN*	*5.0*	*65d*	*16.667*	*0.061*	*235966.9*	*612.1*	*243474.9*	*89.4*	*2943.1*	*32.8*	*447.3*	*4.0*	*4.32*	*2.37*	*2891.0*	*330.0*	*38.6*	*1.2*	*74.9*	*2.8*	*570.9*	*2.0*	*94.19*	*1.50*	*0.86*	*32.2*	*9.9*	*0.012*	*0.000*	*99.5*	*28.67*	*0.14*	*0.17*
1058-01E	*FCT-San*	*SAN*	*8.0*	*65d*	*16.667*	*0.061*	*117194.8*	*514.7*	*118211.5*	*70.5*	*1308.4*	*21.8*	*205.3*	*3.8*	*0.00*	*2.35*	*3964.0*	*370.0*	*40.4*	*1.3*	*81.9*	*4.3*	*565.7*	*2.0*	*94.36*	*1.50*	*0.42*	*15.6*	*0.0*	*0.012*	*0.000*	*101.6*	*29.93*	*0.23*	*0.25*
1062-01A	*FCT-San*	*SAN*	*0.4*	*65d*	*16.913*	*0.095*	*353723.6*	*765.9*	*366701.2*	*115.8*	*4445.3*	*35.5*	*675.4*	*4.2*	*4.88*	*2.37*	*3964.0*	*370.0*	*40.4*	*1.3*	*81.9*	*4.3*	*565.7*	*2.0*	*94.36*	*1.50*	*1.29*	*33.7*	*13.3*	*0.012*	*0.000*	*99.6*	*28.99*	*0.11*	*0.20*
1062-01B	*FCT-San*	*SAN*	*0.7*	*65d*	*16.913*	*0.095*	*125201.1*	*555.7*	*128600.7*	*100.7*	*1629.3*	*40.5*	*246.6*	*3.8*	*2.43*	*2.37*	*3964.0*	*370.0*	*40.4*	*1.3*	*81.9*	*4.3*	*565.7*	*2.0*	*94.36*	*1.50*	*0.45*	*11.8*	*9.7*	*0.013*	*0.000*	*99.5*	*29.21*	*0.22*	*0.28*
1062-01C	*FCT-San*	*SAN*	*1.2*	*65d*	*16.913*	*0.095*	*421848.5*	*861.3*	*432083.4*	*122.1*	*4991.9*	*71.9*	*794.0*	*4.8*	*7.96*	*2.55*	*3964.0*	*370.0*	*40.4*	*1.3*	*81.9*	*4.3*	*565.7*	*2.0*	*94.36*	*1.50*	*1.52*	*39.7*	*9.6*	*0.012*	*0.000*	*99.5*	*29.30*	*0.11*	*0.20*
1062-01D	*FCT-San*	*SAN*	*5.0*	*65d*	*16.913*	*0.095*	*164122.7*	*553.3*	*162115.7*	*80.6*	*1974.0*	*29.8*	*313.0*	*3.7*	*9.10*	*2.41*	*1386.0*	*390.0*	*38.1*	*1.4*	*51.7*	*11.0*	*564.1*	*2.0*	*95.93*	*1.40*	*0.57*	*14.9*	*3.3*	*0.013*	*0.000*	*98.4*	*30.04*	*0.18*	*0.25*
1060-01A	FCT-San	SAN	0.4	65d	16.779	0.059	206151.8	998.5	15748.9	22.7	371.8	14.8	71.9	4.5	629.09	5.67	2353.0	340.0	33.3	1.0	70.1	5.3	503.3	1.8	78.39	1.30	0.06	1.5	0.0	0.035	0.002	8.9	34.84	3.70	3.71
1060-01B	FCT-San	SAN	0.7	65d	16.779	0.059	784505.2	3470.7	298897.6	428.0	5034.1	151.2	699.8	7.6	1871.89	17.20	2353.0	340.0	33.3	1.0	70.1	5.3	503.3	1.8	78.39	1.30	1.05	28.6	0.0	0.018	0.000	28.7	22.64	0.63	0.63
1060-01C	FCT-San	SAN	1.2	65d	16.779	0.059	1168076.0	4907.5	444925.1	302.1	5820.3	25.7	734.2	7.6	2569.24	15.27	2353.0	340.0	33.3	1.0	70.1	5.3	503.3	1.8	78.39	1.30	1.57	42.5	0.0	0.013	0.000	34.3	26.99	0.46	0.46
1060-01D	FCT-San	SAN	5.0	65d	16.779	0.059	2702617.0	11333.9	287257.1	214.0	5109.1	58.1	493.8	6.3	8336.12	43.72	2353.0	340.0	33.3	1.0	70.1	5.3	503.3	1.8	78.39	1.30	1.01	27.4	0.0	0.013	0.000	7.9	22.31	1.80	1.80
1048-01A	FCT-San	SAN	0.4	65c	16.262	0.049	33934.2	502.1	29911.4	25.2	353.4	24.4	100.5	3.5	29.94	2.54	2436.0	370.0	31.0	0.9	63.8	4.9	510.4	2.1	77.42	1.40	0.11	2.9	0.4	0.026	0.001	73.7	24.28	0.88	0.89
1048-01B	FCT-San	SAN	0.7	65c	16.262	0.049	223172.3	879.4	224297.5	705.0	2908.1	59.4	381.2	4.0	25.43	2.62	2436.0	370.0	31.0	0.9	63.8	4.9	510.4	2.1	77.42	1.40	0.79	21.4	1.6	0.013	0.000	96.7	27.90	0.19	0.21
1048-01C	FCT-San	SAN	1.2	65c	16.262	0.049	208246.7	853.5	208413.4	705.0	2474.1	58.1	358.9	4.1	8.71	2.30	2436.0	370.0	31.0	0.9	63.8	4.9	510.4	2.1	77.42	1.40	0.74	19.9	4.5	0.013	0.000	98.8	28.64	0.19	0.21
1048-01D	FCT-San	SAN	5.0	65c	16.262	0.049	341017.5	1272.8	344869.9	1120.4	4054.5	55.6	545.7	4.4	17.10	2.50	2436.0	370.0	31.0	0.9	63.8	4.9	510.4	2.1	77.42	1.40	1.22	33.0	3.5	0.012	0.000	98.6	28.27	0.17	0.19
1048-01E	FCT-San	SAN	8.0	65c	16.262	0.049	235027.7	631.8	238426.1	94.4	2818.8	27.9	373.5	3.8	14.75	2.58	3628.0	350.0	35.4	1.4	65.6	3.6	516.0	2.2	84.05	1.50	0.84	22.8	2.8	0.012	0.000	98.2	28.07	0.14	0.16
1050-01A	*FCT-San*	*SAN*	*0.5*	*65c*	*16.209*	*0.049*	*130743.3*	*1017.2*	*134729.1*	*64.2*	*1621.4*	*15.5*	*246.9*	*5.5*	*17.91*	*2.66*	*3628.0*	*350.0*	*35.4*	*1.4*	*65.6*	*3.6*	*516.0*	*2.2*	*84.05*	*1.50*	*0.48*	*17.4*	*1.5*	*0.014*	*0.000*	*96.0*	*26.93*	*0.29*	*0.30*
1050-01B	*FCT-San*	*SAN*	*0.8*	*65c*	*16.209*	*0.049*	*216754.7*	*1546.6*	*227532.2*	*352.5*	*2719.2*	*29.2*	*370.2*	*6.0*	*13.92*	*2.47*	*3628.0*	*350.0*	*35.4*	*1.4*	*65.6*	*3.6*	*516.0*	*2.2*	*84.05*	*1.50*	*0.80*	*29.3*	*2.9*	*0.013*	*0.000*	*98.1*	*27.04*	*0.23*	*0.25*
1050-01C	*FCT-San*	*SAN*	*1.8*	*65c*	*16.209*	*0.049*	*81768.9*	*754.8*	*88341.5*	*264.4*	*1080.7*	*27.9*	*143.4*	*5.2*	*1.93*	*2.45*	*3628.0*	*350.0*	*35.4*	*1.4*	*65.6*	*3.6*	*516.0*	*2.2*	*84.05*	*1.50*	*0.31*	*11.4*	*8.2*	*0.013*	*0.000*	*99.4*	*26.60*	*0.36*	*0.37*
1050-01D	*FCT-San*	*SAN*	*8.0*	*65c*	*16.209*	*0.049*	*308414.7*	*2343.0*	*325442.8*	*1258.8*	*3854.5*	*85.7*	*490.2*	*6.5*	*6.84*	*2.55*	*3628.0*	*350.0*	*35.4*	*1.4*	*65.6*	*3.6*	*516.0*	*2.2*	*84.05*	*1.50*	*1.15*	*41.9*	*7.9*	*0.012*	*0.000*	*99.4*	*27.24*	*0.25*	*0.27*
1052-01A	*FCT-San*	*SAN*	*0.5*	*65c*	*16.181*	*0.049*	*220333.2*	*1034.5*	*227874.4*	*81.8*	*2831.7*	*42.1*	*368.4*	*4.2*	*28.32*	*4.10*	*12433.0*	*340.0*	*61.5*	*1.2*	*192.9*	*6.9*	*572.1*	*2.0*	*219.63*	*2.50*	*0.80*	*16.7*	*1.8*	*0.016*	*0.000*	*96.2*	*26.86*	*0.21*	*0.23*
1052-01B	*FCT-San*	*SAN*	*0.8*	*65c*	*16.181*	*0.049*	*118925.4*	*717.6*	*124464.8*	*56.7*	*1613.6*	*34.7*	*190.2*	*4.2*	*9.83*	*4.32*	*12433.0*	*340.0*	*61.5*	*1.2*	*192.9*	*6.9*	*572.1*	*2.0*	*219.63*	*2.50*	*0.44*	*9.1*	*2.6*	*0.015*	*0.000*	*97.6*	*26.92*	*0.35*	*0.36*
1052-01C	*FCT-San*	*SAN*	*1.8*	*65c*	*16.181*	*0.049*	*768680.3*	*3107.2*	*815213.3*	*151.1*	*9959.5*	*52.1*	*1115.7*	*5.1*	*37.07*	*4.12*	*12433.0*	*340.0*	*61.5*	*1.2*	*192.9*	*6.9*	*572.1*	*2.0*	*219.63*	*2.50*	*2.88*	*59.8*	*4.1*	*0.013*	*0.000*	*98.6*	*26.84*	*0.14*	*0.16*
1052-01D	*FCT-San*	*SAN*	*8.0*	*65c*	*16.181*	*0.049*	*178797.6*	*891.8*	*187289.3*	*80.6*	*2313.3*	*33.4*	*245.7*	*4.2*	*29.31*	*4.27*	*12433.0*	*340.0*	*61.5*	*1.2*	*192.9*	*6.9*	*572.1*	*2.0*	*219.63*	*2.50*	*0.66*	*13.7*	*1.1*	*0.013*	*0.000*	*95.2*	*26.23*	*0.25*	*0.26*
1052-01E	*FCT-San*	*SAN*	*7.0*	*65c*	*16.181*	*0.049*	*11619.6*	*476.9*	*8094.7*	*15.2*	*88.9*	*18.1*	*13.8*	*3.5*	*3.54*	*4.21*	*12688.0*	*310.0*	*62.2*	*1.7*	*206.7*	*10.0*	*571.0*	*2.0*	*226.29*	*2.10*	*0.03*	*0.6*	*0.5*	*0.016*	*0.004*	*90.9*	*37.61*	*4.75*	*4.75*
1034-02A	FCT-San	SAN	5.0	65a	16.784	0.050	1175907.0	3213.7	1242485.0	226.6	14931.3	98.3	797.2	6.7	68.62	3.40	18099.0	350.0	23.0	0.8	108.2	4.2	241.6	1.4	131.44	1.90	4.38	100.0	4.2	0.016	0.000	98.3	27.85	0.11	0.14
1036-02A	FCT-San	SAN	5.0	65a	16.780	0.050	1184701.0	3457.0	1266916.0	214.0	15096.3	76.9	711.1	6.6	35.10	3.28	18099.0	350.0	23.0	0.8	108.0	4.0	241.6	1.4	131.40	1.90	4.47	100.0	7.3	0.014	0.000	99.2	27.75	0.11	0.14
1038-01A	FCT-San	SAN	5.0	65a	16.780	0.050	1244837.0	922.0	1331445.0	214.0	15860.4	62.0	819.0	5.2	44.61	3.20	18940.0	380.0	23.6	0.9	110.0	7.0	241.3	1.4	126.90	1.80	4.70	100.0	6.7	0.016	0.000	99.0	27.70	0.08	0.11
1040-01A	FCT-San	SAN	5.0	65a	16.780	0.050	1645707.0	1102.4	1742097.0	239.2	21243.5	70.8	1019.0	5.7	87.58	3.46	18940.0	380.0	23.6	0.9	110.0	7.0	241.3	1.4	126.90	1.80	6.15	100.0	4.3	0.015	0.000	98.5	27.84	0.08	0.11
1042-01A	FCT-San	SAN	5.0	65b	16.460	0.040	1606527.0	1093.1	1670095.0	239.2	20224.6	104.7	946.2	5.6	59.54	3.64	18940.0	380.0	23.6	0.9	110.0	7.0	241.3	1.4	126.90	1.80	5.89	100.0	5.8	0.015	0.000	99.0	27.94	0.08	0.11
1044-01A	FCT-San	SAN	5.0	65b	16.460	0.040	1329503.0	1035.2	1382691.0	226.6	16837.7	74.6	769.6	5.5	46.35	3.41	18940.0	380.0	23.6	0.9	110.0	7.0	241.3	1.4	126.90	1.80	4.88	100.0	6.1	0.014	0.000	99.0	27.94	0.08	0.11
1046-01A	FCT-San	SAN	5.0	65b	16.460	0.040	1097786.0	862.6	1138757.0	226.6	13727.7	78.4	673.5	4.8	26.84	3.36	20453.0	380.0	25.5	1.4	142.0	7.0	249.4	1.3	132.00	1.90	4.02	100.0	9.2	0.015	0.000	99.3	28.10	0.08	0.11
1054-01A	FCT-San	SAN	5.0	65c	16.120	0.050	1147273.0	931.9	1155075.0	201.4	13590.6	163.8	639.1	4.6	51.21	3.40	20453.0	380.0	25.5	1.4	142.0	7.0	249.4	1.3	132.00	1.90	4.08	100.0	4.6	0.014	0.000	98.7	28.19	0.08	0.12
1052-02A	FCT-San	SAN	5.0	65c	16.180	0.050	1164926.0	1058.0	1177825.0	214.0	13895.2	151.2	742.0	5.3	95.09	3.79	20453.0	380.0	25.5	1.4	142.0	7.0	249.4	1.3	132.00	1.90	4.16	100.0	2.9	0.016	0.000	97.6	27.86	0.08	0.12
1050-02A	FCT-San	SAN	5.0	65c	16.210	0.050	1050026.0	566.8	1076080.0	226.6	13035.7	93.3	575.5	3.3	21.27	3.09	18784.0	360.0	24.5	1.4	136.0	6.0	248.5	1.5	133.00	1.80	3.80	100.0	10.0	0.014	0.000	99.5	28.05	0.08	0.11
1048-02A	FCT-San	SAN	5.0	65c	16.260	0.050	1737709.0	567.0	1759779.0	251.8	21344.4	70.7	886.0	3.7	58.58	3.31	18784.0	360.0	24.5	1.4	136.0	6.0	248.5	1.5	133.00	1.80	6.21	100.0	5.6	0.013	0.000	99.1	28.36	0.07	0.11
1056-02A	*FCT-San*	*SAN*	*5.0*	*65d*	*16.560*	*0.090*	*1190637.0*	*552.2*	*1228287.0*	*239.2*	*14603.2*	*49.4*	*608.8*	*3.7*	*25.33*	*3.42*	*18784.0*	*360.0*	*24.5*	*1.4*	*136.0*	*6.0*	*248.5*	*1.5*	*133.00*	*1.80*	*4.33*	*100.0*	*8.8*	*0.013*	*0.000*	*99.4*	*28.44*	*0.08*	*0.17*
1058-02A	FCT-San	SAN	6.0	65d	16.670	0.060	1155534.0	3249.9	1215465.0	214.0	14337.6	138.7	554.9	5.7	19.40	3.11	12695.0	370.0	20.2	0.9	76.0	8.0	222.4	1.3	110.70	1.50	4.29	100.0	12.3	0.014	0.000	99.6	28.12	0.11	0.15
1060-02A	FCT-San	SAN	6.0	65d	16.780	0.060	1422816.0	3945.7	1493797.0	226.6	18179.8	92.2	695.9	6.4	64.40	3.33	12695.0	370.0	20.2	0.9	76.0	8.0	222.4	1.3	110.70	1.50	5.27	100.0	4.6	0.014	0.000	98.7	28.12	0.11	0.15
1062-02A	*FCT-San*	*SAN*	*6.0*	*65d*	*16.910*	*0.090*	*1074139.0*	*3030.7*	*1122275.0*	*115.8*	*13626.7*	*40.4*	*522.7*	*5.5*	*25.70*	*2.52*	*16002.0*	*350.0*	*33.5*	*1.9*	*118.0*	*3.0*	*226.7*	*1.3*	*111.10*	*1.70*	*3.96*	*100.0*	*8.7*	*0.014*	*0.000*	*99.4*	*28.67*	*0.11*	*0.20*

Notes:
a: Relative isotopic abundances corrected for blank, radioactive decay, and mass discrimination
b: 4-digit number indicates the RunID number in Mass Spec, -01 denotes the aliquot number, letter suffix indicates the heating step
c: Number indicates the irradiation batch number, letter refers to the tube in which the sample was loaded in the irradiation can. Rads #64 and #65 were both 960 MWH, done in medium-flux positions at McMaster Nuclear Reactor (positions 8D and 8C, respectively), with Cd shielding.
Data in italics were analyses excluded from integrated age calculations.
All negative values in the table were replaced with "0".
Decay constants and isotopic abundances after Steiger and Jäger (1977).
Ages calculated relative to PP20 Hornblende flux monitor at 1074 Ma (Jourdan et al., 2006)
Nucleogenic interference correction factors (±2σ)
(^{39}Ar/^{37}Ar)Ca = 0.0007 ± 0.000054
(^{36}Ar/^{37}Ar)Ca = 0.00028 ± 0.00017
(^{40}Ar/^{39}Ar)K = 0.003 ± 0.005
Bkgd = background

Appendix B

Table A2. Analytical data for GA-1550 biotite secondary standards from irradiation batch #66.

Lab ID#[b]	Sample	Material	Watts	Irrad.[c]	J		Relative isotopic abundances[a]										Background relative isotopic abundances										Derived results								w/±J
							^{40}Ar		^{39}Ar		^{38}Ar		^{37}Ar		^{36}Ar		^{40}Ar Bkgd		^{39}Ar Bkgd		^{38}Ar Bkgd		^{37}Ar Bkgd		^{36}Ar Bkgd		^{39}Ar Mol	^{39}Ar %	%(^{36}Ar)$_{Ca}$	Ca/K		%^{40}Ar*	Age (Ma)		
					(x 10^{-3})	±1σ		±1σ		±1σ		±1σ		±1σ		±1σ		±1σ		±1σ		±1σ		±1σ		±1σ	x 10^{-14}	of total			±1σ			±1σ	±1σ
1066-01A	*GA-1550*	*BT*	*0.3*	*66a*	*1.990*	*0.010*	*27748.3*	*54.2*	*318.4*	*4.1*	*191.6*	*5.6*	*5.22*	*5.90*	*68.80*	*4.88*	*9861.4*	*20.0*	*43.3*	*1.6*	*227.1*	*2.4*	*420.5*	*3.8*	*129.49*	*2.60*	*0.00112*	*0.5*	*0.01*	*0.0877*	*0.0992*	*26.0*	*79.35*	*15.75*	*15.76*
1066-01B	*GA-1550*	*BT*	*0.5*	*66a*	*1.990*	*0.010*	*26645.5*	*37.3*	*642.8*	*5.8*	*297.1*	*4.5*	*0*	*6.29*	*20.46*	*4.24*	*9581.2*	*20.0*	*40.8*	*2.6*	*225.7*	*2.5*	*426.1*	*3.8*	*133.12*	*2.30*	*0.00227*	*1.1*	*0.00*	*0*	*0.0524*	*77.1*	*111.01*	*6.72*	*6.74*
1066-01C	*GA-1550*	*BT*	*0.8*	*66a*	*1.990*	*0.010*	*202050.7*	*86.7*	*6791.0*	*16.6*	*3119.2*	*11.3*	*0*	*5.21*	*1.98*	*3.90*	*9581.2*	*20.0*	*40.8*	*2.6*	*225.7*	*2.5*	*426.1*	*3.8*	*133.12*	*2.30*	*0.02395*	*11.5*	*0.00*	*0*	*0.0041*	*99.8*	*103.29*	*0.63*	*0.81*
1066-01D	*GA-1550*	*BT*	*1.0*	*66a*	*1.990*	*0.010*	*406005.5*	*152.4*	*14038.2*	*22.8*	*6442.7*	*16.2*	*4.45*	*5.74*	*0*	*4.01*	*9581.2*	*20.0*	*40.8*	*2.6*	*225.7*	*2.5*	*426.1*	*3.8*	*133.12*	*2.30*	*0.04951*	*23.7*	*0.00*	*0.0017*	*0.0022*	*100.1*	*100.81*	*0.33*	*0.59*
1066-01E	*GA-1550*	*BT*	*1.2*	*66a*	*1.990*	*0.010*	*335326.9*	*103.8*	*11534.4*	*35.4*	*5187.7*	*12.5*	*0*	*5.40*	*0*	*5.77*	*9428.4*	*25.0*	*49.0*	*3.0*	*237.4*	*2.3*	*426.2*	*3.7*	*142.25*	*4.20*	*0.04068*	*19.5*	*0.03*	*0*	*0.0025*	*101.8*	*103.02*	*0.59*	*0.78*
1066-01F	*GA-1550*	*BT*	*1.5*	*66a*	*1.990*	*0.010*	*162998.1*	*71.2*	*5678.8*	*12.3*	*2522.1*	*11.9*	*8.88*	*5.86*	*0*	*4.87*	*9428.4*	*25.0*	*49.0*	*3.0*	*237.4*	*2.3*	*426.2*	*3.7*	*142.25*	*4.20*	*0.02003*	*9.6*	*0.00*	*0.0084*	*0.0055*	*103.4*	*103.28*	*0.90*	*1.03*
1066-01G	*GA-1550*	*BT*	*1.7*	*66a*	*1.990*	*0.010*	*262869.3*	*178.0*	*9165.8*	*20.4*	*4022.2*	*13.7*	*0*	*5.76*	*0*	*5.33*	*9428.4*	*25.0*	*49.0*	*3.0*	*237.4*	*2.3*	*426.2*	*3.7*	*142.25*	*4.20*	*0.03233*	*15.5*	*0.07*	*0*	*0.0034*	*102.9*	*102.72*	*0.63*	*0.81*
1066-01H	*GA-1550*	*BT*	*2.0*	*66a*	*1.990*	*0.010*	*117643.9*	*62.3*	*4065.7*	*16.5*	*1806.3*	*7.5*	*5.11*	*6.70*	*0*	*4.51*	*9394.7*	*23.0*	*43.4*	*1.8*	*224.3*	*2.4*	*414.8*	*3.4*	*131.10*	*3.10*	*0.01434*	*6.9*	*0.00*	*0.0067*	*0.0088*	*101.2*	*101.91*	*1.19*	*1.29*
1066-01I	*GA-1550*	*BT*	*2.5*	*66a*	*1.990*	*0.010*	*95876.3*	*62.3*	*3348.2*	*12.1*	*1512.0*	*7.7*	*13.94*	*5.38*	*0*	*3.96*	*9394.7*	*23.0*	*43.4*	*1.8*	*224.3*	*2.4*	*414.8*	*3.4*	*131.10*	*3.10*	*0.01181*	*5.7*	*0.00*	*0.0223*	*0.0086*	*100.3*	*100.06*	*1.25*	*1.34*
1066-01J	*GA-1550*	*BT*	*5.0*	*66a*	*1.990*	*0.010*	*103766.5*	*94.7*	*3594.7*	*12.7*	*1577.6*	*7.9*	*0*	*5.77*	*0*	*4.04*	*9394.7*	*23.0*	*43.4*	*1.8*	*224.3*	*2.4*	*414.8*	*3.4*	*131.10*	*3.10*	*0.01268*	*6.1*	*0.19*	*0*	*0.0086*	*102.8*	*103.23*	*1.20*	*1.30*
1102-01A	*GA-1550*	*BT*	*0.3*	*66e*	*2.122*	*0.006*	148254.9	83.8	*2796.9*	*10.8*	*1382.6*	*7.9*	*0*	*6.35*	*272.92*	*6.81*	8985.3	18.0	37.9	1.2	206.3	3.1	394.3	3.5	114.79	3.50	*0.00986*	*5.6*	*0.00*	*0*	*0.0131*	*45.0*	*88.98*	*2.67*	*2.68*
1102-01B	GA-1550	BT	0.4	66e	2.122	0.006	128981.0	83.8	4528.4	13.9	2182.8	9.3	0	5.36	36.55	4.49	8985.3	18.0	37.9	1.2	206.3	3.1	394.3	3.5	114.79	3.50	0.01597	9.0	0.00	0	0.0068	91.6	96.98	1.11	1.15
1102-01C	GA-1550	BT	0.5	66e	2.122	0.006	233246.1	99.8	8370.3	18.9	3926.0	14.0	0	5.37	48.13	4.86	8985.3	18.0	37.9	1.2	206.3	3.1	394.3	3.5	114.79	3.50	0.02952	16.6	0.00	0	0.0037	93.9	97.25	0.67	0.72
1102-01D	GA-1550	BT	0.6	66e	2.122	0.006	104659.1	70.3	3775.7	13.9	1803.5	8.2	6.47	5.57	28.39	3.13	8970.6	18.0	38.8	1.4	206.7	2.9	382.2	3.8	120.84	2.00	0.01332	7.5	0.02	0.0099	0.0085	91.9	94.81	0.96	1.00
1102-01E	GA-1550	BT	0.7	66e	2.122	0.006	205721.8	98.6	7566.1	18.9	3512.3	14.0	0	5.30	8.76	3.86	8970.6	18.0	38.8	1.4	206.7	2.9	382.2	3.8	120.84	2.00	0.02669	15.0	0.00	0	0.0040	98.8	99.77	0.61	0.66
1102-01F	GA-1550	BT	0.8	66e	2.122	0.006	90839.8	75.2	3337.7	13.9	1575.5	7.6	0	5.65	6.05	3.18	8970.6	18.0	38.8	1.4	206.7	2.9	382.2	3.8	120.84	2.00	0.01177	6.6	0.00	0	0.0098	98.1	99.16	1.11	1.14
1102-01G	GA-1550	BT	0.9	66e	2.122	0.006	184851.2	70.9	6565.1	15.1	3076.1	11.2	7.60	5.98	49.07	3.38	8936.8	24.0	36.9	1.1	198.9	2.8	371.3	3.4	112.14	2.00	0.02316	13.0	0.01	0.0067	0.0053	92.1	96.44	0.60	0.66
1102-01H	GA-1550	BT	1.0	66e	2.122	0.006	84948.6	52.4	3060.4	17.7	1452.0	9.3	20.66	5.39	19.38	3.36	8936.8	24.0	36.9	1.1	198.9	2.8	371.3	3.4	112.14	2.00	0.01079	6.1	0.09	0.0390	0.0102	93.2	96.24	1.31	1.34
1102-01I	*GA-1550*	*BT*	*1.1*	*66e*	*2.122*	*0.006*	*21160.5*	*40.6*	*769.3*	*6.4*	*357.5*	*5.6*	*10.52*	*5.29*	*19.13*	*3.31*	*8936.8*	*24.0*	*36.9*	*1.1*	*198.9*	*2.8*	*371.3*	*3.4*	*112.14*	*2.00*	*0.00271*	*1.5*	*0.05*	*0.0791*	*0.0398*	*73.0*	*75.12*	*4.75*	*4.76*
1102-01J	*GA-1550*	*BT*	*1.2*	*66e*	*2.122*	*0.006*	*28137.4*	*58.1*	*1015.3*	*6.9*	*496.5*	*5.4*	*5.63*	*6.55*	*0*	*3.03*	*8964.9*	*29.0*	*35.6*	*1.1*	*200.1*	*2.1*	*374.7*	*4.2*	*113.45*	*1.90*	*0.00358*	*2.0*	*0.00*	*0.0321*	*0.0373*	*106.6*	*109.42*	*3.30*	*3.31*
1102-01K	GA-1550	BT	1.5	66e	2.122	0.006	214692.5	91.6	7891.8	18.9	3656.5	13.6	0	6.55	19.08	3.49	8964.9	29.0	35.6	1.1	200.1	2.1	374.7	4.2	113.45	1.90	0.02783	15.7	0.00	0	0.0048	97.4	98.46	0.53	0.60
1102-01L	GA-1550	BT	1.7	66e	2.122	0.006	10262.5	42.8	320.6	4.7	146.2	4.0	10.66	5.92	0.89	3.73	8964.9	29.0	35.6	1.1	200.1	2.1	374.7	4.2	113.45	1.90	0.00113	0.6	0.98	0.1925	0.1069	97.5	115.43	12.59	12.59
1102-01M	GA-1550	BT	2.0	66e	2.122	0.006	4376.3	41.0	59.9	2.7	35.5	3.9	0	6.74	10.71	3.38	8964.9	29.0	35.6	1.1	200.1	2.1	374.7	4.2	113.45	1.90	0.00021	0.1	0.00	0	0.6535	26.8	73.40	62.09	62.09
1102-01N	GA-1550	BT	2.5	66e	2.122	0.006	9234.1	30.9	144.9	4.8	89.2	4.5	6.32	5.33	20.09	3.84	8958.4	16.0	33.5	1.1	193.5	2.1	374.4	3.3	114.44	1.90	0.00051	0.3	0.03	0.2528	0.2131	35.0	83.41	29.04	29.04
1102-01O	GA-1550	BT	5.0	66e	2.122	0.006	49211.0	52.8	183.0	3.0	114.6	4.5	0.12	4.77	157.41	5.08	8958.4	16.0	33.5	1.1	193.5	2.1	374.4	3.3	114.44	1.90	0.00065	0.4	0.00	0.0039	0.1510	4.5	45.55	30.93	30.93
1086-01A	GA-1550	BT	0.3	66c	2.175	0.006	14167.2	35.2	266.7	4.5	141.9	4.9	27.65	5.45	40.59	5.11	8075.5	13.0	29.0	1.1	166.3	2.5	312.3	3.2	94.88	3.10	0.00094	0.8	0.06	0.6920	0.1369	14.5	29.84	22.09	22.09
1086-01B	GA-1550	BT	0.5	66c	2.175	0.006	35889.5	38.8	1144.4	7.3	584.8	6.6	9.53	5.43	29.25	3.96	8075.5	13.0	29.0	1.1	166.3	2.5	312.3	3.2	94.88	3.10	0.00404	3.5	0.03	0.0556	0.0317	75.7	90.60	3.89	3.90
1086-01C	GA-1550	BT	0.7	66c	2.175	0.006	137047.0	104.0	4747.7	15.1	2486.6	14.4	26.07	5.77	50.32	4.06	8075.5	13.0	29.0	1.1	166.3	2.5	312.3	3.2	94.88	3.10	0.01675	14.6	0.05	0.0367	0.0081	89.1	97.94	1.00	1.03
1086-01D	GA-1550	BT	0.8	66c	2.175	0.006	54881.2	58.1	2044.5	8.6	1065.8	10.0	23.77	5.88	13.81	4.03	8075.5	13.0	29.0	1.1	166.3	2.5	312.3	3.2	94.88	3.10	0.00721	6.3	0.16	0.0776	0.0192	92.6	94.69	2.23	2.24
1086-01E	GA-1550	BT	0.9	66c	2.175	0.006	158679.2	81.6	5879.2	15.1	3078.8	17.1	10.57	6.01	3.47	2.94	8024.5	19.0	30.3	0.9	171.0	2.2	323.2	3.6	101.34	1.60	0.02074	18.1	0.29	0.0120	0.0068	99.4	102.06	0.61	0.67
1086-01F	GA-1550	BT	1.0	66c	2.175	0.006	38675.2	62.1	1431.3	6.9	744.4	7.5	16.30	6.36	0	2.72	8024.5	19.0	30.3	0.9	171.0	2.2	323.2	3.6	101.34	1.60	0.00505	4.4	0.00	0.0761	0.0297	101.2	103.95	2.16	2.18
1086-01G	GA-1550	BT	1.2	66c	2.175	0.006	42357.7	50.3	1603.7	7.4	823.2	7.0	23.70	7.42	0.69	3.40	8024.5	19.0	30.3	0.9	171.0	2.2	323.2	3.6	101.34	1.60	0.00566	4.9	3.28	0.0988	0.0309	99.6	100.11	2.39	2.41
1086-01H	GA-1550	BT	1.5	66c	2.175	0.006	125188.6	63.3	4690.3	20.2	2446.1	13.6	15.86	5.63	14.30	3.31	8024.5	19.0	30.3	0.9	171.0	2.2	323.2	3.6	101.34	1.60	0.01654	14.5	0.11	0.0226	0.0080	96.7	98.23	0.89	0.93
1086-01I	GA-1550	BT	1.7	66c	2.175	0.006	48582.8	56.2	1809.5	8.6	938.6	7.6	18.48	5.68	8.10	3.25	7924.5	15.0	34.8	1.9	169.3	1.9	323.9	2.7	97.14	2.10	0.00638	5.6	0.22	0.0683	0.0210	95.1	97.24	2.05	2.07
1086-01J	GA-1550	BT	2.0	66c	2.175	0.006	52062.0	47.7	1937.7	10.0	1001.1	8.8	14.33	5.06	5.95	2.78	7924.5	15.0	34.8	1.9	169.3	1.9	323.9	2.7	97.14	2.10	0.00683	6.0	0.23	0.0495	0.0175	96.7	98.87	1.67	1.69
1086-01K	GA-1550	BT	2.5	66c	2.175	0.006	59748.3	57.4	2255.8	7.4	1177.6	7.5	10.06	5.25	4.87	2.93	7924.5	15.0	34.8	1.9	169.3	1.9	323.9	2.7	97.14	2.10	0.00796	7.0	0.20	0.0298	0.0156	97.6	98.46	1.48	1.50
1086-01L	GA-1550	BT	5.0	66c	2.175	0.006	121062.1	54.2	4626.1	12.7	2372.5	12.8	21.61	4.79	0.23	4.31	7879.4	23.0	31.3	1.3	166.8	1.9	324.5	2.9	103.93	1.90	0.01632	14.3	8.89	0.0313	0.0069	100.0	99.62	1.07	1.10
1095-01A	GA-1550	BT	0.3	66d	2.229	0.010	104626.4	84.7	3425.4	10.3	1776.1	11.9	6.04	4.96	74.31	3.57	7944.5	22.0	31.4	1.1	166.8	2.4	322.7	3.3	92.03	1.70	0.01208	14.1	0.01	0.0119	0.0098	78.8	94.09	1.22	1.28
1095-01B	GA-1550	BT	0.5	66d	2.229	0.010	152044.4	85.9	5665.1	15.1	2832.8	15.0	0	6.53	31.39	4.77	7944.5	22.0	31.4	1.1	166.8	2.4	322.7	3.3	92.03	1.70	0.01998	23.4	0.00	0	0.0078	93.9	98.34	0.99	1.08
1095-01C	GA-1550	BT	0.7	66d	2.229	0.010	95737.8	59.7	3600.3	9.9	1787.5	12.4	0	5.84	16.32	3.93	7998.2	19.0	27.6	0.9	173.3	2.4	330.7	3.5	96.85	2.40	0.01270	14.9	0.00	0	0.0110	95.0	98.54	1.27	1.34
1095-01D	GA-1550	BT	0.8	66d	2.229	0.010	25578.5	38.9	954.6	6.7	479.8	6.4	0	6.78	15.85	3.44	7998.2	19.0	27.6	0.9	173.3	2.4	330.7	3.5	96.85	2.40	0.00337	3.9	0.00	0	0.0482	81.5	85.56	4.17	4.19
1095-01E	GA-1550	BT	0.9	66d	2.229	0.010	39798.8	49.1	1493.9	10.0	739.8	6.4	0	5.80	5.93	3.35	7998.2	19.0	27.6	0.9	173.3	2.4	330.7	3.5	96.85	2.40	0.00527	6.2	0.00	0	0.0264	95.6	99.37	2.63	2.67
1095-01F	GA-1550	BT	1.0	66d	2.229	0.010	78948.6	55.0	2912.1	11.6	1434.0	10.9	0	5.96	17.06	3.48	7998.2	19.0	27.6	0.9	173.3	2.4	330.7	3.5	96.85	2.40	0.01027	12.0	0.00	0	0.0139	93.6	99.01	1.41	1.47
1095-01G	GA-1550	BT	1.2	66d	2.229	0.010	74301.2	62.5	2775.0	11.3	1159.3	8.6	0	5.14	9.11	3.20	7981.8	20.0	24.3	1.8	166.6	2.3	318.4	3.0	98.75	1.90	0.00979	11.4	0.00	0	0.0126	96.4	100.65	1.37	1.44
1095-01H	GA-1550	BT	1.5	66d	2.229	0.010	37715.6	48.4	1375.4	6.5	594.9	7.3	1.19	4.75	16.19	3.86	7981.8	20.0	24.3	1.8	166.6	2.3	318.4	3.0	98.75	1.90	0.00485	5.7	0.01	0.0059	0.0235	87.2	93.46	3.23	3.26
1095-01I	GA-1550	BT	1.7	66d	2.229	0.010	33581.9	57.7	1223.2	7.6	514.3	5.7	11.15	4.75	4.85	2.90	7981.8	20.0	24.3	1.8	166.6	2.3	318.4	3.0	98.75	1.90	0.00431	5.0	0.22	0.0619	0.0264	95.7	102.47	2.77	2.80
1095-01J	GA-1550	BT	2.0	66d	2.229	0.010	6525.6	31.5	248.1	5.0	105.6	3.5	0	4.75	0	3.32	7983.1	15.0	28.8	1.0	171.6	2.0	325.6	3.4	109.68	2.70	0.00088	1.0	0.00	0	0.1301	148.4	150.07	15.07	15.09
1095-01K	GA-1550	BT	2.5	66d	2.229	0.010	13600.3	48.9	515.0	3.9	220.7	4.5	0	5.29	0	4.20	7983.1	15.0	28.8	1.0	171.6	2.0	325.6	3.4	109.68	2.70	0.00182	2.1	0.02	0	0.0698	137.5	140.01	9.12	9.14
1095-01L	GA-1550	BT	5.0	66d	2.229	0.010	1627.3	28.2	55.8	2.1	24.9	3.7	0	5.20	0	3.73	7983.1	15.0	28.8	1.0	171.6	2.0	325.6	3.4	109.68	2.70	0.00020	0.2	0.04	0	0.6335	306.3	326.72	67.88	67.90
1095-02A	GA-1550	BT	0.3	66d	2.229	0.010	129050.7	79.7	3528.8	11.5	1775.3	11.6	0.44	2.72	145.53	2.68	7991.1	16.0	16.5	0.8	48.5	1.0	127.2	1.8	76.61	1.30	0.01246	5.5	0.00	0.0062	0.0378	66.4	94.86	0.92	1.00
1095-02B	GA-1550	BT	0.5	66d	2.229	0.010	472030.8	151.9	18116.6	21.4	8851.0	41.1	0	3.19	48.13	2.53	7991.1	16.0	16.5	0.8	48.5	1.0	127.2	1.8	76.61	1.30	0.06395	28.1	0.00	0	0.0086	97.1	98.68	0.20	0.46
1095-02C	GA-1550	BT	0.7	66d	2.229	0.010	238591.1	82.0	9321.1	16.4	4562.8	20.7	2.81	3.35	2.17	2.80	8034.3	15.0	20.0	1.1	47.5	1.3	123.5	2.1	80.36	1.50	0.03290	14.5	0.90	0.0148	0.0176	99.9	99.69	0.38	0.57
1095-02D	GA-1550	BT	0.8	66d	2.229	0.010	202342.8	98.1	7981.3	30.2	3925.6	18.6	0	2.89	7.99	3.77	8034.3	15.0	20.0	1.1	47.5	1.3	123.5	2.1	80.36	1.50	0.02817	12.4	0.00	0	0.0178	99.0	97.88	0.65	0.77
1095-02E	GA-1550	BT	0.9	66d	2.229	0.010	174683.5	78.2	6836.9	21.4	3360.7	17.4	0.37	3.26	0	2.30	8034.3	15.0	20.0	1.1	47.5	1.3	123.5	2.1	80.36	1.50	0.02413	10.6	0.00	0.0026	0.0233	100.4	99.94	0.49	0.65
1095-02F	GA-1550	BT	1.0	66d	2.229	0.010	136300.6	61.0	5374.2	11.0	2560.9	14.2	0	3.16	0	2.22	8034.3	15.0	20.0	1.1	47.5	1.3	123.5	2.1	80.36	1.50	0.01897	8.3	6.45	0	0.0289	100.3	99.20	0.51	0.66
1095-02G	GA-1550	BT	1.2	66d	2.229	0.010	196151.0	94.1	7779.5	15.2	3646.3	21.7	0	3.13	7.04	2.38	7858.4	13.0	13.7	1.2	50.6	1.1	124.9	2.0	73.71	1.60	0.02746	12.1	0.00	0	0.0197	99.1	97.46	0.40	0.57
1095-02H	GA-1550	BT	1.5	66d	2.229	0.010	48772.9	52.0	1927.8	9.3	951.8	9.3	0	3.05	1.06	2.66	7858.4	13.0	13.7	1.2	50.6	1.1	124.9	2.0	73.71	1.60	0.00680	3.0	0.00	0	0.0777	99.5	98.19	1.64	1.69
1095-02I	GA-1550	BT	1.7	66d	2.229	0.010	12355.1	35.2	492.3	4.0	232.8	3.9	0	3.24	3.27	2.29	7858.4	13.0	13.7	1.2	50.6	1.1	124.9	2.0	73.71	1.60	0.00174	0.8	0.00	0	0.3230	92.2	90.44	5.37	5.38
1095-02J	GA-1550	BT	2.0	66d	2.229	0.010	42152.6	60.1	1701.8	12.1	807.5	6.6	4.16	2.84	0	3.37	7744.3	16.0	16.8	0.9	49.2	0.9	121.3	1.7	75.35	1.60	0.00601	2.6	0.00	0.1201	0.0818	101.4	97.94	2.36	2.39

Table A2. (Continued)

Lab ID#[b]	Sample	Material	Watts	Irrad.[c]	J		Relative isotopic abundances[a]										Background relative isotopic abundances										Derived results								
					(x 10^{-3}) ± 1σ		^{40}Ar ±1σ		^{39}Ar ±1σ		^{38}Ar ±1σ		^{37}Ar ±1σ		^{36}Ar ±1σ		^{40}Ar Bkgd ±1σ		^{39}Ar Bkgd ±1σ		^{38}Ar Bkgd ±1σ		^{37}Ar Bkgd ±1σ		^{36}Ar Bkgd ±1σ		^{39}Ar Mol x 10^{-14}	^{39}Ar % of total	%(^{36}Ar)$_{Ca}$	Ca/K ±1σ		%^{40}Ar*	Age (Ma) ±1σ		w/±J ±1σ
1095-02K	GA-1550	BT	2.5	66d	2.229	0.010	15025.3	32.0	610.5	6.2	281.3	3.9	0	2.91	0.82	2.56	7744.3	16.0	16.8	0.9	49.2	0.9	121.3	1.7	75.35	1.60	0.00215	0.9	0.00	0.	0.2344	98.4	94.54	4.86	4.88
1095-02L	GA-1550	BT	5.0	66d	2.229	0.010	19211.8	34.2	757.2	5.1	383.8	4.5	6.77	2.73	0.00	2.37	7744.3	16.0	16.8	0.9	49.2	0.9	121.3	1.7	75.35	1.60	0.00267	1.2	0.00	0.4391	0.1769	103.6	102.37	3.62	3.64
1086-02A	GA-1550	BT	0.3	66c	2.175	0.006	78326.4	57.7	2274.3	10.6	1124.3	7.3	7.23	3.02	70.84	3.09	7744.3	16.0	16.8	0.9	49.2	0.9	121.3	1.7	75.35	1.60	0.00803	8.4	0.07	0.1561	0.0652	73.1	95.91	1.57	1.59
1086-02B	GA-1550	BT	0.5	66c	2.175	0.006	280945.9	99.5	10609.5	15.1	5094.1	24.6	2.96	3.30	16.66	2.57	7651.6	16.0	15.8	1.0	52.2	1.1	124.0	2.4	73.88	1.60	0.03745	39.4	0.12	0.0137	0.0153	98.4	99.12	0.30	0.40
1086-02C	GA-1550	BT	0.7	66c	2.175	0.006	167247.6	85.8	6411.1	12.6	3083.3	16.7	5.89	3.49	15.36	2.58	7651.6	16.0	15.8	1.0	52.2	1.1	124.0	2.4	73.88	1.60	0.02263	23.8	0.27	0.0451	0.0267	97.4	96.75	0.49	0.55
1086-02D	GA-1550	BT	0.8	66c	2.175	0.006	73271.8	66.2	2794.1	7.6	1337.5	9.7	0	3.32	0	2.87	7651.6	16.0	15.8	1.0	52.2	1.1	124.0	2.4	73.88	1.60	0.00986	10.4	1.84	0	0.0584	100.7	100.40	1.17	1.20
1086-02E	GA-1550	BT	0.9	66c	2.175	0.006	65803.2	57.4	2499.8	8.7	1228.8	9.4	4.51	2.70	8.13	2.45	7728.6	15.0	16.8	0.8	46.3	1.2	122.4	1.4	74.97	1.80	0.00882	9.3	0.39	0.0887	0.0531	96.5	96.69	1.14	1.17
1086-02F	GA-1550	BT	1.0	66c	2.175	0.006	16738.0	39.5	646.2	5.0	311.0	3.6	0	2.68	0	2.61	7728.6	15.0	16.8	0.8	46.3	1.2	122.4	1.4	74.97	1.80	0.00228	2.4	1.77	0	0.2040	101.9	100.37	4.53	4.54
1086-02G	GA-1550	BT	1.2	66c	2.175	0.006	17899.8	39.5	714.0	4.1	329.8	4.6	0	2.78	0	2.60	7728.6	15.0	16.8	0.8	46.3	1.2	122.4	1.4	74.97	1.80	0.00252	2.6	0.68	0	0.1914	103.4	98.58	4.08	4.09
1086-02H	GA-1550	BT	1.5	66c	2.175	0.006	17460.1	31.5	667.5	7.8	327.5	3.9	4.90	2.89	0	2.88	7728.6	15.0	16.8	0.8	46.3	1.2	122.4	1.4	74.97	1.80	0.00236	2.5	0.00	0.3609	0.2127	103.0	102.34	4.91	4.92
1086-02I	GA-1550	BT	1.7	66c	2.175	0.006	7891.0	37.8	282.9	3.4	130.9	3.0	0	2.83	0	3.59	7571.9	21.0	18.7	0.9	47.2	1.2	121.4	1.7	75.45	1.30	0.00100	1.0	0.36	0	0.4919	108.7	114.82	14.02	14.02
1086-02L	GA-1550	BT	5.0	66c	2.175	0.006	1644.3	30.9	48.9	1.7	22.0	2.1	1.07	2.83	0	2.61	7571.9	21.0	18.7	0.9	47.2	1.2	121.4	1.7	75.45	1.30	0.00017	0.2	0.00	1.0795	2.8437	100.5	127.54	58.32	58.33
1102-02A	GA-1550	BT	0.3	66e	2.122	0.006	76120.3	65.0	1730.0	8.0	718.0	13.0	0.34	4.36	155.79	5.15	7763.8	24.0	16.7	1.2	47.7	1.0	122.4	1.8	79.51	1.40	0.00610	0.4	0.00	0.010	0.1200	38.9	64.00	3.00	3.30
1102-02B	GA-1550	BT	0.3	66e	2.122	0.006	46981.2	55.8	1262.0	7.0	568.0	11.0	1.71	3.79	49.55	2.99	7763.8	24.0	16.7	1.2	47.7	1.0	122.4	1.8	79.51	1.40	0.00446	0.3	0.02	0.070	0.1500	68.6	95.00	3.00	2.63
1102-02C	GA-1550	BT	0.4	66e	2.122	0.006	196479.9	139.6	5368.0	15.0	2340.0	40.0	8.85	4.11	227.79	5.75	7718.7	18.0	20.3	1.2	47.4	0.9	122.5	2.0	72.75	1.70	0.01895	1.3	0.03	0.080	0.0400	65.5	89.20	1.20	1.22
1102-02D	GA-1550	BT	0.5	66e	2.122	0.006	254824.5	88.7	8305.0	16.0	3670.0	60.0	9.72	3.84	124.20	6.08	7718.7	18.0	20.3	1.2	47.4	0.9	122.5	2.0	72.75	1.70	0.02932	1.9	0.06	0.060	0.0200	85.6	97.50	0.80	0.86
1102-02E	GA-1550	BT	0.6	66e	2.122	0.006	360857.6	152.1	13330.0	20.0	5840.0	90.0	13.24	4.08	51.81	3.39	7718.7	18.0	20.3	1.2	47.4	0.9	122.5	2.0	72.75	1.70	0.04706	3.1	0.18	0.049	0.0150	95.9	96.40	0.30	0.41
1102-02F	GA-1550	BT	0.7	66e	2.122	0.006	483440.9	152.7	18160.0	20.0	7770.0	120.0	3.65	3.87	23.23	3.69	7804.2	22.0	20.1	1.3	48.9	1.4	123.3	1.9	77.48	1.90	0.06411	4.2	0.11	0.010	0.0100	98.7	97.60	0.20	0.37
1102-02G	GA-1550	BT	0.8	66e	2.122	0.006	509055.9	215.1	19340.0	30.0	8280.0	130.0	4.68	4.03	23.29	3.10	7804.2	22.0	20.1	1.3	48.9	1.4	123.3	1.9	77.48	1.90	0.06825	4.5	0.14	0.012	0.0100	98.8	96.60	0.20	0.35
1102-02H	GA-1550	BT	0.8	66e	2.122	0.006	382943.9	119.1	14510.0	30.0	6150.0	100.0	0	4.05	12.43	2.96	7804.2	22.0	20.1	1.3	48.9	1.4	123.3	1.9	77.48	1.90	0.05122	3.4	0.00	0	0.0140	99.2	97.20	0.30	0.41
1102-02I	GA-1550	BT	0.9	66e	2.122	0.006	753700.1	227.7	28630.0	20.0	12200.0	190.0	4.79	3.88	31.52	3.56	7804.2	22.0	20.1	1.3	48.9	1.4	123.3	1.9	77.48	1.90	0.10107	6.7	0.11	0.008	0.0070	98.9	96.71	0.16	0.31
1102-02J	GA-1550	BT	1.0	66e	2.122	0.006	1711253.0	979.7	65900.0	100.0	27700.0	400.0	15.86	17.02	6.34	9.83	7800.2	19.0	17.4	0.9	50.0	1.0	124.7	2.0	78.57	1.70	0.23261	15.4	1.77	0.012	0.0130	100.0	96.50	0.20	0.35
1102-02K	GA-1550	BT	1.1	66e	2.122	0.006	1734865.0	459.6	66660.0	100.0	28000.0	400.0	0	15.95	0	10.21	7800.2	19.0	17.4	0.9	50.0	1.0	124.7	2.0	78.57	1.70	0.23528	15.5	1.65	0	0.0120	100.2	96.90	0.20	0.34
1102-02L	GA-1550	BT	1.2	66e	2.122	0.006	1941735.0	569.7	74010.0	100.0	30500.0	500.0	0	19.00	34.05	11.45	7800.2	19.0	17.4	0.9	50.0	1.0	124.7	2.0	78.57	1.70	0.26125	17.2	0.00	0	0.0130	99.6	97.10	0.20	0.34
1102-02M	GA-1550	BT	1.5	66e	2.122	0.006	2415449.0	796.1	92630.0	130.0	38700.0	600.0	28.15	20.32	13.58	12.28	7800.2	19.0	17.4	0.9	50.0	1.0	124.7	2.0	78.57	1.70	0.32697	21.6	1.46	0.015	0.0110	100.0	96.85	0.20	0.33
1102-02N	GA-1550	BT	1.7	66e	2.122	0.006	269073.9	95.5	10190.0	20.0	4290.0	70.0	10.34	4.47	16.54	3.08	7949.3	21.0	28.5	0.9	52.6	1.0	125.7	2.3	76.94	1.30	0.03596	2.4	0.44	0.050	0.0200	98.3	96.50	0.40	0.47
1102-02O	GA-1550	BT	2.0	66e	2.122	0.006	172511.8	90.6	6515.0	11.0	2780.0	50.0	2.85	4.18	9.00	2.94	7949.3	21.0	28.5	0.9	52.6	1.0	125.7	2.3	76.94	1.30	0.02300	1.5	0.22	0.020	0.0300	98.6	97.00	0.50	0.58
1102-02P	GA-1550	BT	2.5	66e	2.122	0.006	37801.2	44.3	1444.0	8.0	599.0	11.0	0	4.43	3.99	2.46	7949.3	21.0	28.5	0.9	52.6	1.0	125.7	2.3	76.94	1.30	0.00510	0.3	0.00	0	0.1500	97.0	94.40	1.90	1.94
1102-02Q	GA-1550	BT	5.0	66e	2.122	0.006	28389.1	43.0	1085.0	6.0	442.0	9.0	0	3.75	0.50	2.60	7726.2	18.0	16.1	0.8	47.3	0.9	127.7	1.6	75.75	1.30	0.00383	0.3	0.00	0	0.1700	99.6	97.00	3.00	2.66
1066-02A	GA-1550	BT	0.3	66a	1.990	0.010	30048.9	139.5	431.0	4.0	261.0	3.0	0	2.21	64.23	2.71	6666.8	17.0	17.6	1.0	25.1	0.7	88.4	1.7	73.96	1.40	0.00152	0.9	0.00	0	0.9000	36.0	88.00	6.00	6.56
1066-02B	GA-1550	BT	0.5	66a	1.990	0.010	83228.4	57.9	2270.0	15.0	1115.0	8.0	0	2.54	58.75	2.70	6666.8	17.0	17.6	1.0	25.1	0.7	88.4	1.7	73.96	1.40	0.00801	5.0	0.00	0	0.1900	79.0	100.80	1.40	1.46
1066-02C	GA-1550	BT	0.7	66a	1.990	0.010	142459.6	77.4	4796.0	11.0	2295.0	15.0	0	2.63	8.34	2.20	6666.8	17.0	17.6	1.0	25.1	0.7	88.4	1.7	73.96	1.40	0.01693	10.5	0.00	0	0.0900	98.4	101.70	0.50	0.72
1066-02D	GA-1550	BT	0.8	66a	1.990	0.010	123972.3	75.0	4294.0	13.0	2053.0	12.0	0	2.55	0	2.20	6666.8	17.0	17.6	1.0	25.1	0.7	88.4	1.7	73.96	1.40	0.01516	9.4	4.35	0	0.1000	100.9	101.30	0.60	0.78
1066-02E	GA-1550	BT	0.9	66a	1.990	0.010	151819.7	81.8	5286.0	13.0	2500.0	16.0	4.70	2.62	5.51	2.42	6611.5	14.0	16.1	0.9	21.9	0.8	79.6	1.8	68.04	1.60	0.01867	11.6	2.07	0.150	0.0800	99.2	99.10	0.50	0.71
1066-02F	GA-1550	BT	1.0	66a	1.990	0.010	118184.8	79.3	4154.0	12.0	1970.0	12.0	4.37	2.52	1.29	2.40	6611.5	14.0	16.1	0.9	21.9	0.8	79.6	1.8	68.04	1.60	0.01467	9.1	8.19	0.180	0.1000	99.9	98.90	0.60	0.82
1066-02G	GA-1550	BT	1.2	66a	1.990	0.010	153226.8	71.9	5341.0	14.0	2467.0	15.0	5.17	2.61	10.04	2.49	6611.5	14.0	16.1	0.9	21.9	0.8	79.6	1.8	68.04	1.60	0.01886	11.7	1.25	0.160	0.0800	98.3	98.20	0.50	0.72
1066-02H	GA-1550	BT	1.5	66a	1.990	0.010	222403.7	96.6	7706.0	15.0	3560.0	20.0	0	2.58	23.33	2.91	6531.7	13.0	16.0	0.8	24.5	0.9	86.2	1.6	62.19	2.20	0.02721	16.9	0.00	0	0.0600	97.0	97.50	0.40	0.64
1066-02I	GA-1550	BT	1.7	66a	1.990	0.010	88830.3	69.2	3111.0	11.0	1463.0	10.0	0	2.25	5.45	2.98	6531.7	13.0	16.0	0.8	24.5	0.9	86.2	1.6	62.19	2.20	0.01099	6.8	0.00	0	0.1200	98.4	97.80	1.00	1.13
1066-02J	GA-1550	BT	2.0	66a	1.990	0.010	119430.3	59.3	4177.0	12.0	1973.0	14.0	0	2.41	11.06	2.90	6531.7	13.0	16.0	0.8	24.5	0.9	86.2	1.6	62.19	2.20	0.01475	9.1	0.00	0	0.1000	97.4	97.00	0.80	0.90
1066-02K	GA-1550	BT	2.5	66a	1.990	0.010	55647.2	45.9	1968.0	6.0	918.0	8.0	0	2.64	5.80	2.51	6433.8	13.0	14.7	0.8	21.8	0.9	82.7	1.8	62.64	1.50	0.00695	4.3	0.00	0	0.2000	97.1	95.60	1.30	1.41
1066-02L	GA-1550	BT	5.0	66a	1.990	0.010	60628.6	47.1	2117.0	8.0	997.0	8.0	0	2.66	10.97	2.61	6433.8	13.0	14.7	0.8	21.8	0.9	82.7	1.8	62.64	1.50	0.00747	4.6	0.00	0	0.2000	94.8	94.60	1.30	1.39

Notes:
a: Relative isotopic abundances corrected for blank, radioactive decay, and mass discrimination
b: 4-digit number indicates the RunID number in Mass Spec, -01 denotes the aliquot number, letter suffix indicates the heating step
c: Number indicates the irradiation batch number, letter refers to the tube in which the sample was loaded in the irradiation can. Rad#66 was irradiated for 160 MWH in medium-flux position 8A at McMaster Nuclear Reactor (no Cd shielding).
Data in italics were analyses excluded from integrated age calculation.
All negative values in the table were replaced with "0".
Decay constants and isotopic abundances after Steiger and Jäger (1977).
Ages calculated relative to FCT-San Fish Canyon Tuff sanidine flux monitor at 28.02 Ma (Renne et al., 1998)
Nucleogenic interference correction factors (±2σ)
(^{39}Ar/^{37}Ar)Ca = 0.0007 ± 0.000054
(^{36}Ar/^{37}Ar)Ca = 0.00028 ± 0.00017
(^{40}Ar/^{39}Ar)K = 0.058 ± 0.005
Bkgd = background

Appendix C

Table A3. Analytical data for PP20 hornblende secondary standards from irradiation batch #66.

							Relative isotopic abundances[a]										Background relative isotopic abundances										Derived results									
					J		^{40}Ar		^{39}Ar		^{38}Ar		^{37}Ar		^{36}Ar		^{40}Ar Bkgd		^{39}Ar Bkgd		^{38}Ar Bkgd		^{37}Ar Bkgd		^{36}Ar Bkgd		^{39}Ar Mol	^{39}Ar %	%(^{36}Ar)$_{Ca}$	Ca/K		%^{40}Ar*	Age (Ma)		w/±*J*
Lab ID#[b]	Sample	Material	Watts	Irrad.[c]	(x 10^{-3})	±1σ	±1σ		±1σ		±1σ		±1σ		±1σ		±1σ		±1σ		±1σ		±1σ		±1σ		x 10^{-14}	of total		±1σ			±1σ		±1σ
1071-01A	*PP20*	*HBL*	*1.0*	*66a*	*1.944*	*0.010*	*5838.0*	*36.0*	*10.4*	*2.8*	*13.8*	*3.8*	*17.9*	*5.4*	*0*	*4.313*	*9394.7*	*23.0*	*43.4*	*1.8*	*224.3*	*2.4*	*414.8*	*3.4*	*131.10*	*3.10*	*0*	*0*	*0*	*9*	*4*	*131.2*	*1600*	*300*	*338*
1071-01B	PP20	HBL	2.0	66a	1.944	0.010	754494.9	239.7	1828.1	7.4	2541.4	9.9	1980.6	10.9	17.11854	3.816	9438.9	16.0	42.8	1.6	218.0	2.1	418.5	4.1	122.47	2.20	0.0064	9.0	8.8	5.82	0.04	99.4	1059	3	5
1071-01C	PP20	HBL	4.0	66a	1.944	0.010	7409476.0	3275.2	18532.4	128.0	25959.4	188.8	20418.6	162.7	0	73.551	9438.9	16.0	42.8	1.6	218.0	2.1	418.5	4.1	122.50	2.20	0.0654	90.9	0.0	5.92	0.06	101.5	1050	6	7
1071-01D	*PP20*	*HBL*	*6.0*	*66a*	*1.944*	*0.010*	*6736.5*	*38.7*	*16.4*	*3.1*	*24.7*	*3.9*	*29.8*	*6.0*	*23.00652*	*4.021*	*9438.9*	*16.0*	*42.8*	*1.6*	*218.0*	*2.1*	*418.5*	*4.1*	*122.47*	*2.20*	*0.0001*	*0.1*	*0.1*	*10*	*3*	*0*	*0*	*300*	*261*
1078-01A	*PP20*	*HBL*	*1.0*	*66b*	*2.003*	*0.010*	*11578.2*	*36.8*	*3.6*	*2.4*	*11.5*	*3.8*	*0*	*6.1*	*18.693*	*3.443*	*9471.9*	*19.0*	*44.4*	*1.3*	*224.5*	*2.9*	*421.5*	*3.8*	*121.64*	*2.70*	*0*	*0*	*0*	*0*	*10*	*51.8*	*2600*	*1000*	*956*
1078-01B	PP20	HBL	2.0	66b	2.003	0.010	343666.5	177.3	846.5	7.2	1669.7	9.0	890.6	10.1	6.312	4.281	9471.9	19.0	44.4	1.3	224.5	2.9	421.5	3.8	121.64	2.70	0.0030	8.1	10.8	5.65	0.08	99.5	1071	8	9
1078-01C	PP20	HBL	4.0	66b	2.003	0.010	558461.0	152.3	1398.7	6.3	2850.7	9.7	1510.8	7.4	9.454	4.054	9471.9	19.0	44.4	1.3	224.5	2.9	421.5	3.8	121.64	2.70	0.0049	13.4	12.2	5.80	0.04	99.6	1058	4	6
1078-01D	PP20	HBL	6.0	66b	2.003	0.010	3248589.0	918.5	8158.0	46.6	16206.1	55.0	8743.2	53.9	0	12.753	9476.2	19.0	37.0	2.3	226.8	2.8	439.9	4.1	128.80	1.80	0.0288	78.4	0	5.76	0.05	100.4	1063	5	6
1080-01A	PP20	HBL	3.5	66b	1.978	0.010	3413378.0	1591.9	8475.0	39.2	19402.0	84.1	6507.9	61.0	27.30625	12.266	7278.5	17.0	20.9	1.5	133.1	1.5	266.8	2.9	88.40	1.40	0.0299	49.9	29.3	6.62	0.07	99.9	1057	4	6
1080-01B	PP20	HBL	4.5	66b	1.978	0.010	176455.3	98.4	429.7	4.7	1007.7	7.4	330.3	6.9	2.927264	2.867	7278.5	17.0	20.9	1.5	133.1	1.5	266.8	2.9	88.43	1.40	0.0015	2.5	13.9	6.63	0.16	99.6	1071	10	10
1080-01C	PP20	HBL	6.0	66b	1.978	0.010	204779.7	103.4	503.1	4.4	1160.9	9.1	405.2	7.7	4.638742	2.640	7278.5	17.0	20.9	1.5	133.1	1.5	266.8	2.9	88.43	1.40	0.0018	3.0	10.7	6.95	0.14	99.4	1062	8	9
1080-01D	*PP20*	*HBL*	*5.0*	*66b*	*1.978*	*0.010*	*2763243.0*	*1775.6*	*7575.0*	*67.4*	*15587.4*	*85.5*	*5145.9*	*40.7*	*0*	*21.404*	7950.2	25.0	20.5	1.0	141.2	2.2	274.7	2.9	98.10	2.70	*0.0267*	*44.6*	*0*	*5.95*	*0.07*	*101.5*	*992*	*7*	*8*
1105-01A	PP20	HBL	3.5	66e	2.121	0.006	3431046.0	1224.6	8380.9	39.8	16221.5	80.9	6747.5	56.7	820.8267	20.157	7278.5	17.0	20.9	1.5	133.1	1.5	266.8	2.9	88.40	1.40	0.0296	60.3	1.0	6.95	0.07	93.0	1069	4	5
1105-01B	PP20	HBL	4.5	66e	2.121	0.006	453343.9	152.1	1183.0	5.9	2301.6	12.5	989.9	9.8	12.67131	2.991	7274.6	18.0	23.3	1.2	136.2	2.1	268.7	3.3	87.85	1.80	0.0042	8.5	9.6	7.22	0.08	99.3	1069	4	5
1105-01C	PP20	HBL	6.0	66e	2.121	0.006	1649245.0	545.2	4323.3	24.5	8854.7	65.7	3652.7	36.4	37.839	11.754	7274.6	18.0	23.3	1.2	136.2	2.1	268.7	3.3	87.90	1.80	0.0153	31.1	11.9	7.29	0.08	99.4	1066	5	5

Notes:
a: Relative isotopic abundances corrected for blank, radioactive decay, and mass discrimination
b: 4-digit number indicates the RunID number in Mass Spec, -01 denotes the aliquot number, letter suffix indicates the heating step
c: Number indicates the irradiation batch number, letter refers to the tube in which the sample was loaded in the irradiation can. Rad#66 was irradiated for 160 MWH in medium-flux position 8A at McMaster Nuclear Reactor (no Cd shielding).
Data in italics were analyses excluded from integrated age calculations.
All negative values in the table were replaced with "0".
Decay constants and isotopic abundances after Steiger and Jäger (1977).
Ages calculated relative to FCT-San Fish Canyon Tuff sanidine flux monitor at 28.02 Ma (Renne et al., 1998)
Nucleogenic interference correction factors (±2s)
(^{39}Ar/^{37}Ar)Ca = 0.0007 ± 0.000054
(^{36}Ar/^{37}Ar)Ca = 0.00028 ± 0.00017
(^{40}Ar/^{39}Ar)K = 0.058 ± 0.005
Bkgd = background